The Institute of Paper Chemistry

Appleton, Wisconsin

Doctor's Dissertation

The Degradation of Selected 1,5-Anhydroalditols by Molecular Oxygen in Alkaline Media

Eugene C. Millard

June, 1976

THE DEGRADATION OF SELECTED 1,5-ANHYDROALDITOLS BY MOLECULAR OXYGEN IN ALKALINE MEDIA

A thesis submitted by

Eugene C. Millard

B.S. 1969, Drexel Institute of Technology

M.S. 1972, Lawrence University

in partial fulfillment of the requirements
of The Institute of Paper Chemistry
for the degree of Doctor of Philosophy
from Lawrence University,
Appleton, Wisconsin

June, 1976

TABLE OF CONTENTS

SUMMARY

The degradation of 1,5-anhydroribitol (AR), 1,5-anhydroxylitol (AX), and 3-O-methyl-1,5-anhydroxylitol (MAX) by molecular oxygen [75 psi (25°C)] was studied in a teflon-lined reactor at constant temperature (120°C) and sodium hydroxide concentration (1.25N). Quantitative gas-liquid chromatographic analyses of the reactions at varying time intervals were used to show that both the number and configuration of hydroxyl groups present on the carbohydrate ring influence the rate of reaction. The order of reactivity of the alditols was AR>AX>MAX.

Kinetic analysis (method of integration and differential method) showed the AR system to be second order in carbohydrate with respect to time. The AX system displayed a complex relationship indicative of autoinhibition by a reactive intermediate. The low reactivity of MAX under the reaction conditions studied made it impossible to reach definite conclusions regarding the order of the reaction with respect to the alditol.

All three model systems produced hydrogen peroxide, with maxima occurring at relatively low percent reaction of the carbohydrate. An organic peroxide intermediate (postulated to be alpha-hydroxyhydroperoxide) was detected in the AX and MAX reactions. This is the first report of a reactive organic peroxide in the degradation of a carbohydrate by molecular oxygen in alkaline media. Formation of an alpha-hydroxyhydroperoxy free radical ($AO_2\cdot$) is postulated to occur by direct attack of molecular oxygen on a free radical derived from the alditol by hydrogen abstraction via the superoxide radical ($O_2^{-}\cdot$) and, to a lesser extent, the hydroxyl free radical ($HO\cdot$). The $AO_2\cdot$, which can be stabilized by hydrogen bonding in the AX system, is proposed to be involved in a reversible reaction with the alpha-hydroxyhydroperoxy anion (AO_2^{-}), which can also be stabilized by hydrogen bonding in the AX system. The AO_2^{-} is postulated to react to acidic products via a carbonyl. It can also proceed to the alpha-hydroxyhydroperoxide (AOOH) which subsequently reacts to products through a carbonyl or another

of its conjugate bases. Thus, hydrogen bonding of $AO_2\cdot$ and AO_2^- in the AX system causes an increase in the concentration of $AO_2\cdot$ and subsequently, increases the importance of $AO_2\cdot$ self-termination reactions.

The complex kinetics of the AX system are proposed to result from these $AO_2\cdot$ self-termination reactions which produce only nonradical species. The termination reactions cause an abnormal decrease in the rate of the free radical propagation reactions which kinetically manifests itself as autoinhibition.

Acidic degradation products of the model compounds were identified as their trimethylsilyl derivatives by gas-liquid chromatography-mass spectrometry. The products of the AX and AR reactions were identical. Lactic and glycolic acids were termination products; while glyceric, 2,3-dihydroxybutyric, 1,4-anhydro-2-C-carboxy-D-, and -L-, erythritol and threitol, and 3-O-carboxymethyl-glyceric acids all displayed maxima in their concentration versus time curves. Other minor degradation products identified in the AX and AR systems were 3-hydroxypropanoic, 2-hydroxybutyric, 2,4-dihydroxybutyric, formic, and acetic acids. However, there was no apparent inhibition related to any of the acidic degradation products. The only major compound produced in the MAX reaction was 3-hydroxy-2-methoxybutyric acid. This fact, in conjunction with the production of 2,3-dihydroxybutyric acid in the AX and AR systems, indicates that cleavage between the ring oxygen and C-5 is an important part of the overall degradation mechanism. Major differences in the relative ratio of the 1,4-anhydro-2-C-carboxy-D-, and -L-, erythritol and threitol between the AX and AR reactions indicate that, besides the frequently postulated alpha-dicarbonyl intermediate, another intermediate with a stereochemical directing effect acts as a precursor to these furanoid acids.

Finally, a mechanism is proposed for the alkaline oxygen degradation of the model compounds that accounts for an induction period, the formation of hydrogen peroxide and organic peroxides, the kinetics of the AX and AR systems, and the formation of final acidic degradation products.

INTRODUCTION

PERSPECTIVE

In recent years, concern over the environment has stirred interest in the use of alkali and molecular oxygen for delignifying and brightening pulps. To take full advantage of these processes, the oxidative degradation of wood polysaccharides has to be minimized. Robert, et al. (1,2) made these processes practical by showing that magnesium compounds can decrease the degradation of carbohydrates during delignification with alkali and oxygen. These stabilized processes have the advantage of greatly reducing effluent toxicity while producing pulps with acceptable papermaking properties.

In order to increase the prospects for better control of carbohydrate degradation in oxygen-alkali, a workable knowledge of the reaction mechanism would be invaluable. The present investigation was designed to study one aspect of the reaction mechanism; the mode of ring cleavage of carbohydrates and how it is affected by the stereochemistry and number of hydroxyl groups present on the carbohydrate ring.

LITERATURE REVIEW

The purpose of the review is to give the reader some background concerning the degradation of carbohydrates by molecular oxygen in alkali. It is not intended to be a comprehensive critique of the voluminous literature on the subject. The review will briefly deal with the reactions of cellulose and cellulosic model compounds and discuss the present state of knowledge regarding the mechanism of degradation. For further detail, the original literature may be consulted.

Oxygen bleaching of pulp (ca. 20% consistency) is normally performed at 0.5-5.0% sodium hydroxide (based on o.d. pulp), 90-130°C, and 5-15 atmospheres oxygen pressure for less than 2 hours. Most of the model studies to date (mechanistic as well as empirical) involved more extensive degradation of the carbohydrates than would be found in the normal oxygen bleach. However, it is believed that the information found in the literature can be very useful in understanding the commercial oxygen bleaching and pulping processes.

CELLULOSIC STUDIES

Golova, et al. (3,4) carried out investigations in which various forms of cellulose were treated with alkali and air. It was found that the extent of degradation was roughly proportional to the degree of accessibility (indicated by crystallinity) of the cellulose. Studies also showed that the carbonyl content of the cellulose influenced the rate of degradation; higher carbonyl content led to faster rates of degradation. Peroxides were detected, and it was concluded that they originated from both carbonyl and hydroxyl groups. Akim (5) has proposed that hydroperoxides play a major role in cellulosic degradation reactions. Although hydrogen peroxide was detected, no experimental evidence for the presence of hydroperoxides was given.

The air oxidation of regenerated cellulose in 1% sodium hydroxide solution at 100°C produced oligosaccharides (cellotriose, cellotetraose, and cellopentaose), saccharinic acids and their lactones (6).

Samuelson and Stolpe (7) and Kolmodin and Samuelson (8) investigated the aldonic acid end groups in cellulose after oxygen bleaching. Treatment of hydrocellulose and cellulose impregnated with sulfate lignin produced only small amounts of metasaccharinic acid end groups, while aldonic acid end groups predominated. It was concluded that the "peeling reaction" is unimportant

when oxygen is present. However, Malinen (9) reported that the "peeling reaction" was of considerable importance during the treatment of cellulose with oyxgen and alkali. The governing factor seems to be accessibility, which is highly dependent on alkali concentration. The higher the alkali concentration, the greater the swelling of the cellulose. Oxygen has good accessibility to cellulose which is swollen, producing aldonic acid end groups which stabilize the cellulose to the "peeling reaction." Samuelson and co-workers (7,8), in analyzing the aldonic acid end groups produced by oxygen bleaching of cellulose, showed that arabinonic, mannonic, and erythronic acids were the major products while minor amounts of gluconic, ribonic, and altronic acids were also present. The relative amounts of aldonic acids detected were similar to the amounts found after the aging of alkali cellulose (10) and after the alkaline degradation of D-glucosone in oxygen-free, dilute sodium hydroxide at 100°C (11). Thus, Kolmodin and Samuelson (8) rationalized that the degradation of cellulose during oxygen bleaching can be explained by the reaction scheme (Fig. 1) proposed by Haskins and Hogsed (12) for the depolymerization of cellulose during the aging of alkali cellulose.

As can be seen, oxidation of hydroxyl groups is proposed to occur along the cellulose chain and, after the glycosidic bonds are broken by β-elimination reactions, the glucose end groups undergo oxidation, fragmentation, or rearrangement to form the aldonic acids previously mentioned. In studying the alkaline oxygen degradation of birch xylan, Kolmodin and Samuelson (13) found acidic products similar to those obtained during the degradation of cellulose. The products includeed xylonic, lyxonic, threonic, glyceric, glycolic, formic, 3-hydroxypropanoic, and 2,4-dihydroxybutyric acids.

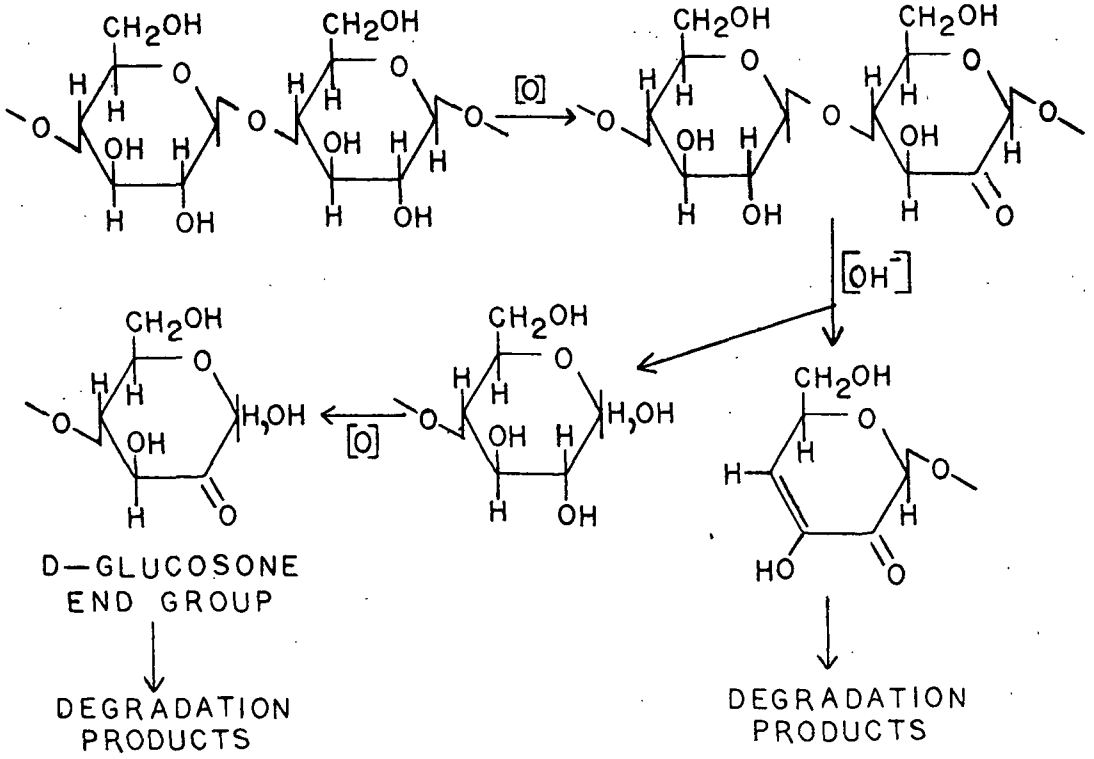

Figure 1. Cleavage of Cellulose by Oxygen in Alkali Proposed by Haskins and Hogsed (12)

MODEL STUDIES

Samuelson and Stolpe (14) studied the degradation of cellobiitol under the influence of alkali and oxygen. Oxygen consumption, formation of peroxides, and organic acids were measured, but direct determination of cellobiitol degradation was not reported. In 0.5% sodium hydroxide at 95°C under oxygen pressure (84 psi), cellobiitol consumed no detectable oxygen for 30 minutes. Subsequently, the rate of oxygen consumption slowly increased to a final constant value. The addition of glucose to the cellobiitol system shortened the induction period, accelerated the initial formation of peroxides, and resulted in the formation of larger concentrations of organic acids. However, once the glucose was consumed, the rate of oxygen consumption returned to the level achieved with cellobiitol alone.

The reaction of glucose was studied separately by Samuelson and Thede (15) using 18% sodium hydroxide and oxygen at a constant pressure of 1 atmosphere. Thirteen monoprotic carboxylic acids were isolated from the reaction mixture. The main products were formic, glycolic, glyceric, and aldonic acids. In the same study, cellobiose was degraded to yield the aforementioned acids along with substantial amounts of aldobionic, 3,4-dihydroxybutyric, 3-deoxypentonic, and glucoisosaccharinic acids.

While studying the alkaline degradation of methyl β-D-glucopyranoside, Brooks (16) observed a large effect of oxygen on the rate of reaction. Depending on the reaction conditions, the increase in the reaction rate was as much as 45 times that in an oxygen-free solution. The effect was rationalized on the basis of a lower activation energy for the oxidation reaction than for alkaline hydroxylsis. The proposed reaction scheme is shown in Fig. 2.

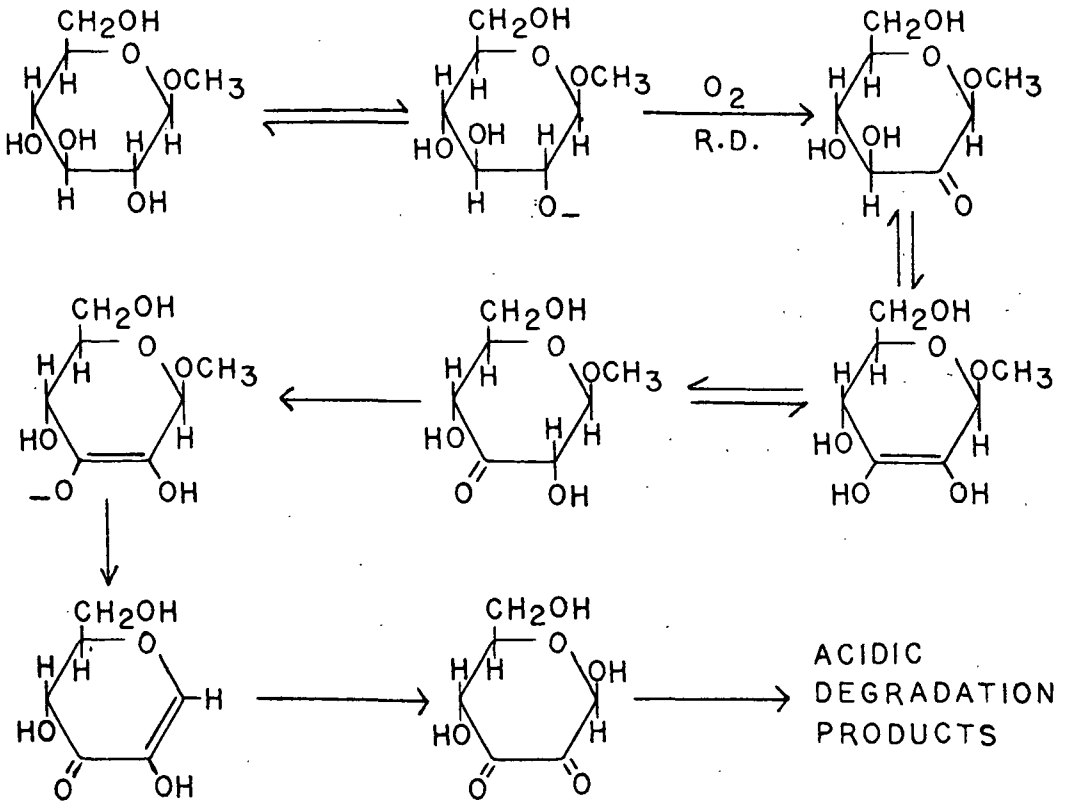

Figure 2. Cleavage of the Glucosidic Bond of Methyl β-D-Glucopyranoside with Alkali and Oxygen Proposed by Brooks (16)

Minor and Sanyer (17) studied the alkaline oxidation of glucitol. Reaction conditions were 0.5M sodium hydroxide and 100 psi oxygen. Hydrogen peroxide was determined to be the reactive peroxidic intermediate. At the start of the reaction, a definite induction period was observed which corresponded in time with the build-up of hydrogen peroxide. The initiation of glucitol degradation was reported to correspond to the peak concentration of hydrogen peroxide. Reevaluation of their data indicates that, as expected, initiation took place when hydrogen peroxide decomposition began to become significant; that is, before the maximum hydrogen peroxide concentration was reached. Also, the detectable hydrogen peroxide disappeared completely with ample glucitol remaining. Transient hydroperoxides were postulated as possible reactive intermediates. A combination of gas chromatography and nuclear magnetic resonance spectroscopy showed that the two major acidic products were glycolic and glyceric acids. The initial step of the reaction was postulated to be ionization of a hydroxyl group followed by hydrogen abstraction by oxygen to form the perhydroxyl anion. This agrees with the reasoning of McCloskey (18) who demonstrated that the maximum concentration of peroxides during the oxidative degradation of a carbohydrate was roughly proportional to the number of hydroxyl groups on the carbohydrate molecule.

McCloskey (18) used initial-rate kinetic studies, perhaps erringly, to show that the alkaline oxygen degradation of methyl β-D-glucopyranoside is approximately fourth order overall; second order in methyl β-D-glucopyranoside and first order in oxygen and sodium hydroxide. Sinkey (19) has since added support to the second order carbohydrate relationship.

McCloskey (18) also showed that oxidation of methyl glycopyranosides does not necessarily result in cleavage of the glycosidic bond. Less than 1 mole of methanol was generated for every mole of glycopyranoside reacted. It was

reasoned that degradation products with the aglycon still attached were responsible for this phenomenon. Acid hydrolysis of the reaction mixture confirmed this fact.

Ericsson, et al. (20) also studied the alkaline oxygen degradation of methyl β-D-glucopyranoside. They succeeded in isolating and identifying a methyl 2-C-carboxy-β-D-pentofuranoside as a product of the reaction (Fig. 3).

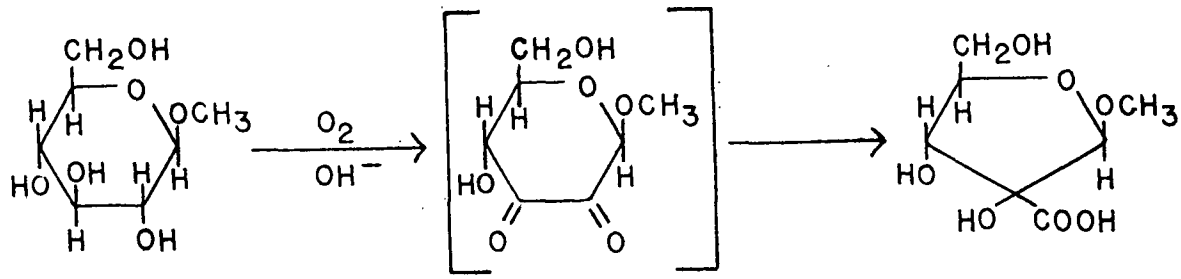

Figure 3. A Product of the Alkaline Oxygen Degradation of Methyl β-D-Glucopyranoside Proposed by Ericsson, et al. (20)

A dicarbonyl intermediate was proposed to form via simultaneous introduction of carbonyl moieties at C-2 and C-3. Unlike the intermediate proposed by Brooks (Fig. 2), the dicarbonyl intermediate suggested by Ericsson (Fig. 3) still has the glycosidic bond intact. The intermediate then reacts by a benzylic acid-type rearrangement to give the furanoid acid. Weaver (21) has identified similar products in the alkaline hydrogen peroxide degradation of methyl β-D-glucopyranoside and methyl 4-O-methyl-β-D-glucopyranoside. These types of products can account for the bound methanol found by McCloskey (18).

REACTION MECHANISM

The present state of knowledge regarding the mechanism of the alkaline oxygen degradation of carbohydrates is based on both experimental fact and speculation. The remainder of this section will attempt to consolidate the literature into an overview of what is known of the reaction mechanism.

The mechanism of oxidation of a carbohydrate by oxygen in alkaline media involves ionization of the carbohydrate to form the carbinolate anion (16-23), followed by formation of hydrogen peroxide (17-19). The hydrogen peroxide is probably produced by hydrogen abstraction via molecular oxygen which is facilitated by the increased electron density provided by the carbinolate ion (Fig. 4).

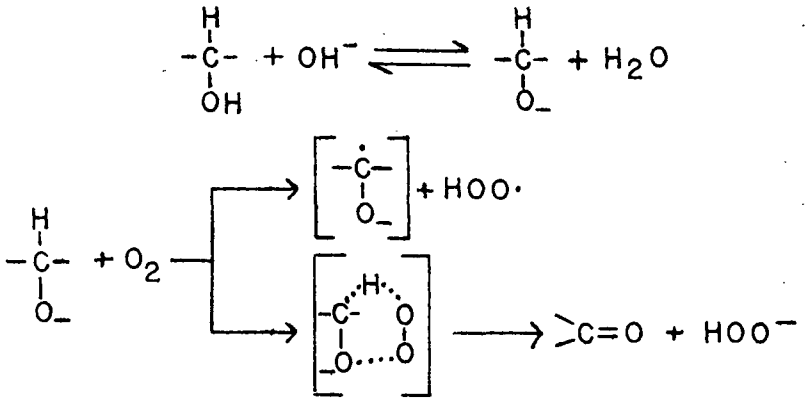

Figure 4. Formation of Hydrogen Peroxide Proposed by McCloskey (18)

The reactions usually exhibit induction periods (14,17-19) corresponding to a build-up in hydrogen peroxide (17-19). Rapid degradation of the carbohydrate is believed to proceed by a free radical mechanism (5,18,19,21,24) with radical species produced directly via hydrogen abstraction by oxygen (Fig. 4) or by the reaction of the hydroperoxy anion with metal ions (18,21,24). The reaction of carbohydrate with radical species is postulated to produce transient hydroperoxides (17,21,25) which react to acidic degradation products through intermediates which probably contain carbonyl functions. Although organic peroxides have been detected in oxygen alkaline degradations (18,25), the presence of hydroperoxides has not been verified. Weaver (21), in studying the alkaline hydrogen peroxide degradation of methyl β-D-glucopyranoside, has presented evidence for the existence of a reactive organic peroxide, believed to be an alpha-hydroxyhydroperoxide.

The acidic degradation products are aldonic acids, methyl C-carboxy-pentofuranoids, and dibasic acids, depending on the starting material. Stable organic peroxides (postulated to be dialkyl peroxides) are also products of the reaction of methyl β-D-glucopyranoside (18,25). They are believed to be the result of termination reactions between hydroperoxy and alkyl free radicals.

THESIS OBJECTIVES

The main objective of the investigation was to gain information about the ring cleavage reactions of selected 1,5-anhydroalditols by molecular oxygen in aqueous alkali. The model compounds were 1,5-anhydroxylitol (AX), 1,5-anhydroribitol (AR), and 3-O-methyl-1,5-anhydroxylitol (MAX). Emphasis was

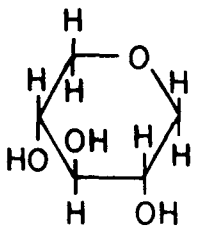

AX

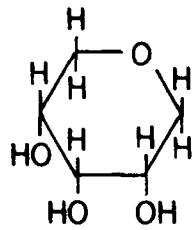

AR

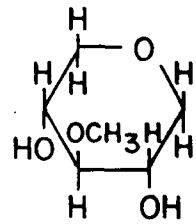

MAX

placed on the effect of altering the configuration and number of hydroxyl groups present on the carbohydrate ring. By studying the differences in the kinetics and products of the model compound reactions, the effect of the alterations was used to gain insight into the reaction mechanism.

RESULTS AND DISCUSSION

ALDITOL DEGRADATION

GENERAL

The following conditions were employed for alkaline oxygen degradations of the selected model compounds: 1.25N sodium hydroxide; 120°C; 75 psi oxygen pressure (25°C)*; and either 0.01N or 0.1N carbohydrate.

Disappearance of the starting materials was followed by quantitative gas-liquid chromatography (GLC) employing the per-O-acetylated derivatives. The GLC conditions are reported in Appendix II, Tables V and VI.

In general, the reproducibility of the alkaline oxygen degradations of the anhydroalditols at 0.01 and 0.1N carbohydrate (Fig. 5 and 6, respectively) (Appendix V, Tables XXI-XXVII) was excellent. One segment of the degradation pattern that was not always reproducible was the induction period. Figure 7 and the data in Appendix V illustrate its variable nature. Sinkey (19) has reported that certain transition metal ions significantly increase the initial degradation rate of the alkaline oxygen reaction of methyl β-D-glucopyranoside by rapidly decomposing hydrogen peroxide to free radicals which can initiate degradation of the carbohydrate. Therefore, variation in the metal ion content of the reaction solutions could possibly account for the varying induction period. In agreement with the work on methyl β-D-glucopyranoside (19), the degradation rate attained after the induction period was essentially the same for duplicate experiments, regardless of the character of the induction period. This is a vital factor in the kinetic treatment employed in this investigation.

*The actual gage pressure was calculated by correcting the needed pressure of 75 psi (25°C) to 120°C and correcting for the vapor pressure of water.

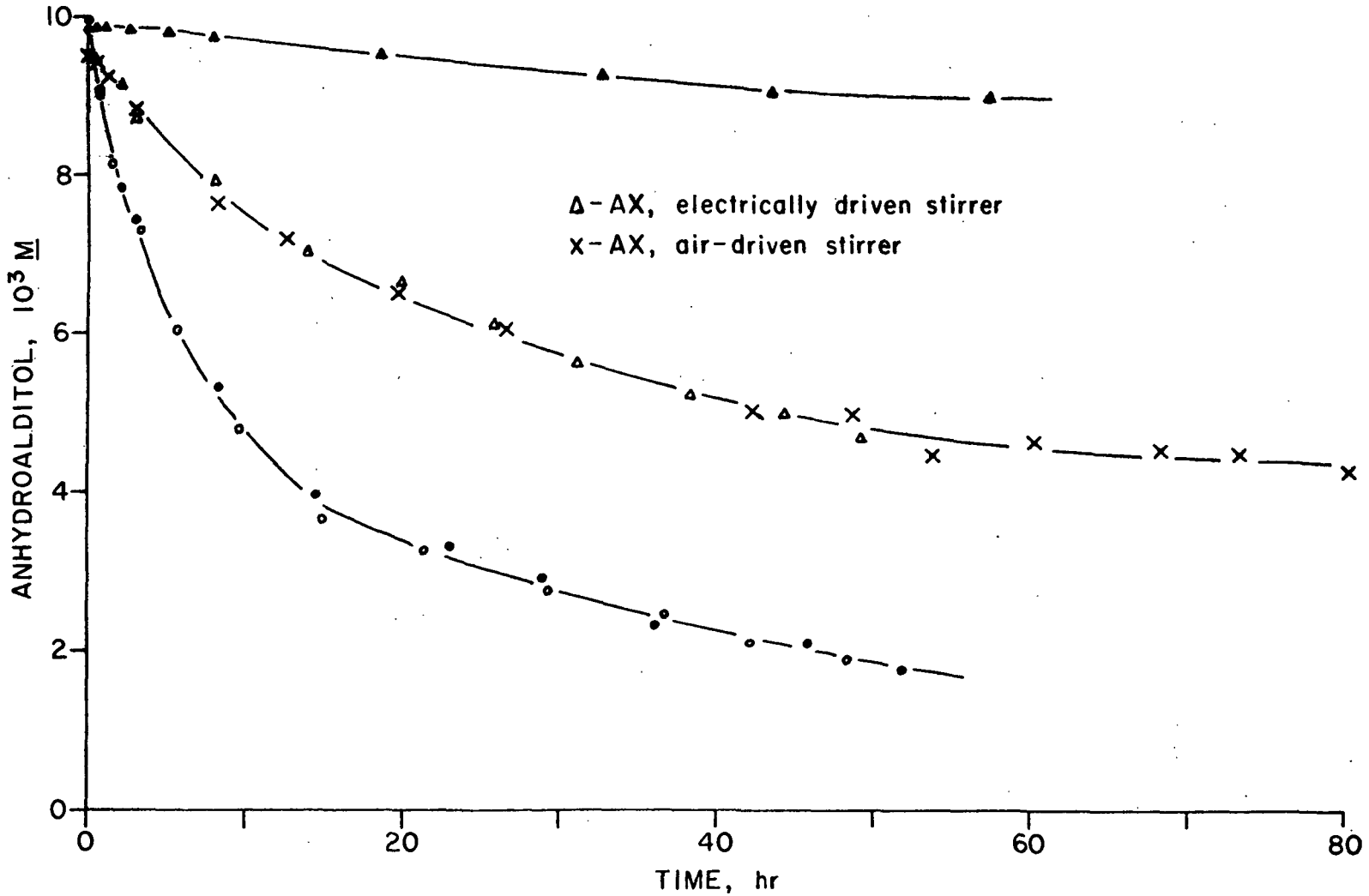

Figure 5. Degradation of 3-O-Methyl-1,5-anhydroxylitol (▲ - 1 MAX), 1,5-Anhydroxylitol (Δ - 2 AX, x - 3 AX), and 1,5-Anhydroribitol (o - 1 AR, ● - 3 AR) in 1.25N NaOH at 120°C, 75 PSI O_2 (25°C), and 0.01N Carbohydrate

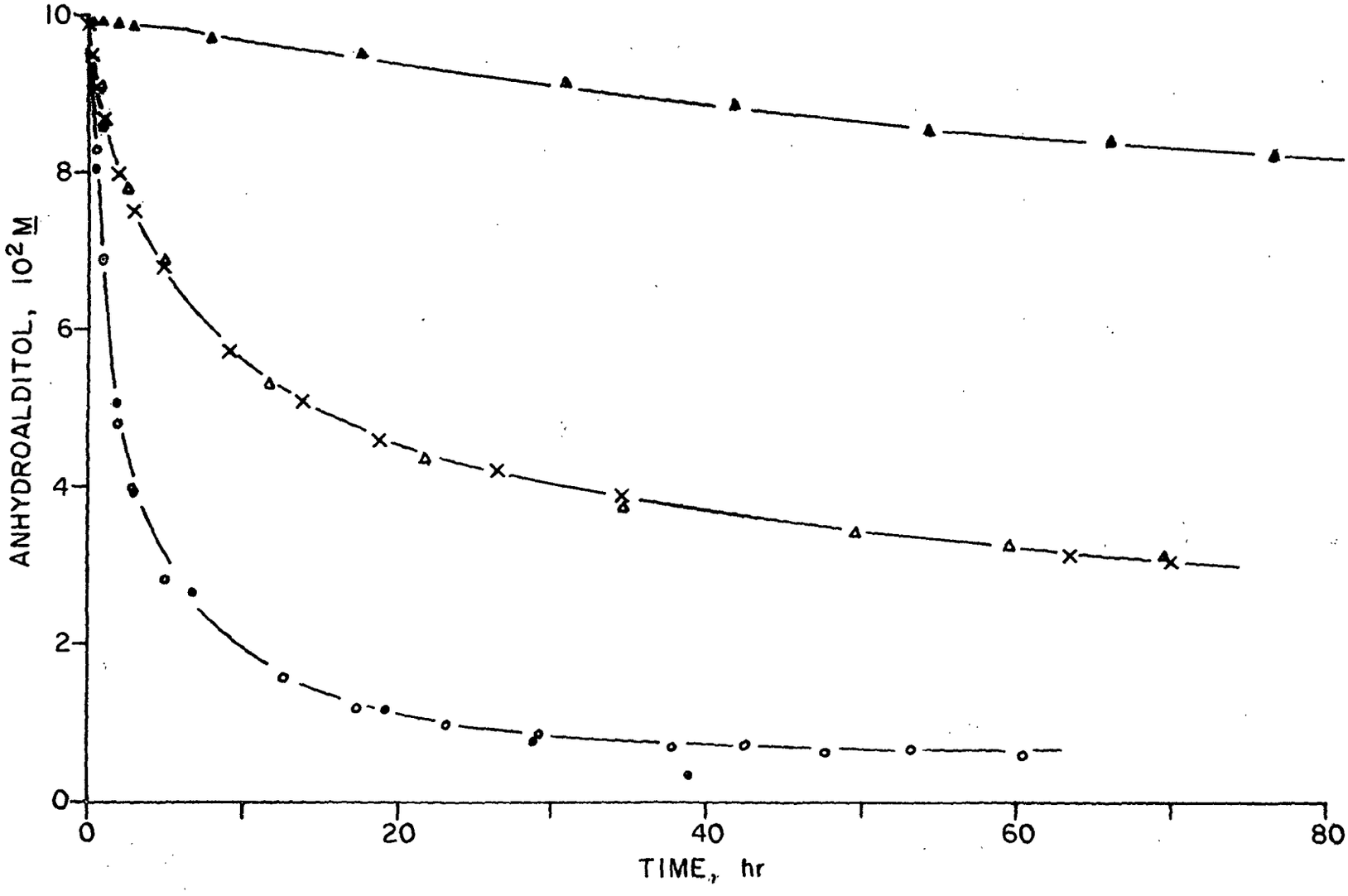

Figure 6. Degradation of 3-O-Methyl-1,5-anhydroxylitol (▲ - 2 MAX), 1,5-Anhydroxylitol (x - 4 AX, Δ - 5 AX), and 1,5-Anhydroribitol (o - 4 AR, ● - 5 AR) in 1.25N NaOH at 120°C, 75 PSI O_2 (25°C), and 0.1N Carbohydrate

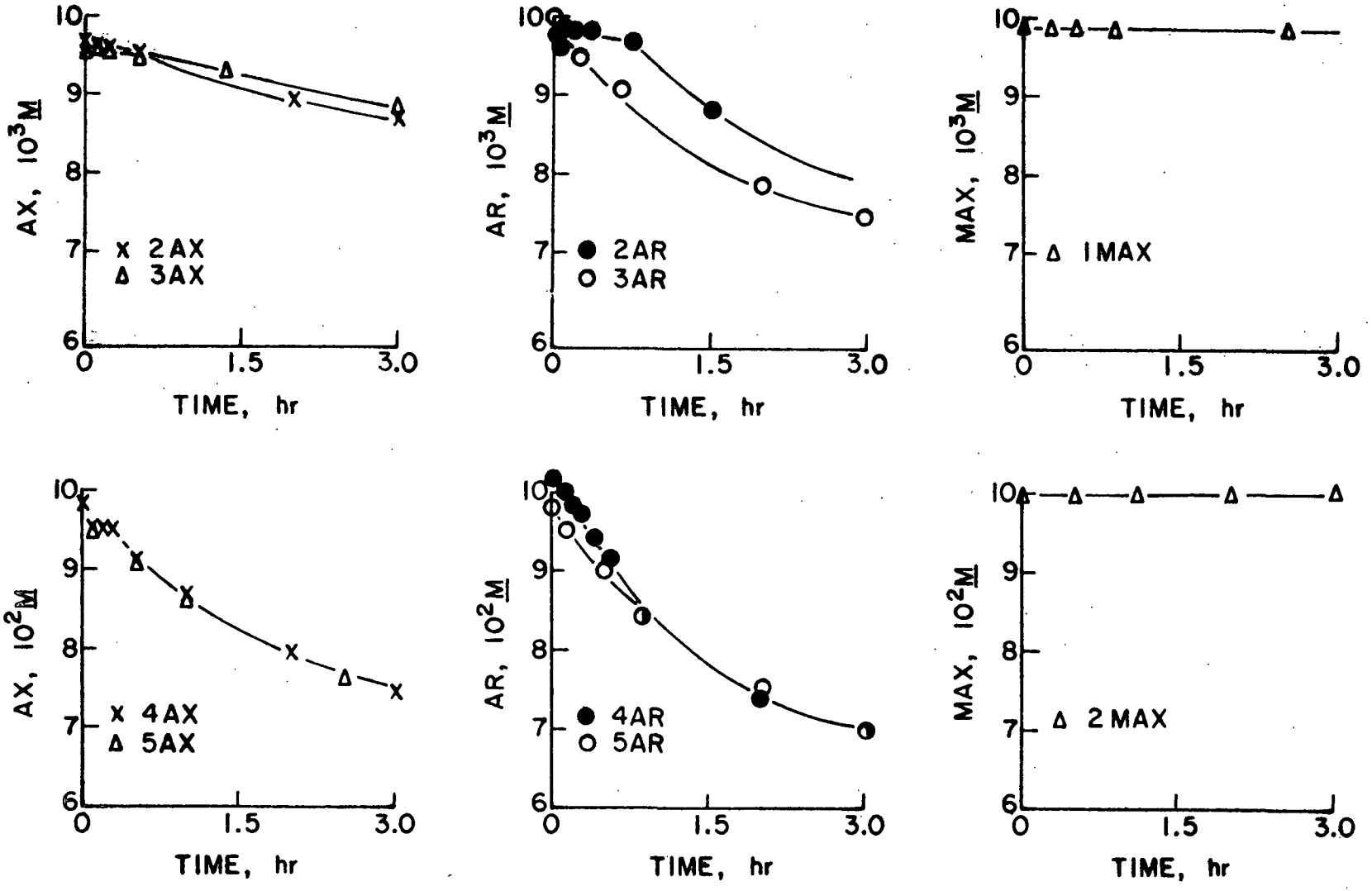

Figure 7. Variable Nature of Induction Period During Degradation of 1,5-Anhydroxylitol, 1,5-Anhydroribitol, and 3-O-Methyl-1,5-anhydroxylitol in 1.25N NaOH at 120°C and 75 PSI O_2 (25°C)

Figure 5 also illustrates that an increased stirring rate had no effect on the rate of degradation of 1,5-anhydroxylitol (AX). The two kinetic experiments for AX shown in Fig. 5 (2AX and 3AX) differ only in the rate of stirring used. The stirrer for one reaction (2AX) was electrically driven and for the other reaction (3AX) air-driven. The air-driven stirrer greatly increased the stirring efficiency but had no effect on the rate of alditol degradation. Thus, diffusion by molecular oxygen into the solution was not a factor in the rate-controlling step of the degradation of the model compounds*. This is in agreement with previous investigators (22,26).

As can be seen in Fig. 5 and 6, the rate of degradation of an anhydroalditol is greatly influenced by both the configuration and number of hydroxyl groups present on the pyranoid ring. The order of reactivity at both carbohydrate concentrations studied was 1,5-anhydroribitol (AR)>1,5-anhydroxyitol (AX)>3-O-methyl-1,5-anhydroxyitol (MAX). The large difference in reaction rates between AR and AX must be attributed to the configurational relationship between hydroxyl groups on the ring. In AR vicinal hydroxyl groups are *cis* to one another, while in AX vicinal hydroxyl groups are in a *trans* relationship (see Introduction). The variation in rates between AX and MAX is caused by the substitution of a methoxy group for the hydroxy group at C-3. The means by which these alterations affect the rates of degradation are discussed in a later section.

*At room temperature, alkaline solutions become saturated with oxygen slowly (27). However, at elevated temperatures, saturation conditions may be achieved much more rapidly.

KINETIC ANALYSIS

Background

There are two main methods of treating kinetic data: the method of integration and the differential method (28). The method of integration uses the integrated form of the rate equation for an assumed reaction order. Although it is the most widely employed method, it is not reliable where complications such as autocatalysis or autoinhibition play a role in the reaction mechanism. The method of integration characterizes a reaction according to the way in which the concentration of reactants varies with time, which could cause misleading deductions about the way the reaction rates vary with the concentration of reactants (28).

The differential method employs the differential form of the rate expression. The reaction rate at a particular reactant concentration is obtained from the slope of the concentration versus time curve at that point. The method may be applied in two ways. Initial rates may be measured at various initial reactant concentrations. The slope of a log-log plot of the initial rates versus the initial concentrations is the reactant order with respect to concentration, or the true order (28). The second procedure involves considering a single kinetic trial, measuring the reaction rate at various times corresponding to a number of reactant concentrations. The slope of the log-log plot of rate versus concentration gives the reactant order with respect to time (28). For a reaction that is autocatalyzed or autoinhibited, the true order derived from initial rate studies does not necessarily equal the order with respect to time derived from a single kinetic experiment.

As stated previously, the degradation reactions of the compounds under investigation generally exhibit induction periods; making utilization of the differential method employing initial reaction conditions impractical. However,

since the degradation rate attained after the induction period was essentially the same for duplicate trials, the differential method employing single kinetic trials seems applicable in the present investigation. This procedure, in combination with the method of integration, was used to obtain the orders of the reactions involved.

If a reaction occurs in a single step, there is a relationship between the stoichiometry of the reaction and the order. However, reactions occurring by a complex mechanism involving a number of steps frequently cannot be characterized by an order (28). Such reactions can have complicated rate expressions in which the reactant concentrations appear in the denominator of the expression. The order of a reaction is strictly an empirical quantity, and merely provides information about the way in which the reaction rate depends on concentration. It should not be used interchangeably with molecularity which represents a conclusion concerning the number of molecules entering into one step of a reaction sequence.

Rate Expressions

It was assumed that the alkaline oxygen degradations of the anhydroalditols would obey the basic rate expression

$$-d[A]/dt = k[A]^a[O_2]^b[NaOH]^c \qquad (1)$$

where $-d[A]/dt$ = rate of disappearance of alditol

k = rate constant

$[A]$ = concentration of alditol

$[O_2]$ = concentration of oxygen

$[NaOH]$ = concentration of sodium hydroxide

a,b,c = orders with respect to the corresponding reactants

In the reactions at 0.01N carbohydrate, the sodium hydroxide was in large excess relative to the carbohydrate and hence its concentration was essentially constant throughout the reaction. At 0.1N carbohydrate, consumption of alkali could have been as much as 15% in the AR reaction. Strictly speaking, this makes the assumption of constant alkali concentration invalid. However, kinetic analysis of the AR degradation data showed the reaction to be second order in alditol at both 0.01 and 0.1N alditol. This would not be the case if the decrease in alkali concentration was enough to significantly affect the reaction rate. Therefore, as a first approximation, the assumption that the alkali concentration remains constant during the degradation reactions at 0.1N carbohydrate seems valid.

The solubility of oxygen in 1.25N alkali at 75 psi oxygen pressure (25°C) and 120°C waS estimated to be $2.46\ 10^{-3}$M based on a linear interpolation of Bruhn's data (29). However, since diffusion of oxygen into solution was not rate limiting, the constant oxygen pressure maintained over the reaction solution insured that the concentration of oxygen was essentially constant throughout the reactions. Thus, Equation (1) can be written as

$$V_a = -d[A]/dt = k'[A]^a \qquad (2)$$

where V_a = reaction velocity at [A]

$k' = k[O_2]^b[NaOH]^c$

The integrated form of Equation (2) depends on the assumed order, a.

$$a = 1 \quad \ln[A] - \ln[A]_o = k_1't \qquad (3)$$

$$a = 2 \quad 1/[A] - 1/[A]_o = k_2't \qquad (4)$$

A reaction which is first order in alditol would give a linear plot of ln[A] against t. A second order reaction would give a linear plot of 1/[A] versus t.

The differential method involves taking the logarithm of Equation (2) to give

$$\log V_a = \log k' + a \log [A] \qquad (5)$$

The slope of a log-log plot of V_a versus [A] at various alditol concentrations for a single kinetic trial is the order of the reaction with respect to the alditol as a function of time.

Analysis by the Method of Integration

The data were plotted according to Equations (3) and (4). Plots assuming a reaction order of one showed severe deviation from linearity (see Appendix V, Fig. 52).

Figure 8 illustrates typical curves derived from data for the degradation of AX and AR* at 0.01N carbohydrate assuming second order dependence on the alditol. The AR plot is linear, indicating the reaction to be second order. A slight deviation from linearity is evident in the AX curve, although a good straight line could be fitted to the data points. Figure 9 gives a curve derived from the 0.01N MAX degradation data. The plot consists of two linear portions, the smallest of which is indicative of the extended induction period in the MAX reactions.

Figure 10 gives a similar curve for AR at 0.1N carbohydrate. Figure 11 illustrates typical AX and MAX data at 0.1N carbohydrate. At the higher concentration of anhydroalditol, the second order relationship still holds for AR and MAX but the deviation from linearity for the AX reaction is now quite distinct.

*Tabulated degradation data is located in Appendix V.

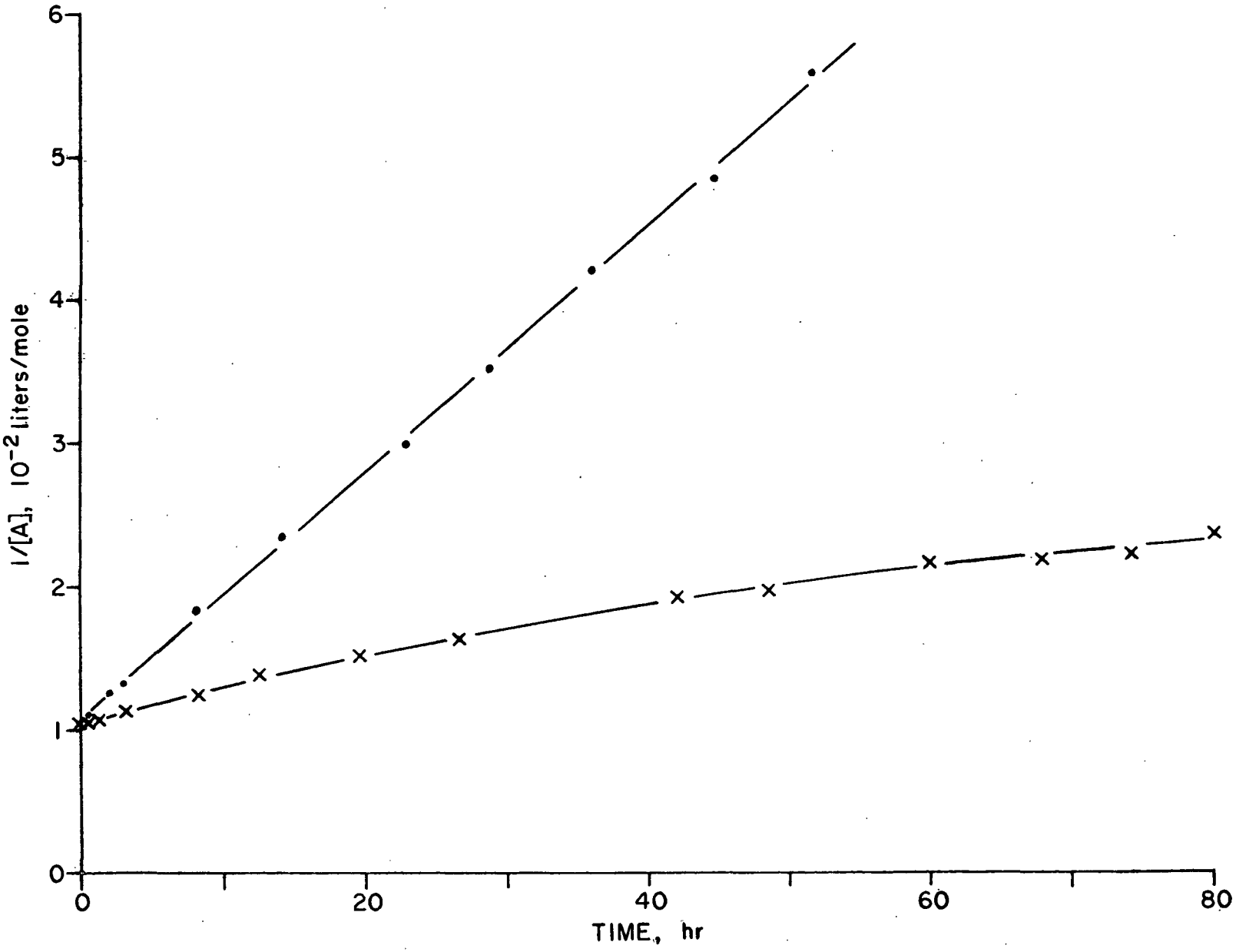

Figure 8. Degradation of 0.01N 1,5-Anhydroxylitol (x - 3 AX) and 0.01N 1,5-Anhydroribitol (o - 3 AR) in 1.25N NaOH at 120°C and 75 PSI O_2 (25°C). Data Plotted According to the Method of Integration Assuming a Carbohydrate Reaction Order of 2.0

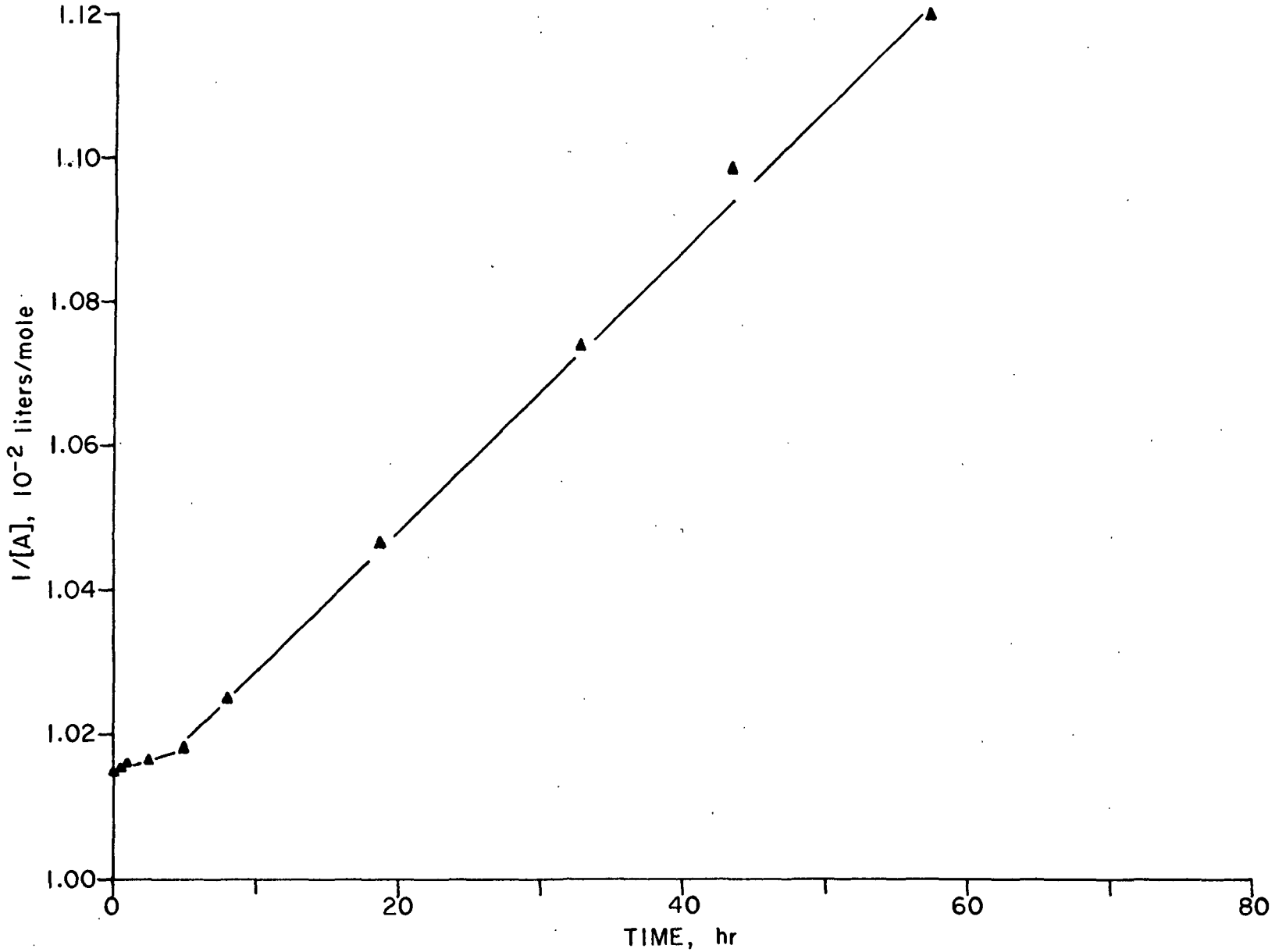

Figure 9. Degradation of 0.01N 3-O-Methyl-1,5-anhydroxylitol (Δ - 1 MAX) in 1.25N NaOH at 120°C and 75 PSI O_2 (25°C). Data Plotted According to the Method of Integration Assuming a Carbohydrate Reaction Order of 2.0

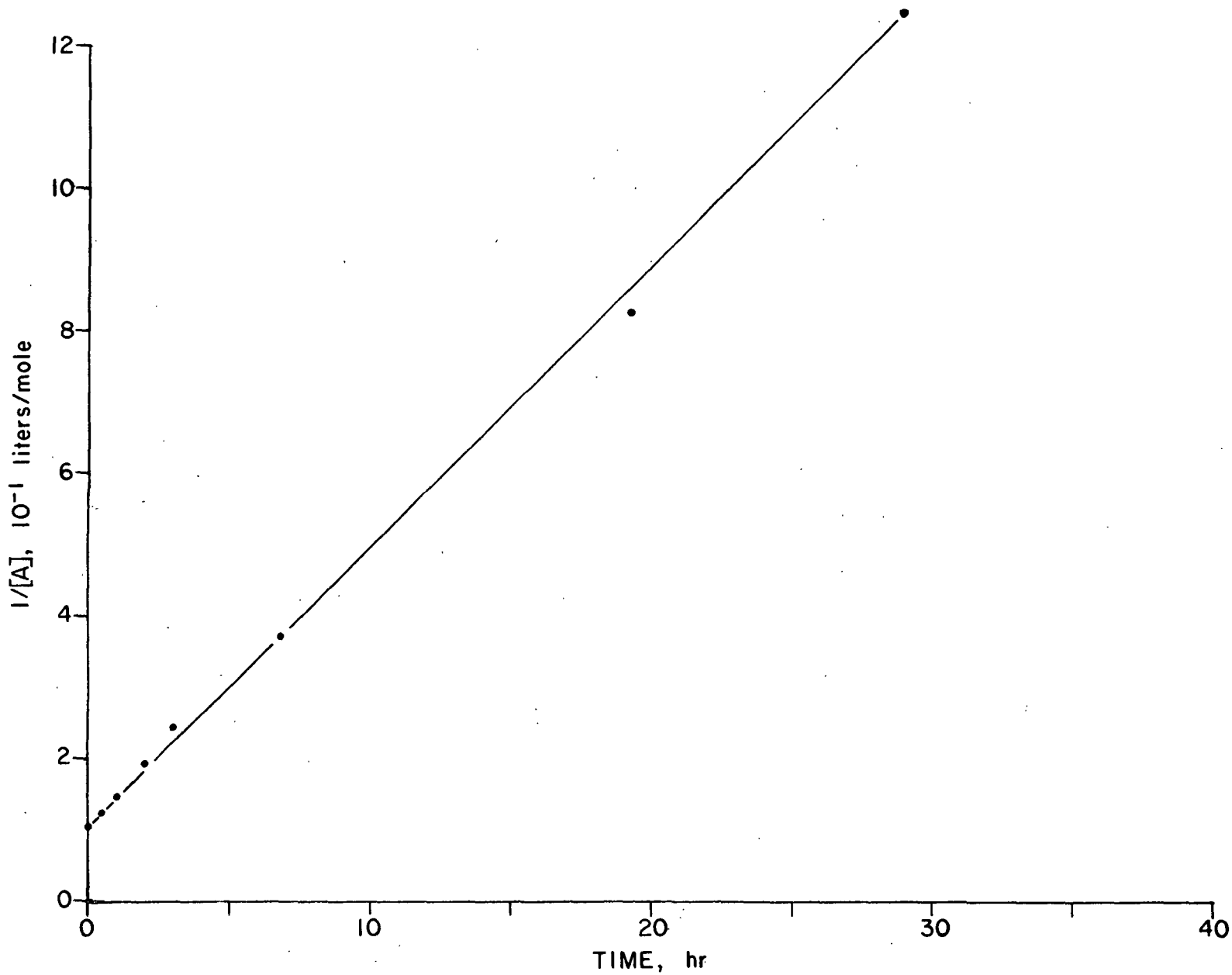

Figure 10. Degradation of 0.1N 1,5-Anhydroribitol (● - 5 AR) in 1.25N NaOH at 120°C and 75 PSI O_2 (25°C). Data Plotted According to the Method of Integration Assuming a Carbohydrate Reaction Order of 2.0

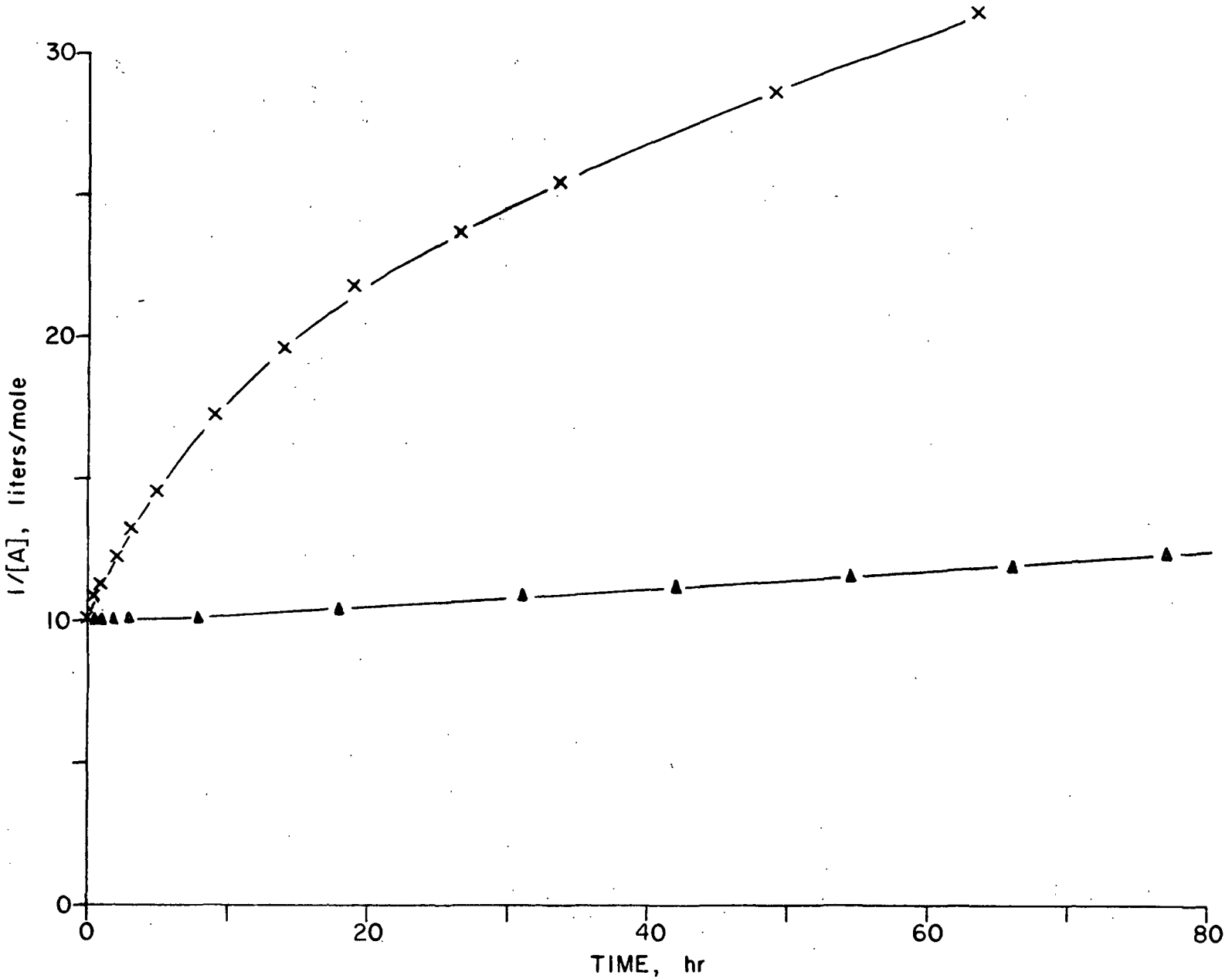

Figure 11. Degradation of 0.1N 1,5-Anhydroxylitol (x - 5 AX) and 0.1N 3-O-Methyl-1,5-anhydroxylitol (Δ - 2 MAX) in 1.25N NaOH at 120°C and 75 PSI O_2 (25°C). Data Plotted According to the Method of Integration Assuming a Carbohydrate Reaction Order of 2.0

Thus, analysis by the method of integration indicates that the order of the AR and MAX reactions with respect to alditol is two while AX exhibits a more complex relationship.

Analysis by the Differential Method

Figures 12 and 13 illustrate application of the differential method of analysis to the degradation data for AX and AR at 0.01 and 0.1N carbohydrate, respectively. The low percentage of MAX reacted under the conditions studied (Fig. 5 and 6) made an accurate determination of order by this method impossible. The data for AR yielded straight lines of slope (order) 2.08 and 2.02 for the 0.01 and 0.1N concentration levels, respectively. The orders of the AX reactions for these concentrations were 3.03 and 3.46, respectively, going to higher values at early reaction times (higher concentration).

Summary

Analysis of the kinetic data by the method of integration and the differential method indicates that the AR reaction is second order in carbohydrate while the AX reaction has an apparent higher order. In addition, the order of the AX reaction with respect to the carbohydrate increases at early reaction times. A possible explanation for this phenomenon is that the order in carbohydrate with respect to time (method employed in the present investigation) in the AX system is greater than the order with respect to concentration (true order). As the reaction proceeds, the rate of reaction decreases more rapidly than it would if the true order were applicable to the entire course of the reaction. Such a situation manifests itself in an apparent higher order reaction with respect to carbohydrate. This abnormally large decrease in the rate of reaction indicates that some intermediate in the reaction is acting as an inhibitor (28). In addition, the inhibitor must be effective only in the AX, and not the AR, system if this explanation is to account for the differences in the kinetics of the degradation of the model compounds.

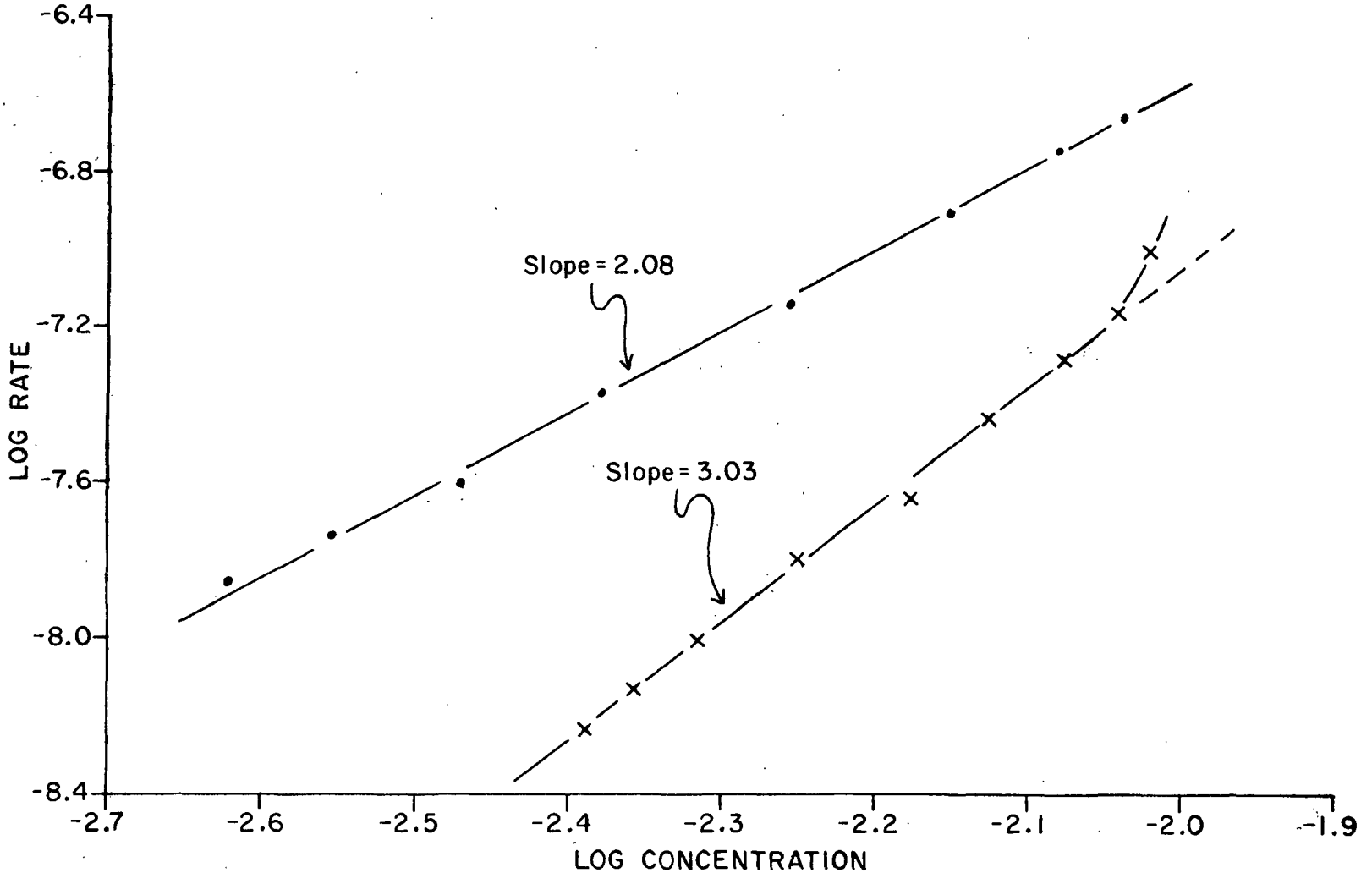

Figure 12. Degradation of 0.01N 1,5-Anhydroribitol (● - 3 AR) and 0.01N 1,5-Anhydroxylitol (x - 3 AX) in 1.25N NaOH at 120°C and 75 PSI O_2 (25°C). Data Plotted According to the Differential Method

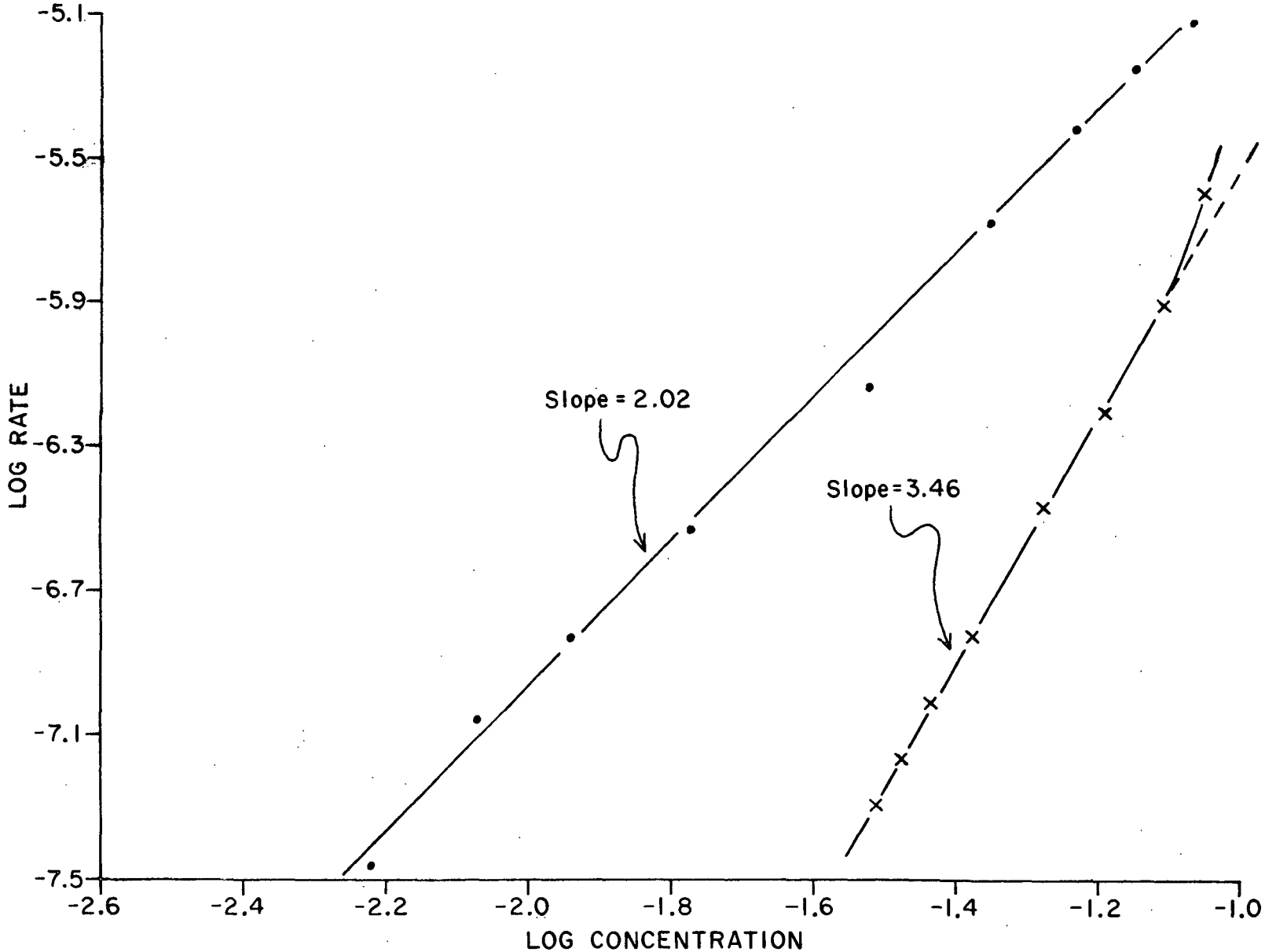

Figure 13. Degradation of 0.1N 1,5-Anhydroribitol (o - 5 AR) and 0.1N 1,5-Anhydroxylitol (x - 5 AX) in 1.25N NaOH at 120°C and 75 PSI O_2 (25°C). Data Plotted According to the Differential Method

No definite conclusions concerning the MAX reaction order could be reached. Although the method of integration indicates the reactions to be second order, this method is not always sensitive enough to reflect complications such as autoinhibition.

PRODUCTS

PEROXIDES

General

The concentration of peroxides (hydrogen peroxide and organic peroxides) was determined by a modified colorimetric method adapted from the work of previous investigators (30-32). The procedure is based on the formation of a titanium(IV) complex with hydrogen peroxide. Organic peroxides with relatively good acid stability (pH 1-2) respond to the titanium reagent only after they are hydrolyzed to hydrogen peroxide. Therefore, hydrogen peroxide which complexes rapidly can be differentiated from organic peroxides which must first hydrolyze to form hydrogen peroxide by measuring the change in absorbancy with time. The colorimetric test for hydrogen peroxide has a precision of ca. $\pm 1 \times 10^{-5}$M, an accuracy of ca. $\pm 2 \times 10^{-5}$M, and a lower sensitivity limit of 2×10^{-5}M. The extent of hydrolysis of the organic peroxides to hydrogen peroxide is not known. The organic peroxides may also undergo decomposition reactions other than hydrolysis. Therefore, the colorimetric test probably gives a low estimate of the organic peroxide concentration.

Hydrogen Peroxide

Hydrogen peroxide analyses were performed in conjunction with all kinetic experiments using 0.1N carbohydrate*. At 0.01N carbohydrate, the level of hydrogen peroxide was too low to detect. Duplicate trials on AX and AR at 0.1N carbohydrate showed similar hydrogen peroxide patterns.

*Experimental data are given in Appendix V, Tables XXIV-XXVI.

The stability of hydrogen peroxide in solution is greatly affected by impurities, especially trace metal ions (19,21,33-36). Reactions 5AX, 5AR, and 2MAX were the only trials in which metal ion determinations were taken (Appendix V, Table XXVII) and since the levels of the various metal ions in the three reactions were essentially the same, these reactions were used to compare hydrogen peroxide formation in the three model systems.

Figures 14, 15, and 16, respectively, illustrate formation of hydrogen peroxide in the degradation of AX, AR, and MAX at 0.1N carbohydrate. The hydrogen peroxide concentrations reached a maximum early in the reaction and subsequently decreased to a low level, similar to methyl β-D-glucopyranoside (19). The rates of hydrogen peroxide production decreased in the order AR>AX> MAX. The maximum hydrogen peroxide concentration in the AR system was approximately twice that in the AX reaction, which, in turn, was approximately twice the level in the MAX system. McCloskey (18) concluded that the maximum concentration of hydrogen peroxide formed during the degradation of carbohydrate by molecular oxygen in alkaline media is a function of the number of hydroxyl groups present on the ring. This possibly accounts for some of the difference in maxima in the AX and MAX systems. An explanation for the large difference between the AX and AR systems is postulated in the Mechanism section.

Previous investigators (17,19) have postulated that a direct relationship exists between hydrogen peroxide build-up and the induction period during the alkaline oxygen degradation of carbohydrates. In his work with methyl β-D-glucopyranoside, Sinkey (19) demonstrated that during the induction period, the slow degradation of glycoside in the magnesium-stabilized system corresponded very well with the increase in the hydrogen peroxide concentration. In addition, there was a correlation between the maximum hydrogen peroxide concentration and the end of the induction period. However, Sinkey also showed that

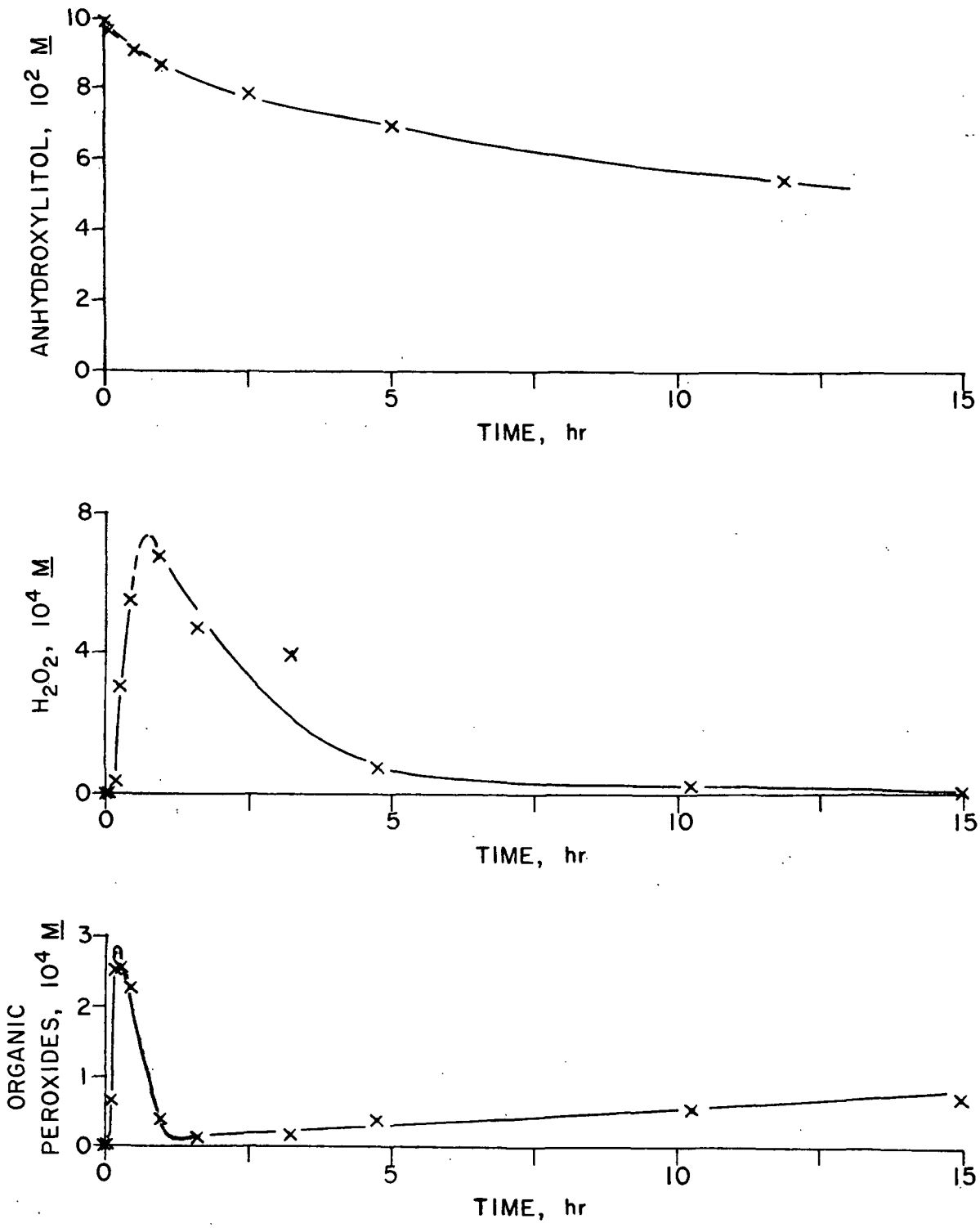

Figure 14. The Production of Peroxides During the Degradation of 0.1N 1,5-Anhydroxylitol (5 AX) in 1.25N NaOH at 120°C and 75 PSI O_2 (25°C)

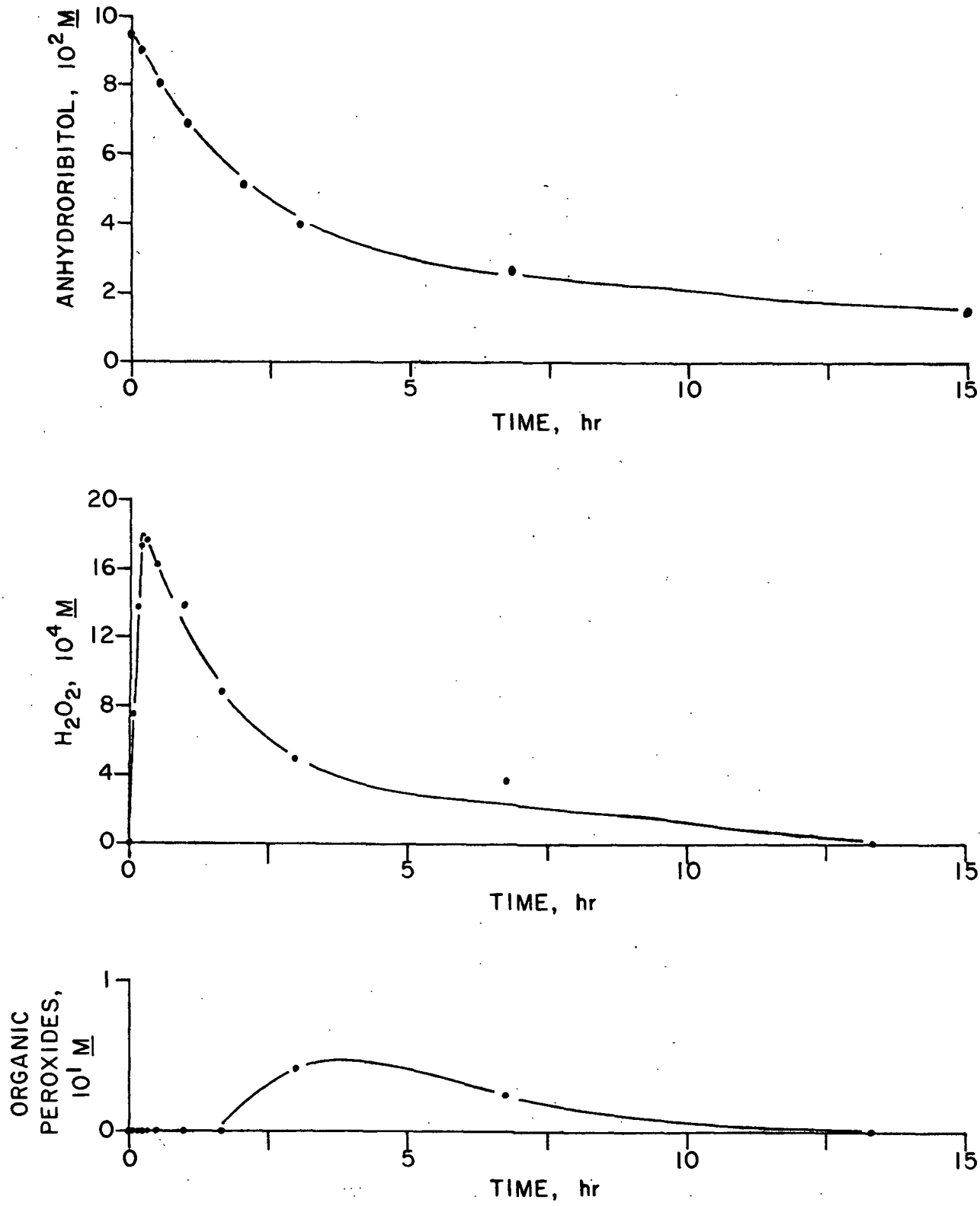

Figure 15. The Production of Peroxides During the Degradation of 0.1N 1,5-Anhydroribitol (5 AR) in 1.25N NaOH at 120°C and 75 PSI O_2 (25°C)

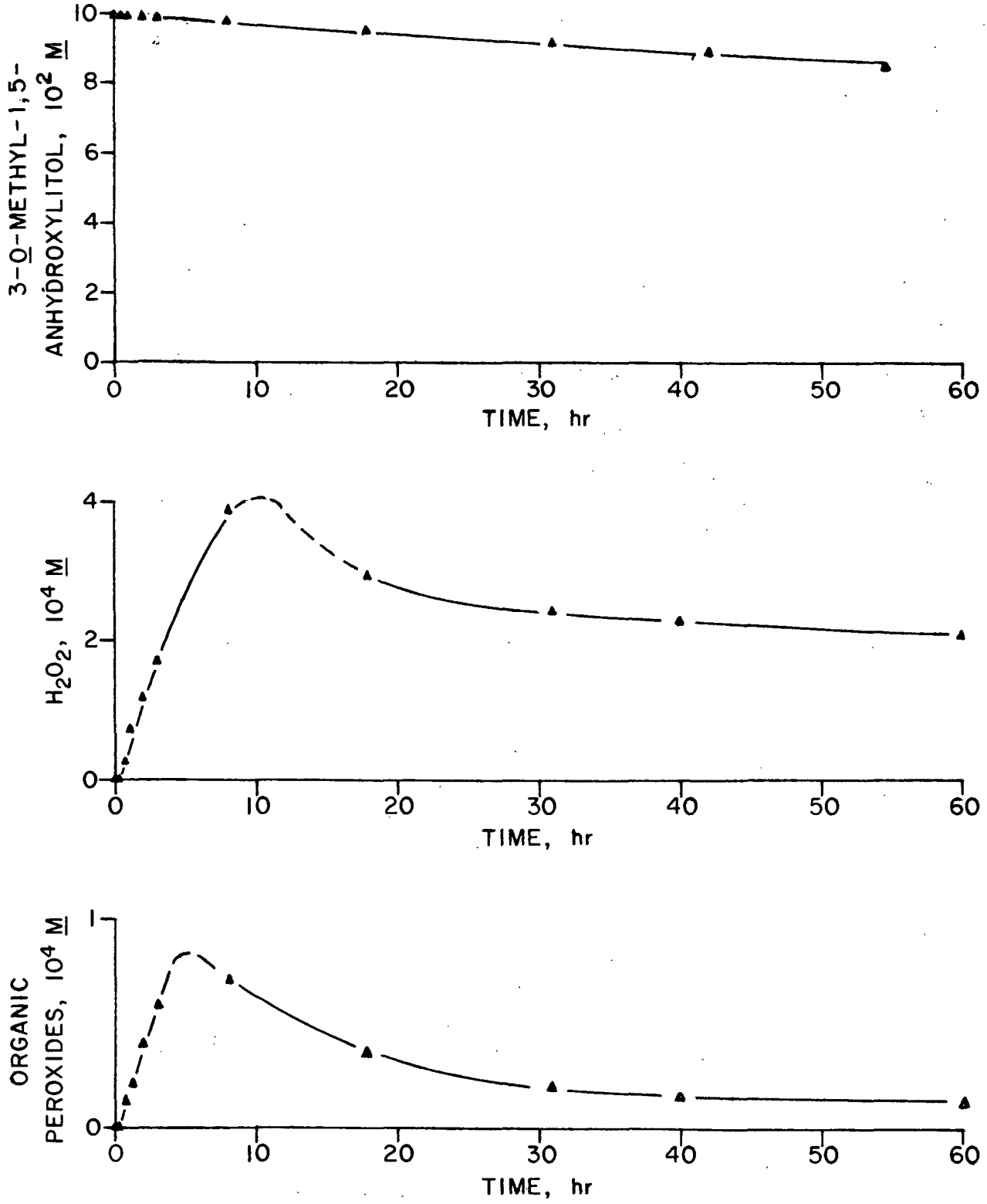

Figure 16. The Production of Peroxides During the Degradation of 0.1N 3-O-Methyl-1,5-anhydroxylitol (2 MAX) in 1.25N NaOH at 120°C and 75 PSI O_2 (25°C)

the length of the induction period of both unstabilized and stabilized methyl β-D-glucopyranoside reactions was extremely variable. In the unstabilized reactions, the postinduction period began before the maximum hydrogen peroxide concentration was reached.

These observations are consistent with the experimental data from the present investigation. No reactions were intentionally stabilized. For the AX and AR systems, the induction periods ranged from 0 to ca. 45 minutes. MAX showed 5-6 hour induction periods (Fig. 7). Postinduction periods always began before the maximum hydrogen peroxide concentration was reached. Where induction periods were evident (Fig. 7), they seemed to be characterized by a slow degradation of the carbohydrate.

Organic Peroxides

Along with hydrogen peroxide, the concentration of organic peroxides was also determined for all kinetic experiments at 0.1N carbohydrate*. At initial alditol concentrations of 0.01N, the level of organic peroxides was too slow to detect. For the reasons discussed previously, only the reactions in which metal ion determinations were taken were used as a basis for comparison between the three model systems.

Figures 14, 15, and 16 also illustrate the formation of organic peroxides in the degradation of AX, AR, and MAX at 0.1N carbohydrate, respectively. No detectable organic peroxides were found in the AR reaction at early reaction times. At later reaction times (after 2 hours), some organic peroxides seem to be forming but the results are inconclusive. However, the AX and MAX systems showed organic peroxide curves similar to their hydrogen peroxide patterns. That is, an initial rise in the concentration to a maximum value followed by a decrease.

*Tabulated experimental data are given in Appendix V, Tables XXIV-XXVI.

This is the first investigation in which a reactive organic peroxide has been reported during the degradation of a carbohydrate by molecular oxygen in alkaline media. In his work with the alkaline hydrogen peroxide degradation of methyl β-D-glucopyranoside, Weaver (21) found evidence for an organic peroxide intermediate (postulated to be an alpha-hydroxyhydroperoxide) which behaved in a manner similar to the organic peroxide in the present investigation. As stated previously, the inhibitor accounting for the difference in kinetics between the AX and AR systems must be effective only in the AX reaction. The organic peroxides detected here have a curve indicative of a reactive intermediate and could be the cause of the autoinhibition in the AX reaction.

Identity of the Organic Peroxide Intermediate

The organic peroxides detected in the present investigation hydrolyzed to hydrogen peroxide in the presence of sulfuric acid (pH 1). The maximum absorbance resulting from the hydrogen peroxide-titanium complex occurred at 20-28 hours. Dialkyl peroxides (ROOR) are known to hydrolyze slowly to hydrogen peroxide under acidic conditions (37). Hydroperoxides also hydrolyze slowly at ca. pH 1 (21)*. Marklund (32) used the procedure to distinguish hydroperoxides from hydrogen peroxide. Therefore, based on hydrolysis behavior alone, the organic peroxides detected in the present investigation could be hydroperoxides and/or dialkyl peroxides. The concentration of organic peroxides attained by this method is probably a low estimate because the extent of hydrolysis to hydrogen peroxide is unknown. Also, organic peroxides undergo decomposition reactions other than hydrolysis.

Although the structure of the organic peroxide intermediate is not known, it is thought to be an alpha-hydroxyhydroperoxide because of the following:

*t-Butylhydroperoxide took 18-24 hours to form the maximum color complex.

1. Hydroperoxides such as cyclohexanone hydroperoxides (19) and t-butylhydroperoxide (21) hydrolyze slowly at ca. pH 1 to form hydrogen peroxide, similar to the intermediate peroxide.
2. Alpha-hydroxyhydroperoxides are considered plausible intermediates in autoxidation reactions of organic compounds in general (38,39). They are also considered plausible intermediates in the autoxidation of cellulose (40) and the alkaline oxygen degradation of cellulose (5) and methyl β-D-glucopyranoside (41), as well as the oxidation of ethanol (42).
3. Alpha-hydroxyhydroperoxides can potentially account for the difference in the reaction kinetics of the AX and AR systems as discussed in the Mechanism section.

Stable Dialkyl Peroxides

The formation of organic peroxides in the AX reaction (Fig. 14) can be rationalized as a rapid production and subsequent degradation of alpha-hydroxy-hydroperoxides in conjunction with a slow build-up of dialkyl peroxides. Thompson, et al. (25) proposed the formation of dialkyl peroxides in the degradation of methyl α- and β-D-glucopyranosides by molecular oxygen in alkali to account for the observed rise in the level of organic peroxides at long reaction times. The formation of dialkyl peroxides can be viewed as a radical termination reaction (43,44).

$$ROO\bullet + R\bullet \longrightarrow ROOR \qquad (6)$$

where ROO• = alpha-hydroxyhydroperoxy free radical

R• = alpha-hydroxy alkyl free radical

In the AR reaction (Fig. 15), some dialkyl peroxides may be forming at extended reaction times. However, since the level of organic peroxides indicated is so close to the lower limit of sensitivity (2×10^{-5}M) of the colorimetric test, the results are inconclusive. The MAX system (Fig. 16) showed no rise in the organic peroxide curve at long reaction times.

CARBOXYLIC ACIDS

Summary of Acidic Products

Acidic reaction products formed in the degradation of carbohydrates by molecular oxygen in alkaline media are believed to arise from formation of keto-derivatives which subsequently degrade by various pathways to the acids (12, 19,20,45-47). These products are aldonic acids, methyl 2-C-carboxy-pentofuranosides, and dibasic acids, depending on the starting material.

The acidic products identified in degradations of AX and AR were identical and are reported in Table I; products of MAX degradations are reported in Table II. Figures 17, 18, and 19 show gas chromatograms of the acidic reaction products from degradations of AX (64% reaction of AX), AR (71% reaction of AR), and MAX (22% reaction of MAX), respectively. Similar chromatograms were obtained from analyses of product mixtures from either 0.1 or 0.01N initial carbohydrate. In addition to the products shown, formic and acetic acids were identified by GLC as their benzyl esters in the AX and AR reaction mixtures; formic acid and only a trace of acetic acid were found in the MAX system.

Although the AX and AR acidic reaction products were identical, they were formed in different ratios. Although the relative ratios of products in the AX and AR reactions changed with time (see Semiquantitative Product Analysis, etc.), no acidic product was identified that could account for the difference in reaction kinetics of the two systems. This is consistent with the postulate

TABLE I

AX AND AR DEGRADATION PRODUCTS

Reaction Product	Method of Identification[a]	Compound Identification
1	MS, R	Lactic acid
2	MS, R	Glycolic acid
3	MS	3-Hydroxypropanoic acid
4	MS	2-Hydroxybutyric acid
5	MS, R	Glyceric acid
6	MS, R	2,3-Dihydroxybutyric acid
7	MS	2,4-Dihydroxybutyric acid
8	--	Unknown
9 and 10	MS	Isomeric mixture of 1,4-anhydro-2-C-carboxy-tetritols
11	MS	3-O-Carboxymethyl-glyceric acid

[a]MS = identified by mass spectrometry.
R = identified by relative retention times compared to authentic samples.

TABLE II

MAX DEGRADATION PRODUCTS

Reaction Product	Method of Identification[a]	Compound Identification
1	R	Lactic acid
2	R	Glyceric acid
3	MS	3-Hydroxy-2-methoxybutyric acid

[a]MS = identified by mass spectrometry.
R = identified by relative retention times compared to authentic samples.

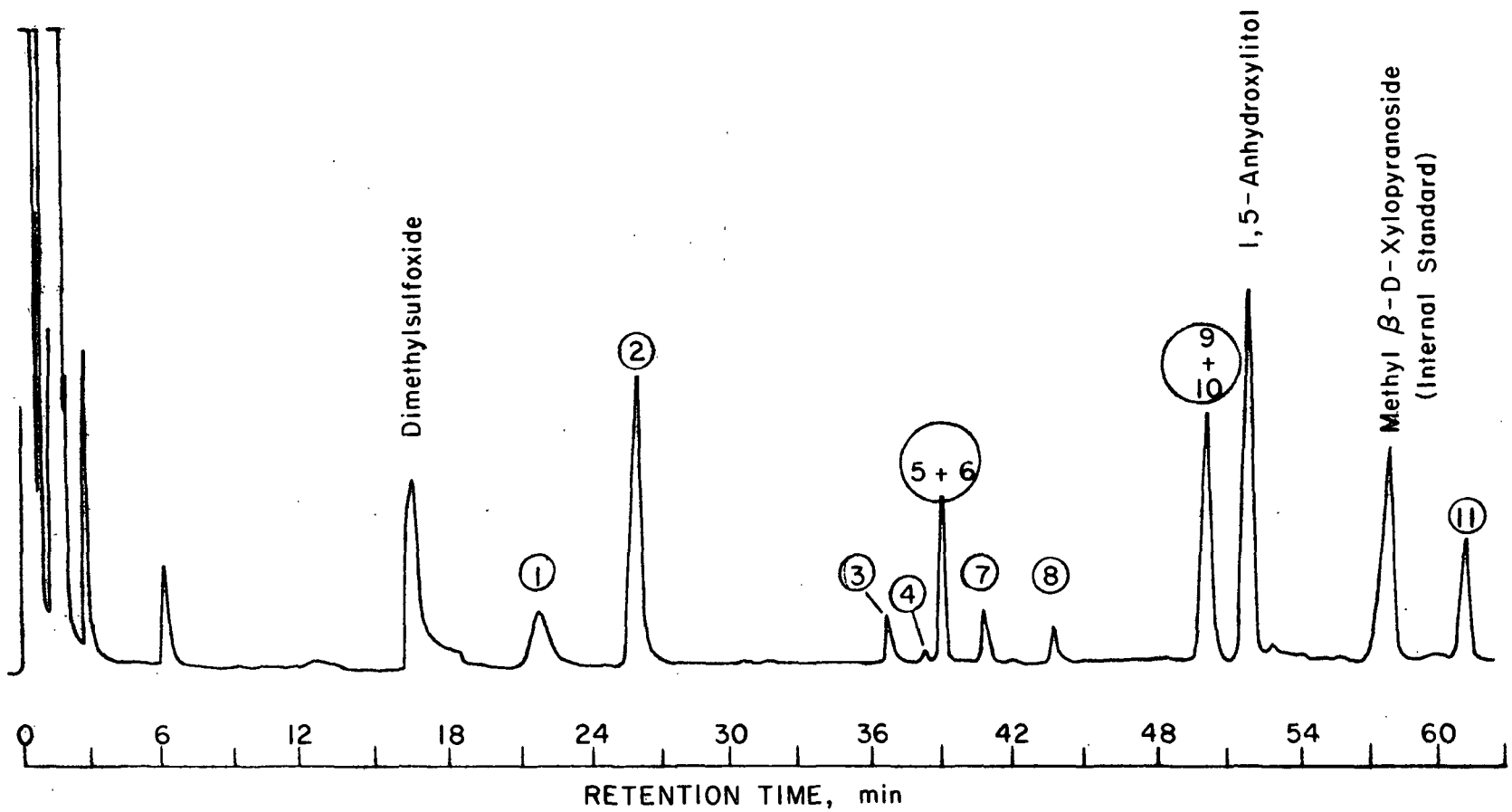

Figure 17. Sample Chromatogram of the Degradation Products of 1,5-Anhydroxylitol (5 AX - 64% Reaction of AX). For Product Identification by Number, see Table I

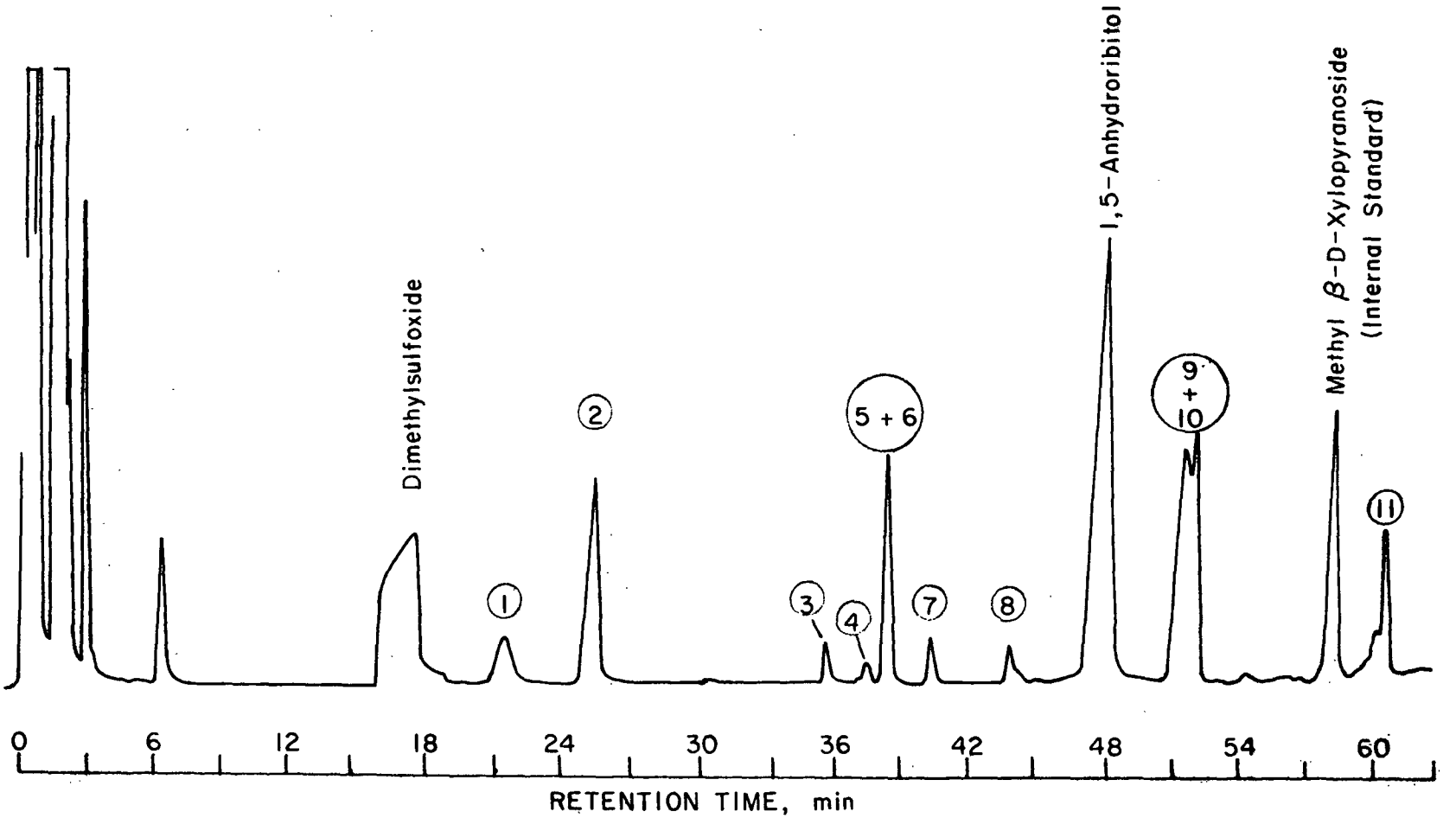

Figure 18. Sample Chromatogram of the Degradation Products of 1,5-Anhydroribitol (5 AR - 71% Reaction of AR). For Product Identification by Number, see Table I

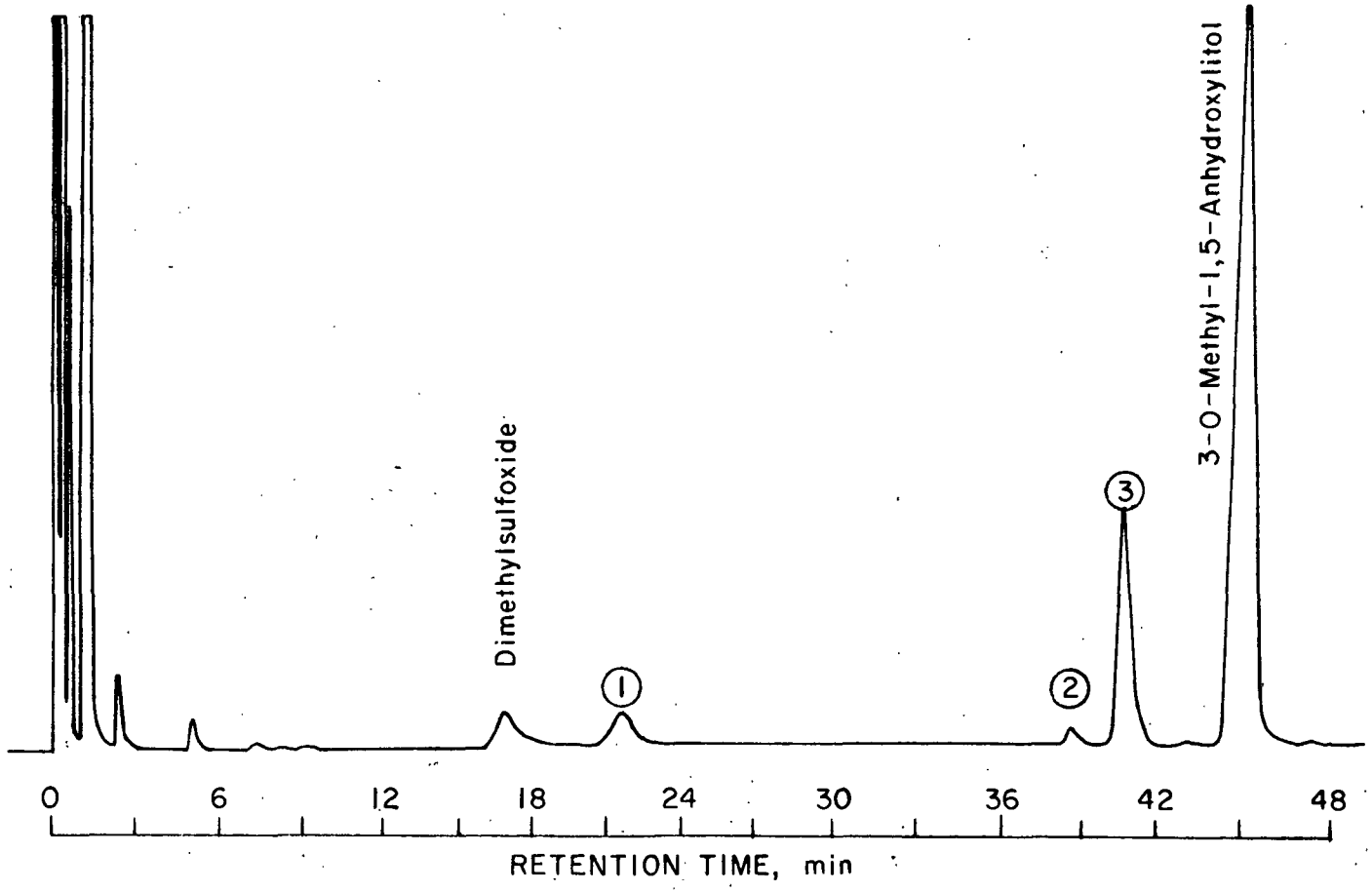

Figure 19. Sample Chromatogram of the Degradation Products of 3-O-Methyl-1,5-anhydroxylitol (2 MAX - 22% Reaction of MAX). For Product Identification by Number, see Table II

that the intermediate organic peroxide (thought to be an alpha-hydroxyhydroperoxide) discussed earlier is responsible for the autoinhibition in the AX system.

Figure 19 shows that the major product of the degradation of MAX was 3-hydroxy-2-methoxybutyric acid. This is the analog of 2,3-dihydroxybutyric acid in the AX and AR reactions. Several minor products were also formed in the MAX reaction. From GLC retention times alone, Compounds 1 and 2 could be lactic and glyceric acids, respectively. Since the relative quantities of these products were so small, their formation does not constitute a major pathway in the MAX reaction mechanism and will not be discussed further.

Product Identification

Identification Techniques

Gas-liquid chromatography-mass spectrometry (GLC-MS) was the major tool used in identifying the per-O-trimethylsilyl (TMS) derivatives of the acidic products from degradations of the three anhydroalditols. In discussion of GLC-MS results, the chemical names used denote either the actual compounds or their TMS derivatives. The complex mixtures of reaction products (AX and AR systems) were readily separated and analyzed by this method. Where possible, reference data and/or authentic samples were used for comparison. GLC conditions and mass spectrometer control settings are given in Appendix IV. GLC alone was used to identify formic and acetic acids (benzyl esters) as reaction products by comparing their retention times to those of authentic samples. GLC conditions are given in Appendix II, Table V.

Reaction Products

Product numbers refer to Figs. 17, 18, and 19 for AX, AR, and MAX reactions, respectively. AX and AR reaction Products ①, ②, ③, and ⑦ were

identified as lactic, glycolic, 3-hydroxypropanoic, and 2,4-dihydroxybutyric acids, respectively. Their mass spectra are illustrated in the upper portion (labeled A) of Fig. 20-23. Below each mass spectrum is a reference spectrum (labeled B) of the same compound. GLC retention times of authentic samples were also used to verify the identity of lactic and glycolic acids in the reaction mixtures.

AX and AR Products ⑤ and ⑥ were identified as glyceric and 2,3-dihydroxybutyric acids, respectively. The presence of 2,3-dihydroxybutyric acid was not readily apparent, since this compound had the identical GLC retention time of glyceric acid under all analysis conditions attempted. The mass spectrum of the combination glyceric acid and 2,3-dihydroxybutyric acid peak is given in Fig. 24, Spectrum A. Comparison of the mass spectra of authentic glyceric acid (Fig. 24, Spectrum B; Appendix IV, Table XIX) and authentic 2,3-dihydroxybutyric acid (Fig. 25, Spectrum A; Appendix IV, Table XIX) shows that the fragmentation pattern of the latter includes four fragments not found (or present at less than the 2% relative abundance level) for glyceric acid; namely m/e 321, 220, 202, and 129. These fragments are possibly accounted for by the following:

1. m/e 321 = P^+-15 (CH_3)
2. m/w 220 = McLafferty-type rearrangement (48)

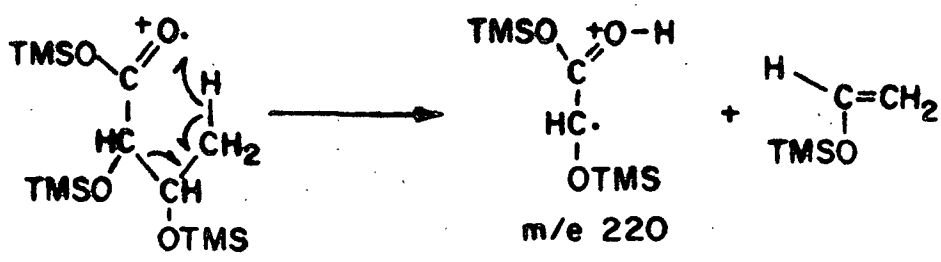

3. m/e 202 = P^+-CO_2-TMSOH
4. m/e 129 = 202-TMS

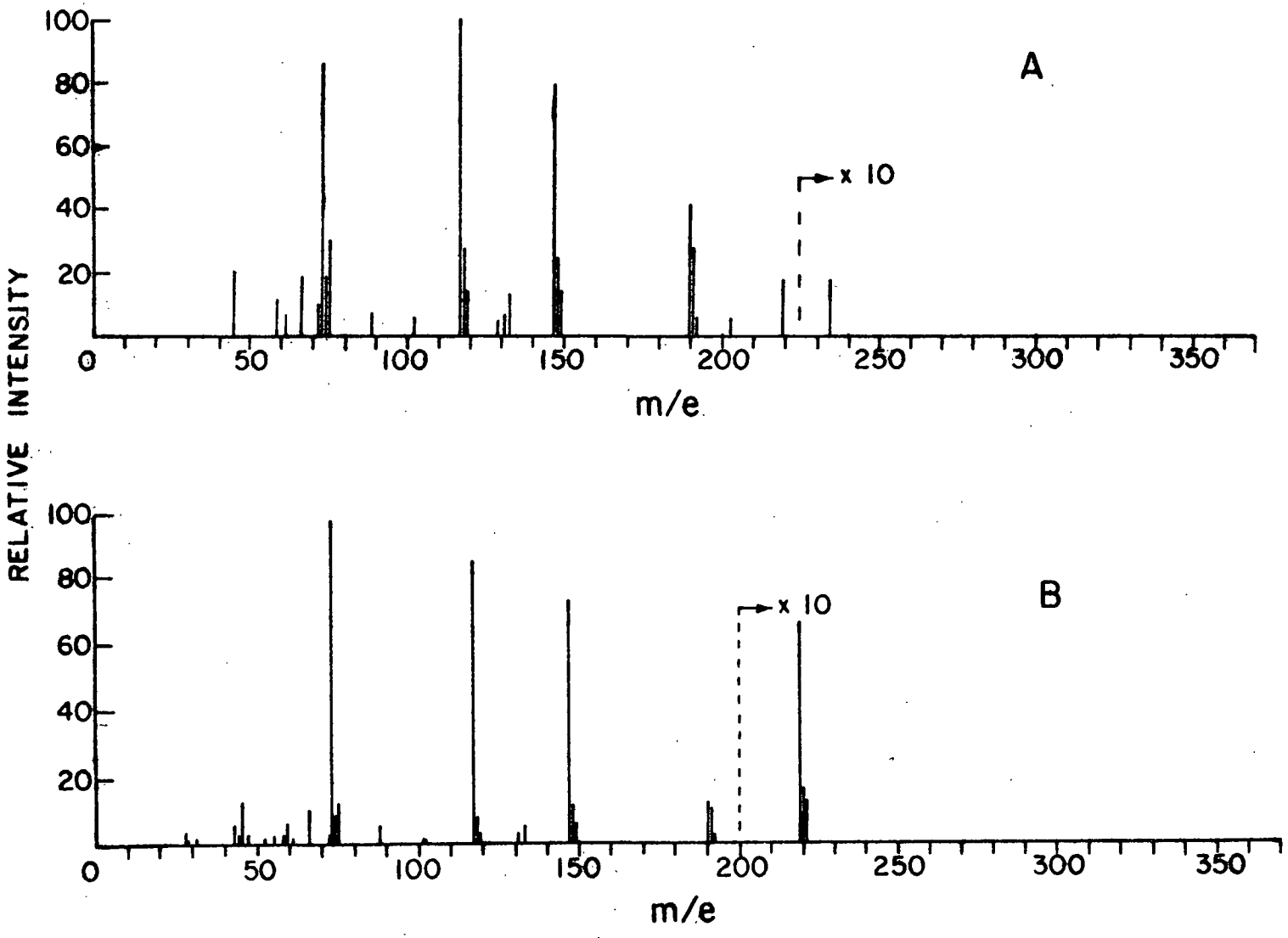

Figure 20. Mass Spectra (70 ev) of the Trimethylsilyl Derivative of Lactic Acid: A - AX and AR Product (1); B - Petersson (48)

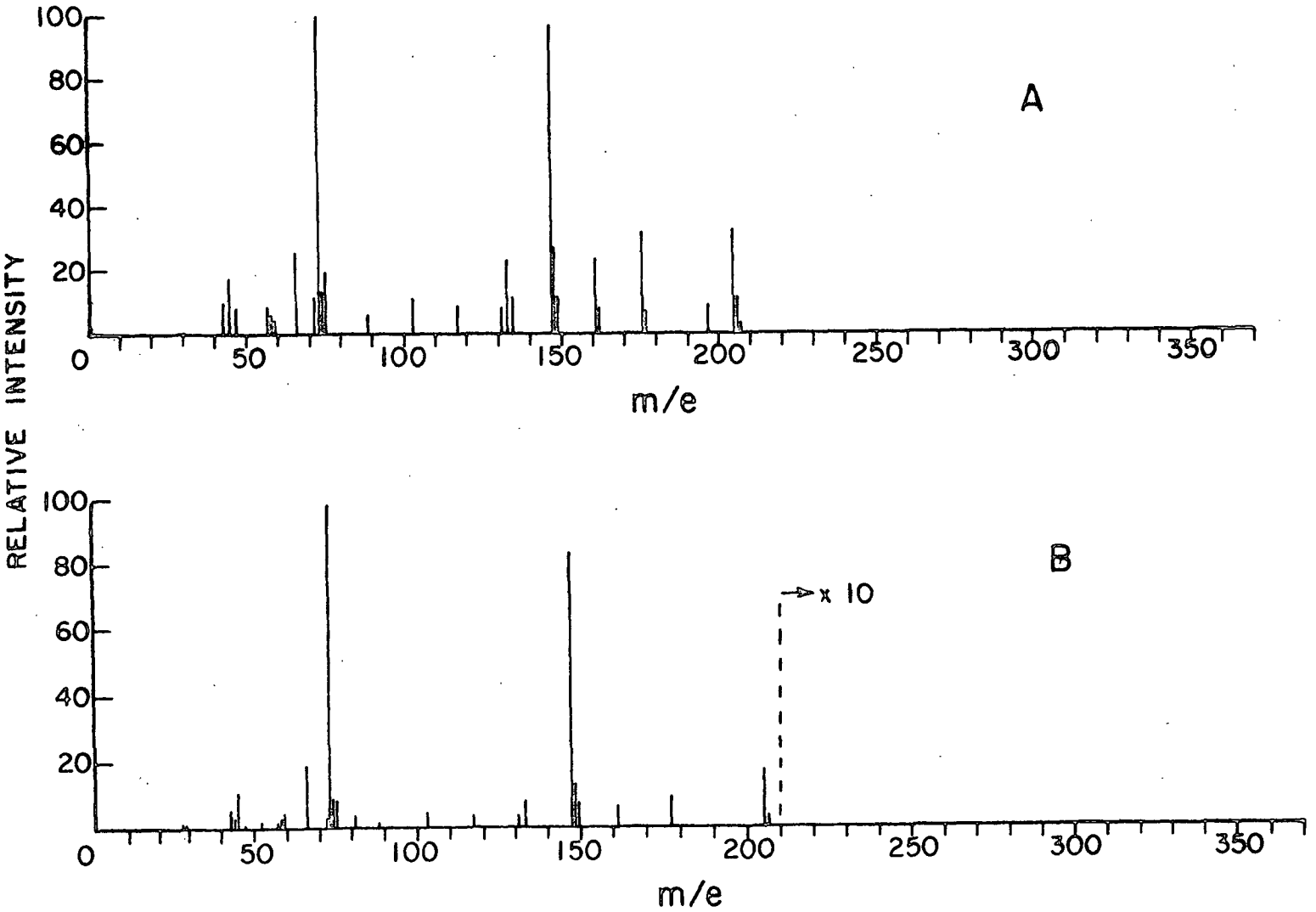

Figure 21. Mass Spectra (70 ev) of the Trimethylsilyl Derivative of Glycolic Acid: A - AX and AR Product (2) ; B - Petersson (48)

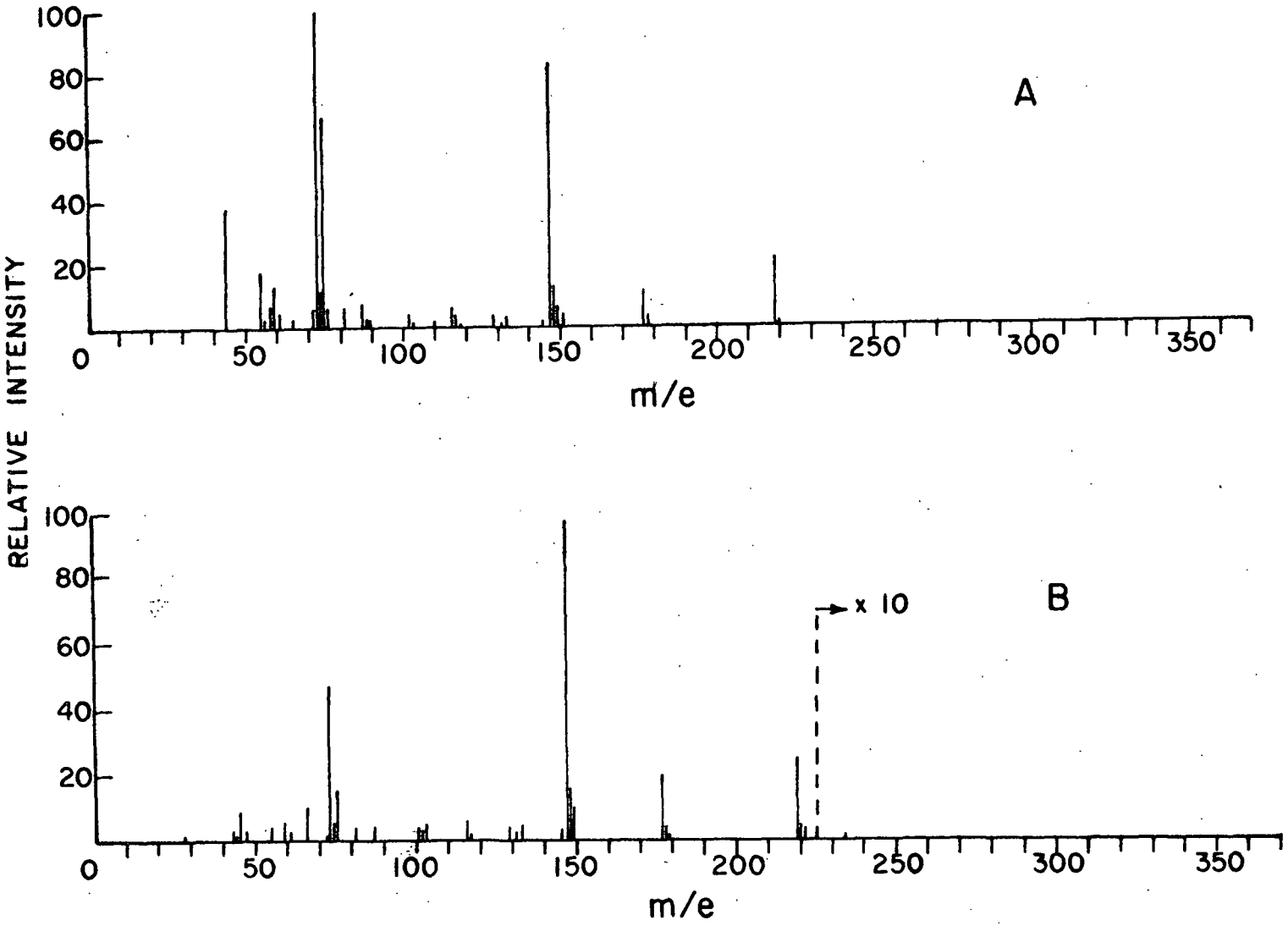

Figure 22. Mass Spectra (70 ev) of the Trimethylsilyl Derivative of 3-Hydroxypropanoic Acid: A - AX and AR Product (3); B - Petersson (48)

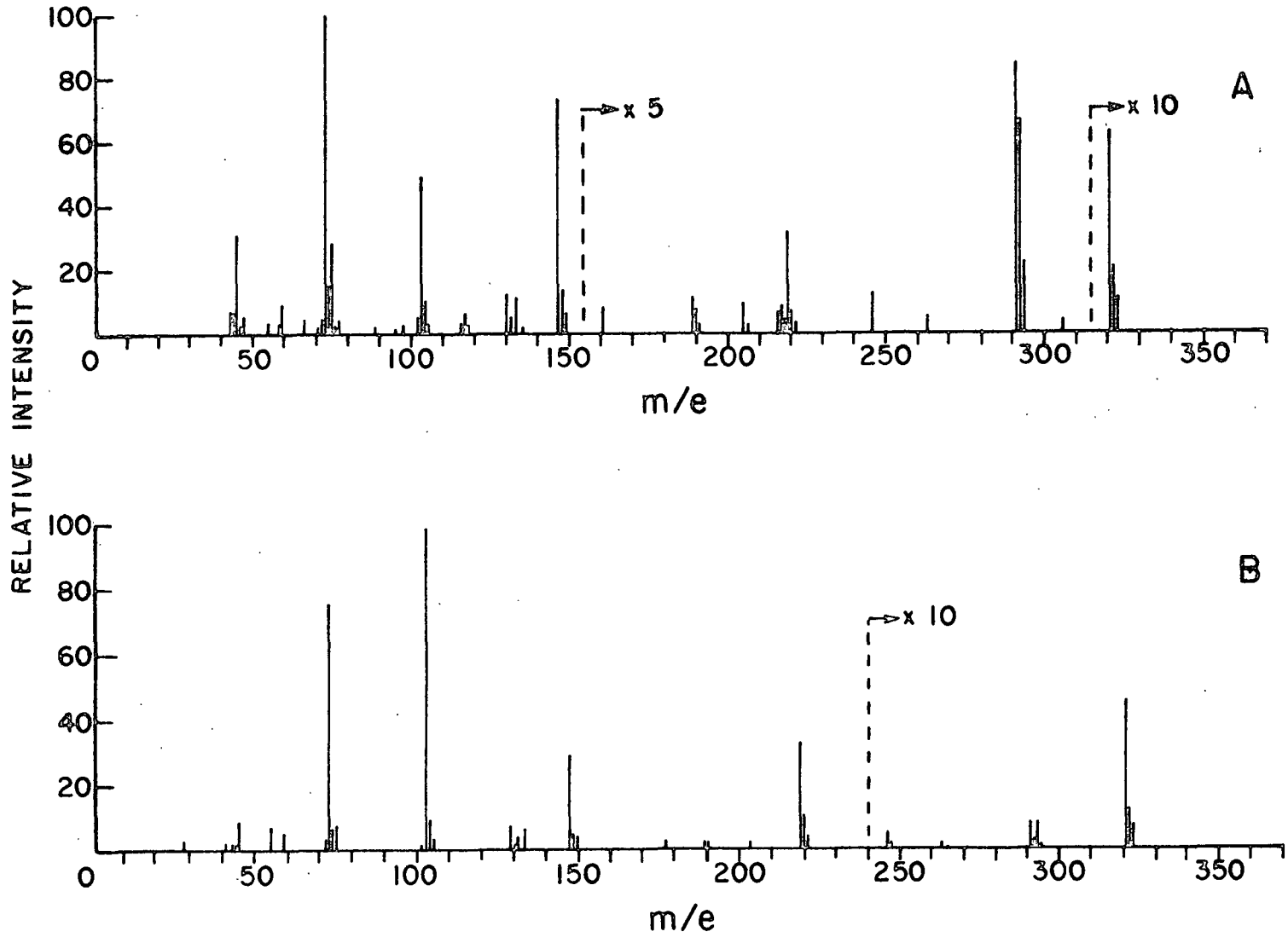

Figure 23. Mass Spectra (70 ev) of the Trimethylsilyl Derivative of 2,4-Dihydroxybutyric Acid: A - AX and AR Product (7); B - Petersson (48)

Although Spectrum A, Fig. 24, appears to be the fragmentation pattern of glyceric acid, a closer look shows the presence of m/e 129 and 220; fragments not found in the spectrum of glyceric acid. This indicates the presence of 2,3-dihydroxybutyric acid in conjunction with glyceric acid in the same GLC peak. The results of the mass spectral analyses performed on the 2,3-dihydroxybutyric acid-glyceric acid peak as a function of percent reaction of AX and AR, respectively, are given in Appendix IV, Tables XIX and XX. The data indicate that 2,3-dihydroxybutyric acid is formed in both systems, reaching a maximum and subsequently degrading to low levels at longer reaction times. This is the first report of 2,3-dihydroxybutyric acid as a reaction product in the degradation of carbohydrates by molecular oxygen in alkaline media. Other systems could produce this compound, but previous investigators may have overlooked it due to the difficulty in separating it from glyceric acid and its relatively low abundance at extended reaction times.

AX and AR Product ④ was identified by GLC-MS as 2-hydroxybutyric acid without aid of a reference spectrum. Because of the relatively small quantity of 2-hydroxybutyric acid produced, the mass spectrum (Fig. 25, Spectrum B) was very weak, especially at high m/e values. Any of the monohydroxybutyric acids would have the same P^+ (m/e 248) and P^+-15 (m/e 233). However, only 2-hydroxybutyric acid accounts for the peak at m/e 219; resulting from carbon-carbon cleavage <u>beta</u> to the carbonyl. Also, the peaks which result from cleavage of the C-1 to C-2 bond (m/e 117 and 131) are usually absent in the 2-deoxyaldonic acids (<u>48</u>).

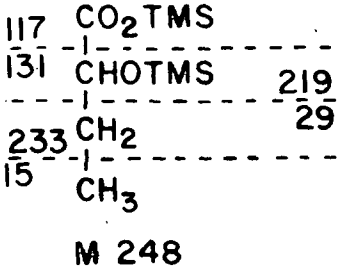

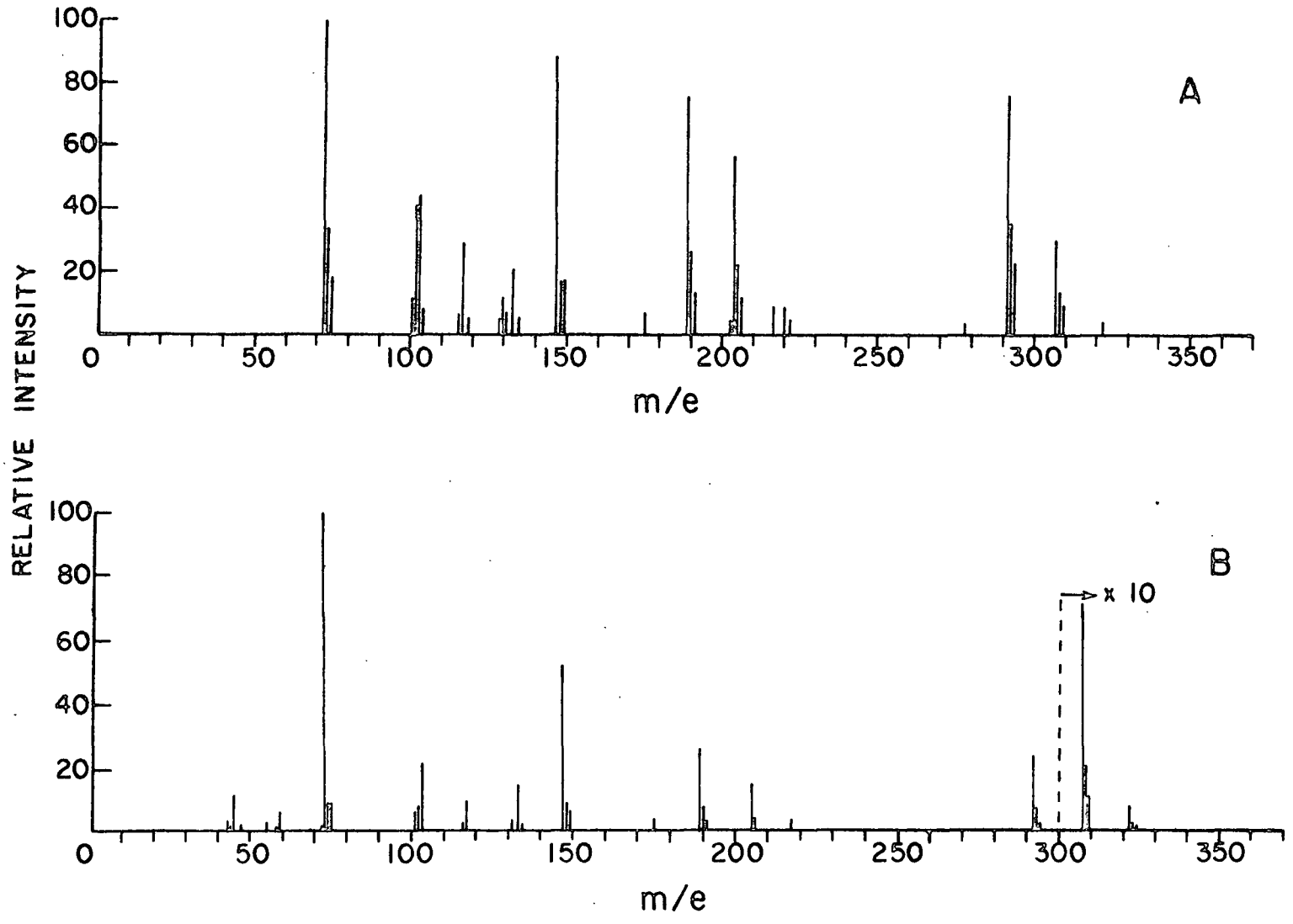

Figure 24. Mass Spectra (70 ev) of Trimethylsilyl Derivatives of: A - Glyceric and 2,3-Dihydroxybutyric Acids (AX and AR Products ⑤ and ⑥; B - Glyceric Acid [Petersson (48)]

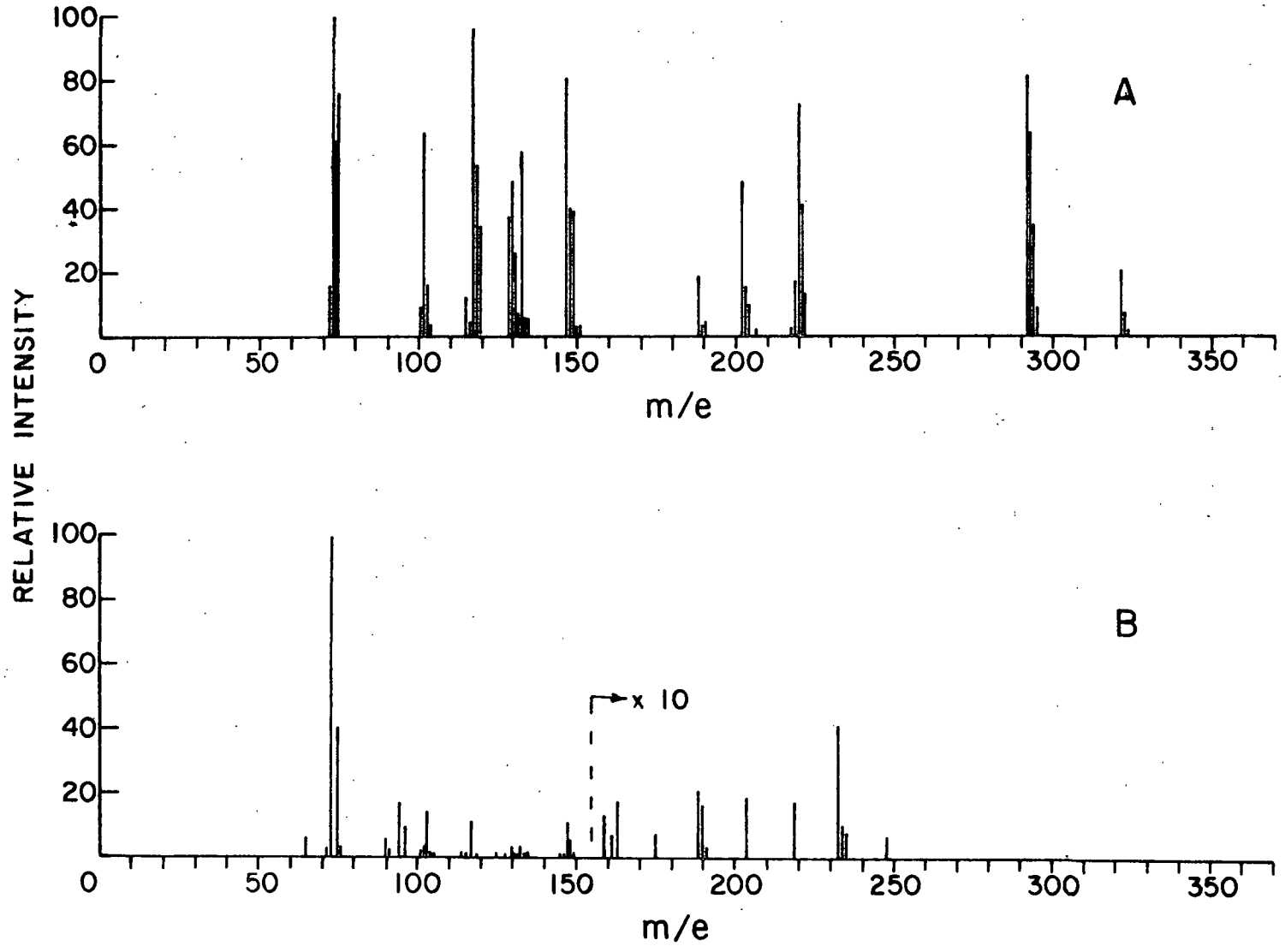

Figure 25. Mass Spectra (70 ev) of Trimethylsilyl Derivatives of 2,3-Dihydroxybutyric Acid (Spectrum A) and 2-Hydroxybutyric Acid (Spectrum B - AX and AR Product (4))

An isomeric mixture of 1,4-anhydro-2-C-carboxy-D-, and -L-, erythritol and threitol was identified as AX and AR Products ⑨ and ⑩ *. The mass spectrum is shown in Fig. 26, Spectrum A. Within the accuracy of the mass spectrometer, spectra taken from Products ⑨ and ⑩ were identical. The P^+ (m/e 364) and P^+-15 (m/e 349) were both present. One of the major diagnostic peaks found at m/e 157 was accounted for by the following:

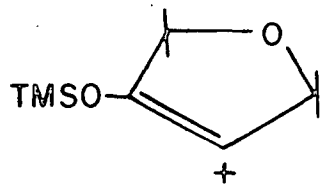

m/e 157

These compounds are the analogs of the methyl 2-C- and 3-C-carboxy-β-D-pentofuranosides reported by Ericsson (20) and Weaver (21) working independently on the degradation of methyl β-D-glucopyranoside in alkali by oxygen and hydrogen peroxide, respectively. Malinen (23) also reported the formation of this type of compound in degradations of various methyl glycosides with oxygen in alkali. In both the AX and AR systems, these compounds accounted for a large percentage of the total reaction over a considerable range of alditol degradation. The 1,4-anhydro-2-C-carboxy-tetritols could form via a benzylic acid-type rearrangement involving a dicarbonyl intermediate as postulated for related compounds (21,24) (Fig. 27).

Another compound which can form via the dicarbonyl intermediate is AX and AR Product ⑪ , identified as 3-O-carboxymethyl-glyceric acid. The compound is formed by the alkali initiated carbon-carbon cleavage between the two carbonyl moieties (see Fig. 41, Mechanism section). The mass spectrum is shown in Fig. 26,

* Although four isomers would be formed, D- and L-enantiomers would not be separated by GLC, resulting in two peaks.

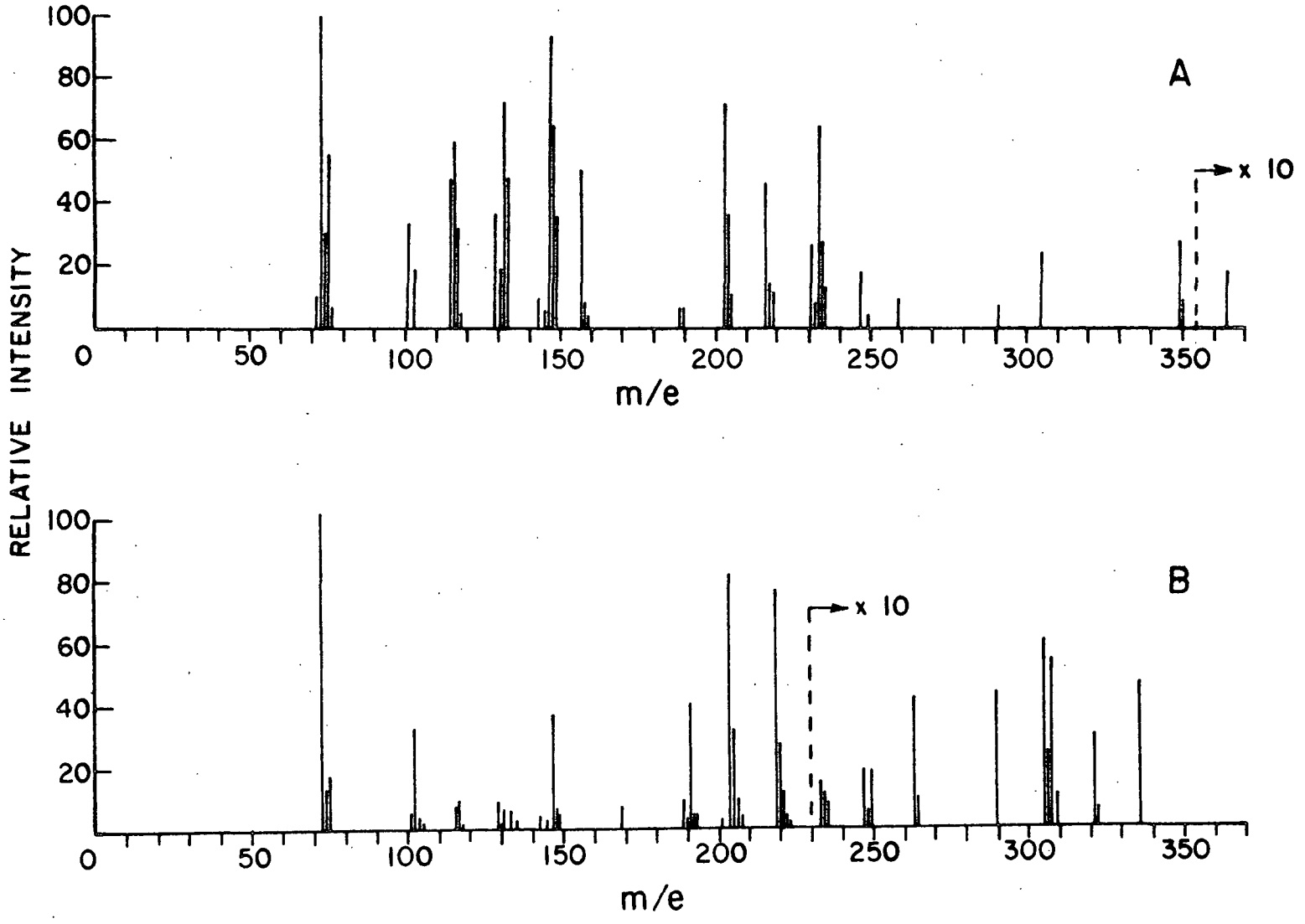

Figure 26. Mass Spectra (70 ev) of the Trimethylsilyl Derivatives of the 1,4-Anhydro-2-C-carboxy-tetritols (Spectrum A - AX and AR Products (9) and (10)) and 3-O-Carboxymethyl-glyceric Acid (Spectrum B - AX and AR Product (11))

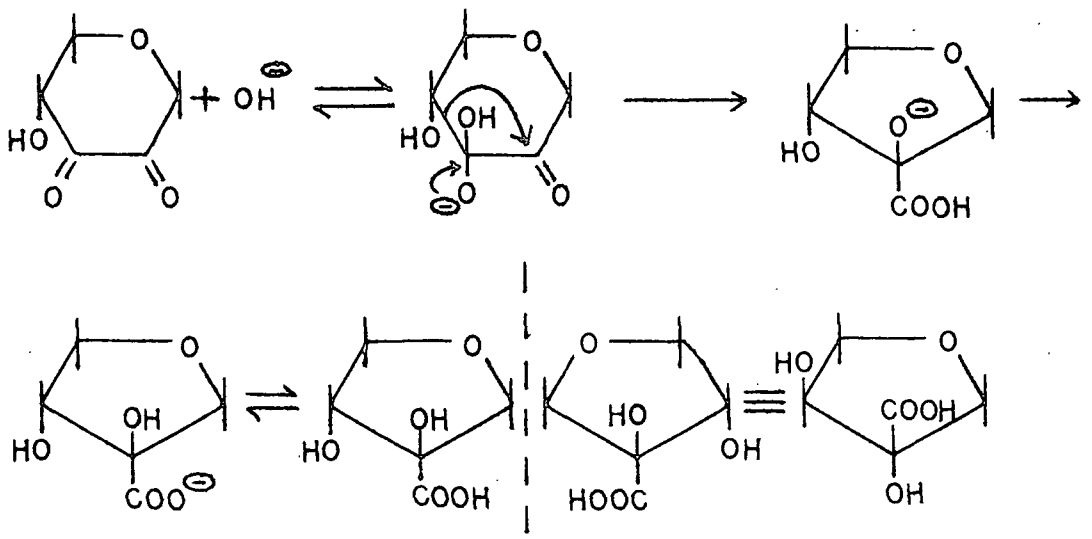

Figure 27. Formation of 1,4-Anhydro-2-C-carboxy-D-threitol Showing the Relationship to the -L- Enantiomer Formed from the C-3, C-4 Dicarbonyl Intermediate

Spectrum B. Like other mass spectral analyses of dibasic acids (24), this compound did not give a P^+ or P^+-15 peak. The first peak in evidence was P^+-CO_2 (m/e 336) (48). Subsequent fragments due to carbon-carbon and carbon-oxygen cleavage as indicated in the diagram were all present.

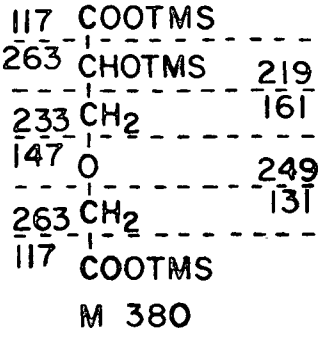

AX and AR Product ⑧ (Fig. 17 and 18) were not identified because a workable mass spectrum could not be obtained.

The major product in the MAX system (Fig. 19, Product ③) was identified as 3-hydroxy-2-methoxybutyric acid. The mass spectrum is given in Fig. 28, Spectrum A. Both the P^+ (m/e 278) and the P^+-15 (m/e 263) were present. All fragments due to carbon-carbon chain cleavage were formed. As stated previously, this compound is the analog of 2,3-dihydroxybutyric acid in the AX and AR systems.

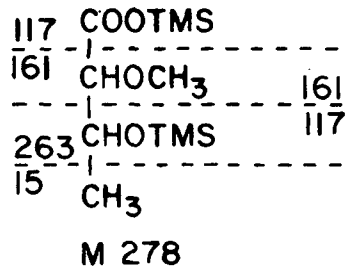

Formic and acetic acids were also detected, as their benzyl esters, in the products of the AX and AR reactions. However, formic acid and only a trace of acetic acid were found in the MAX system. See Appendix II, Tables V and VI for the GLC conditions and retention times.

Finally, mass spectra of MAX, AX, and AR are presented in Fig. 28 (Spectrum B), 29 (Spectrum A), and 29 (Spectrum B), respectively. The spectra were analyzed employing the nomenclature of Kochetkov and Chizhov (49) (see Appendix IV, Fig. 47 and 48). Unlike most carbohydrate derivatives, the three model compounds gave strong parent ions. This is probably due to the absence of a glycosidic oxygen atom which normally facilities the D, F, J, B, and E fragmentation series.

Semiquantitative Product Analysis for 1,5-Anhydroxylitol and 1,5-Anhydroribitol Reaction Systems

In conjunction with the AX and AR kinetic experiments performed at 0.1N carbohydrate, 1.25N sodium hydroxide, 75 psi oxygen pressure (25°C), and 120°C (Appendix V, Reactions 5AX and 5AR), semiquantitative analyses were performed

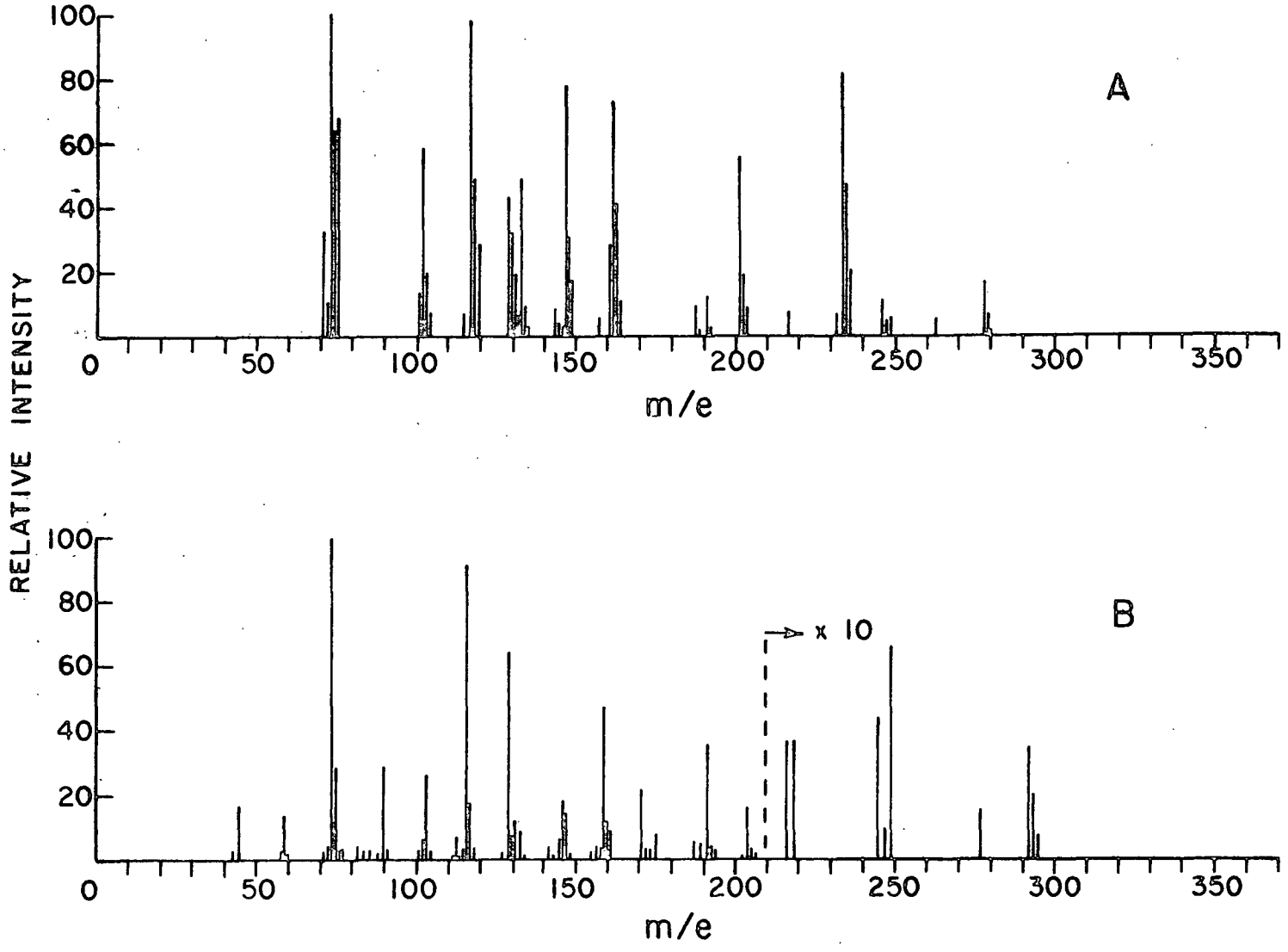

Figure 28. Mass Spectra (70 ev) of the Trimethylsilyl Derivatives of 3-Hydroxy-2-methoxybutyric Acid (Spectrum A - MAX Product (3)) and 3-O-Methyl-1,5-anhydroxylitol (Spectrum B)

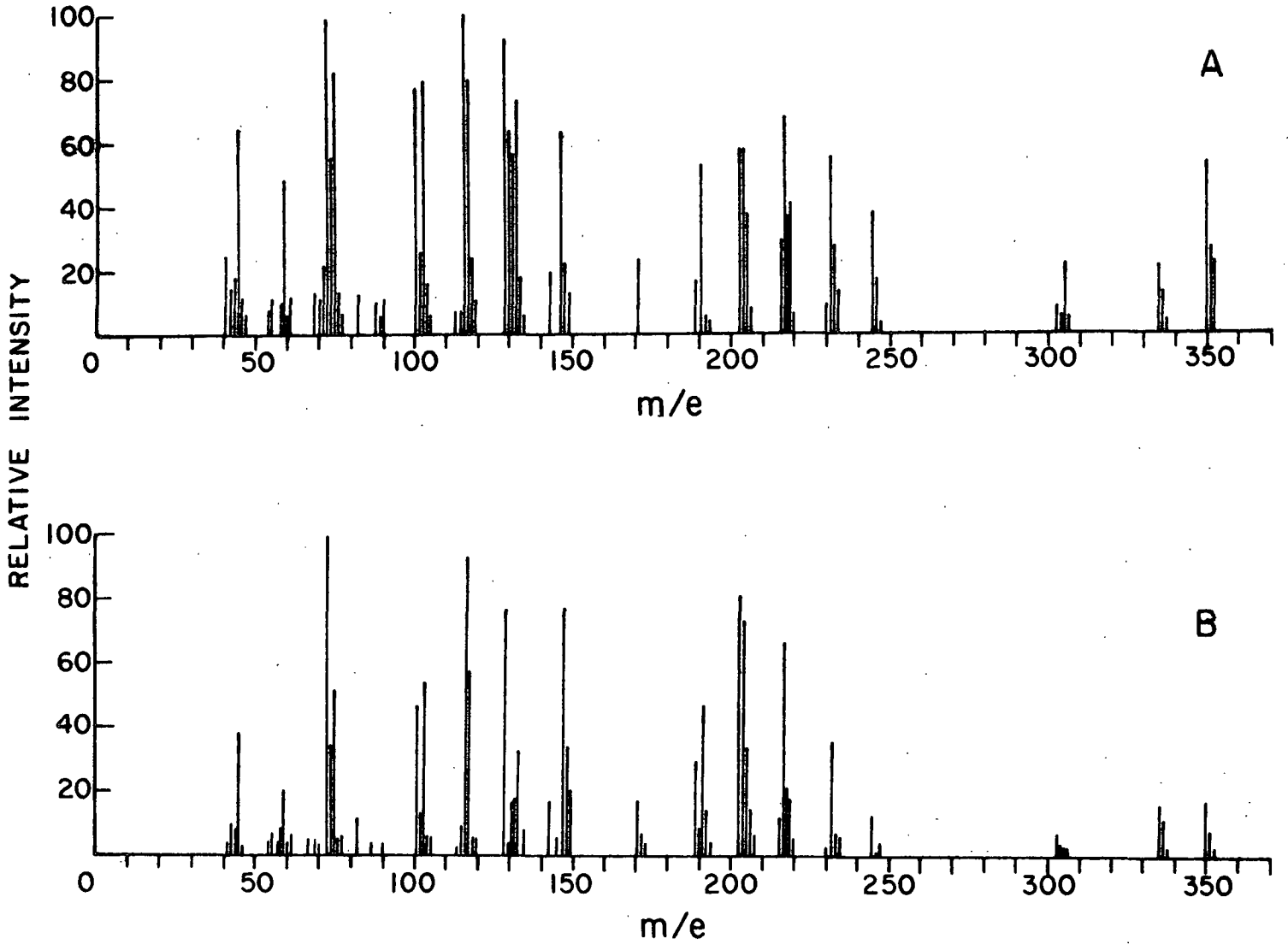

Figure 29. Mass Spectra (70 ev) of the Trimethylsilyl Derivatives of 1,5-Anhydroxylitol (Spectrum A) and 1,5-Anhydroribitol (Spectrum B)

on the acidic reaction products as their TMS derivatives. GLC conditions are given in Appendix II, Table V. Typical chromatograms are shown in Fig. 17 and 18.

The product analyses were "semiquantitative" because response factors were determined for only lactic acid, glycolic acid, glyceric acid, AX, and AR relative to the internal standard, methyl β-D-xylopyranoside (Appendix II, Table VI). The response factors used for the other products were estimates, assuming there is a correlation between the response factor and the molecular weight (Appendix II, Table VI). The data presented in Tables III and IV and Fig. 30-33 should be considered with this fact in mind.

Tables III and IV give the semiquantitative product analyses for the AX and AR systems, respectively. Figures 30-33 give a graphical representation of the data in Tables III and IV.

As can be seen from Tables III and IV, 91-100% of the AX and AR reacted at any given time can be accounted for through the degradation products using the estimated response factors. The calculations were made assuming that 1 mole of reactant produced 1 mole of products, regardless of the species (see Mechanism, Fig. 40 and 41).

The general pattern of major product formation (Fig. 30 and 32) in the AX and AR systems was the same. The trends in the AX system were more drastic, with rapid production and degradation of reactant products occurring at ca. 50% reaction of AX (Fig. 30) as compared to 72% reaction of AR (Fig. 32). In both systems, lactic and glycolic acids were termination products in the sense that their rates of formation were at all times equal to, or greater than, their rates of degradation. The pattern for glyceric and 2,3-dihydroxybutyric acis was not entirely clear. The concentration versus time curves representing

TABLE III

SEMIQUANTITATIVE ANALYSIS OF 1,5-ANHYDROXYLITOL REACTION PRODUCTS

AX Reacted, 10^2M	Products,[a] 10^2M									Total Product, 10^2M	Accounted for (%), total[b]
	1	2	3	4	5+6	7	8	9+10	11		
1.5824	0.0250	0.4004	0.0860	0.0730	0.4515	0.0410	0.0140	0.4100	0.0486	1.1405	91.0
2.8879	0.1060	0.7541	0.0590	0.0200	0.8012	0.0460	P[c]	0.7766	0.0509	2.6678	92.4
4.1142	0.2783	1.1591	0.0790	0.0600	0.9351	0.0750	0.0410	1.1755	0.1419	4.2733	103.8
4.9351	0.3771	1.4611	--[d]	0.0820	1.2060	0.1170	0.1110	1.3430	P	4.9162	99.6
5.4890	0.5190	1.6933	--	0.0810	1.0023	0.1580	0.1080	1.2430	0.3861	5.2276	95.2
5.9933	0.6067	2.1548	--	0.1040	0.8122	0.1840	0.1770	1.2096	0.3475	5.6358	94.0
6.2703	0.8765	2.6084	--	0.1680	0.5783	0.2220	0.2180	0.9503	0.4016	6.0111	95.9

[a] Numbers correspond to the following acids: 1 = lactic; 2 = glycolic; 3 = 3-hydroxypropanoic; 4 = 2-hydroxybutyric; 5 = glyceric; 6 = 2,3-dihydroxybutyric; 7 = 2,4-dihydroxybutyric; 8 = unknown; 9 and 10 = 1,4-anhydro-2-C-carboxy-tetritols; and 11 = 3-O-carboxymethyl-glyceric acid.

[b] Percentages were derived from the curves in Fig. 30 and 31 and not from the data in the table.

[c] P = Unanalyzed peak, less than 0.03 x 10^{-2}M.

[d] No peak in evidence.

TABLE IV

SEMIQUANTITATIVE ANALYSIS OF 1,5-ANHYDRORIBITOL REACTION PRODUCTS

AR Reacted, 10^2M	Products,[a] 10^2M									Total Product, 10^2M	Accounted for (%), total[b]
	1	2	3	4	5+6	7	8	9+10	11		
1.531	0.163	0.392	P[c]	0.094	0.340	0.032	P	0.389	0.043	1.433	93.4
2.718	0.321	0.686	0.066	0.101	0.464	0.064	P	0.812	0.113	2.563	94.3
3.522	0.415	0.845	0.062	0.111	0.668	0.010	P	1.029	0.131	3.391	96.3
4.230	0.404	1.007	0.086	0.093	0.776	0.104	P	1.367	0.221	4.146	98.0
5.168	0.471	1.294	0.032	0.038	0.979	0.096	0.052	1.727	0.271	5.220	101.0
6.871	0.683	1.845	0.160	0.072	1.273	0.196	0.163	1.939	0.476	6.828	99.4
8.431	0.816	2.727	0.060	0.026	1.045	0.290	0.430	2.045	0.523	8.069	95.7
8.766	0.879	3.009	0.105	0.042	0.961	0.337	0.480	2.002	0.562	8.335	95.1

[a] Numbers correspond to the following acids: 1 = lactic; 2 = glycolic; 3 = 3-hydroxypropanoic, 4 = 2-hydroxybutyric; 5 = glyceric; 6 = 2,3-dihydroxybutyric; 7 = 2,4-dihydroxybutyric; 8 = unknown; 9 and 10 = 1,4-anhydro-2-C-carboxy-tetritols; and 11 = 3-O-carboxymethyl-glyceric acid.

[b] Percentages were derived from the curves in Fig. 32 and 33 and not from the data in the table.

[c] P = Unanalyzed peak, less than 0.03 x 10^{-2}M.

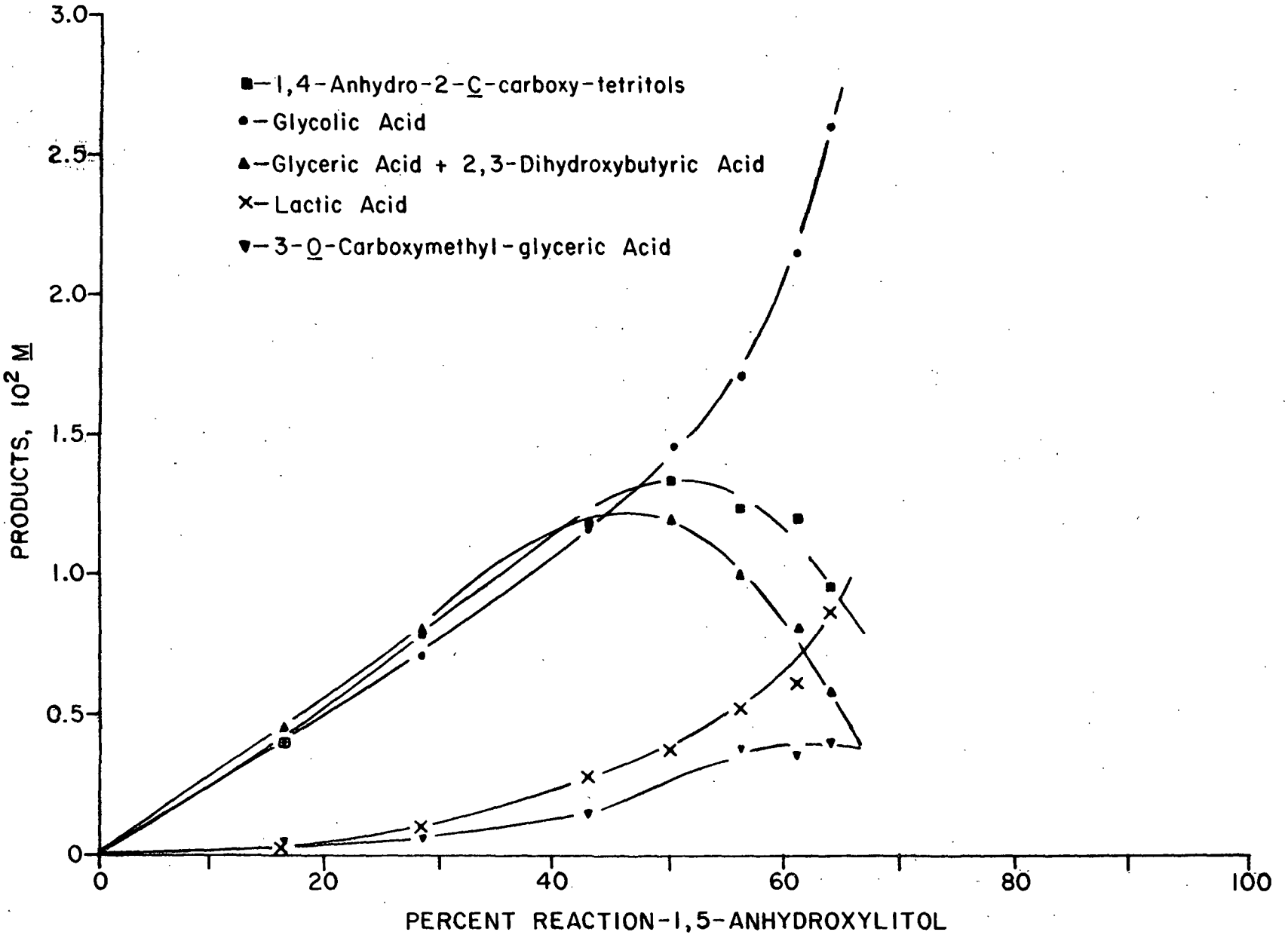

Figure 30. Formation of the Major Acidic Products in the Degradation of 1,5-Anhydroxylitol (Reaction 5 AX) in 1.25N NaOH at 120°C and 75 PSI O_2 (25°C)

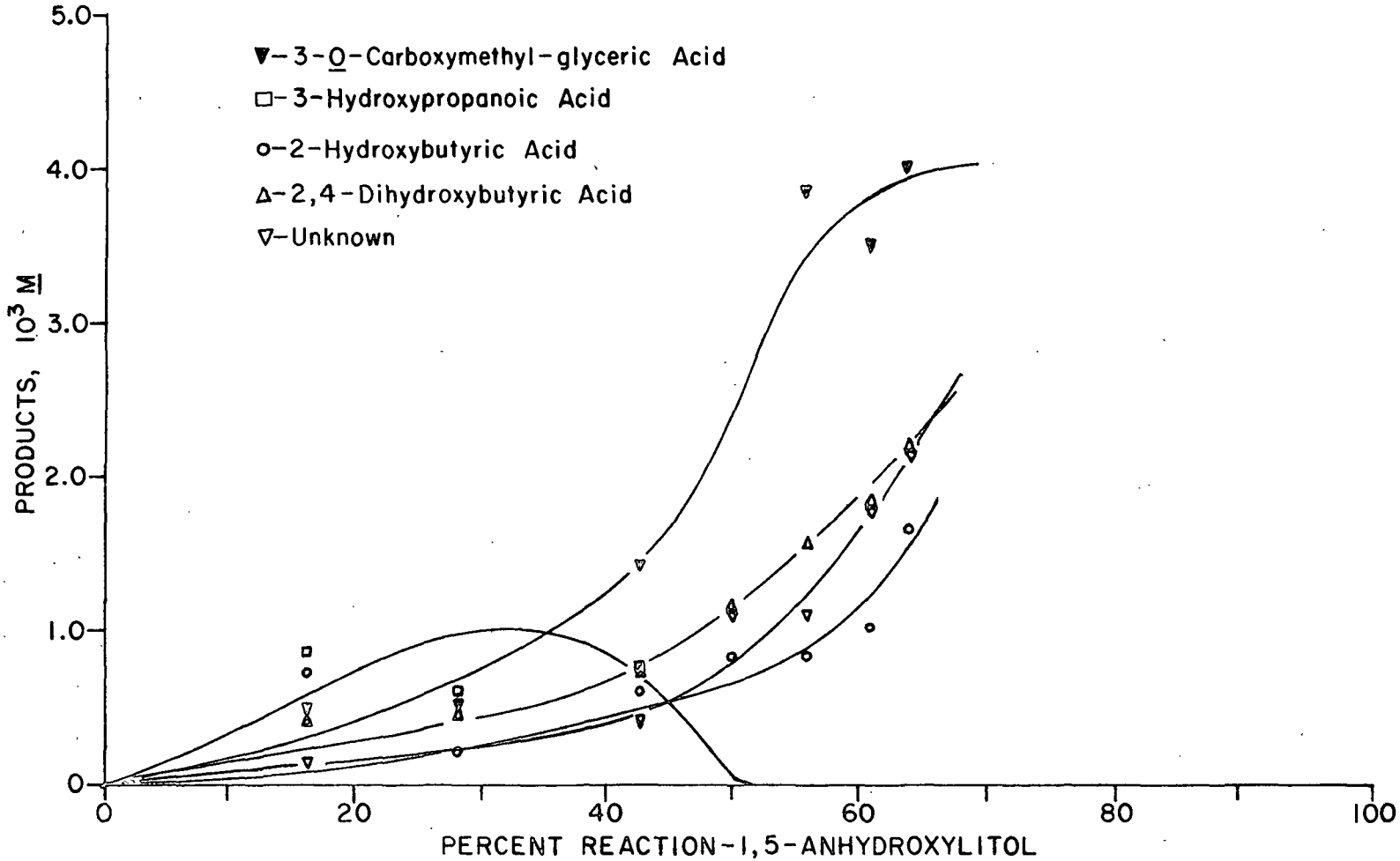

Figure 31. Formation of the Minor Acidic Products in the Degradation of 1,5-Anhydroxylitol (Reaction 5 AX) in 1.25N NaOH at 120°C and 75 PSI O_2 (25°C)

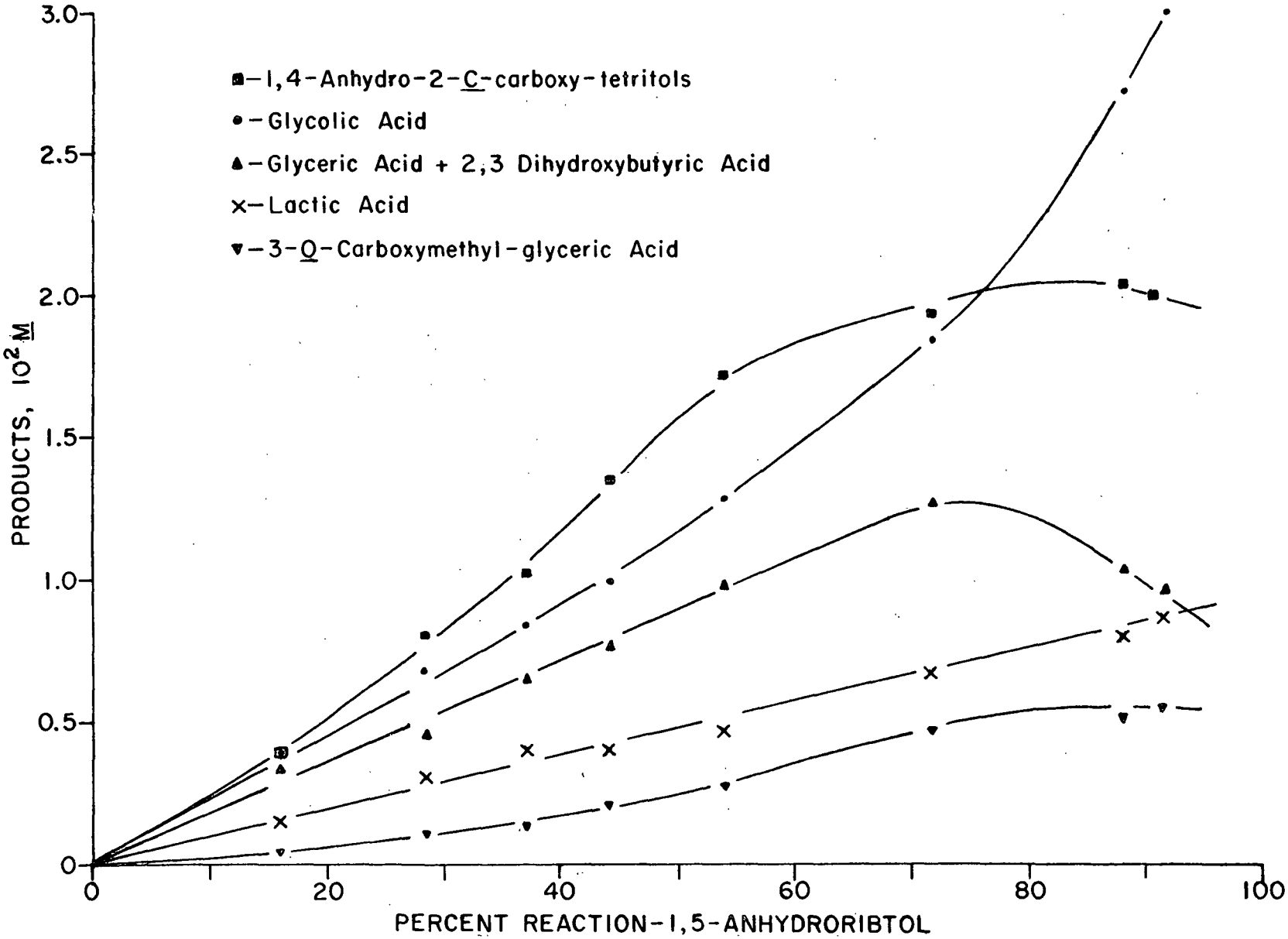

Figure 32. Formation of the Major Acidic Products in the Degradation of 1,5-Anhydroribitol (Reaction 5 AR) in 1.25N NaOH at 120°C and 75 PSI O_2 (25°C)

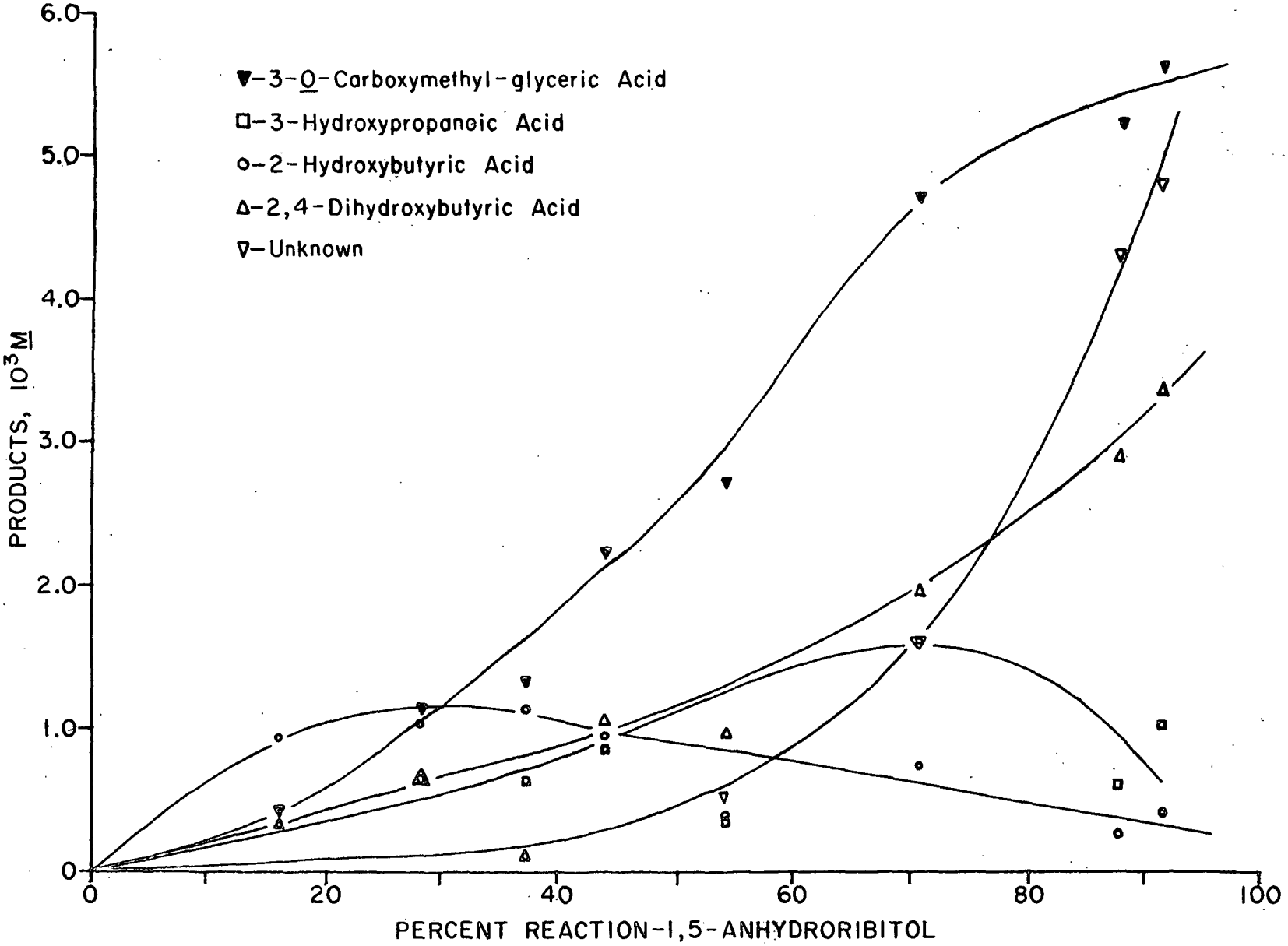

Figure 33. Formation of the Minor Acidic Products in the Degradation of 1,5-Anhydroribitol (Reaction 5 AR) in 1.25N NaOH at 120°C and 75 PSI O_2 (25°C)

the sum of the two acids displayed maxima in both systems. As indicated earlier (Product Identification section), 2,3-dihydroxybutyric acid displayed the same behavior. Therefore, in theory, the pattern of glyceric acid and 2,3-dihydroxybutyric acid production in the reaction systems could be viewed as a steady build-up in glyceric acid in conjunction with formation and subsequent decomposition of 2,3-dihydroxybutyric acid. However, this seems unlikely based on the extent of decomposition shown in Fig. 30. A better explanation is that concurrent formation and degradation of both acids are involved.

The concentration of the 1,4-anhydro-2-C-carboxy-tetritols also went through a maximum. Although the general pattern for the sum of these acids was the same in both systems, some distinct qualitative differences were noted (Fig. 34). Over the time course of the AX reaction, the dominant product was (9). The relative amount of Product (10) continually decreased as the reaction proceeded to a point where it was not noticeable in the gas chromatogram (Fig. 34). Conversely, Product (10) dominated at early reaction times in the degradation of AR, but became increaseingly less important as the reaction proceeded (Fig. 34). The data seem to indicate that there is preferential formation of Product (9) in the AX system and Product (10) in the AR system. The data also indicate that Product (10) is probably more reactive than Product (9) under the degradation conditions employed. These observations raise questions concerning the accepted mechanism of formation of these furanoid acids. They are generally considered to form via a benzylic acid-type rearrangement of a dicarbonyl precursor as shown earlier (21,24) (Reaction Product section). In the AX and AR systems, the dicarbonyl intermediates would be identical. Therefore, the differences in the relative ratios of the isomeric products observed in the two systems would not be expected. Although the dicarbonyl species may be an intermediate,

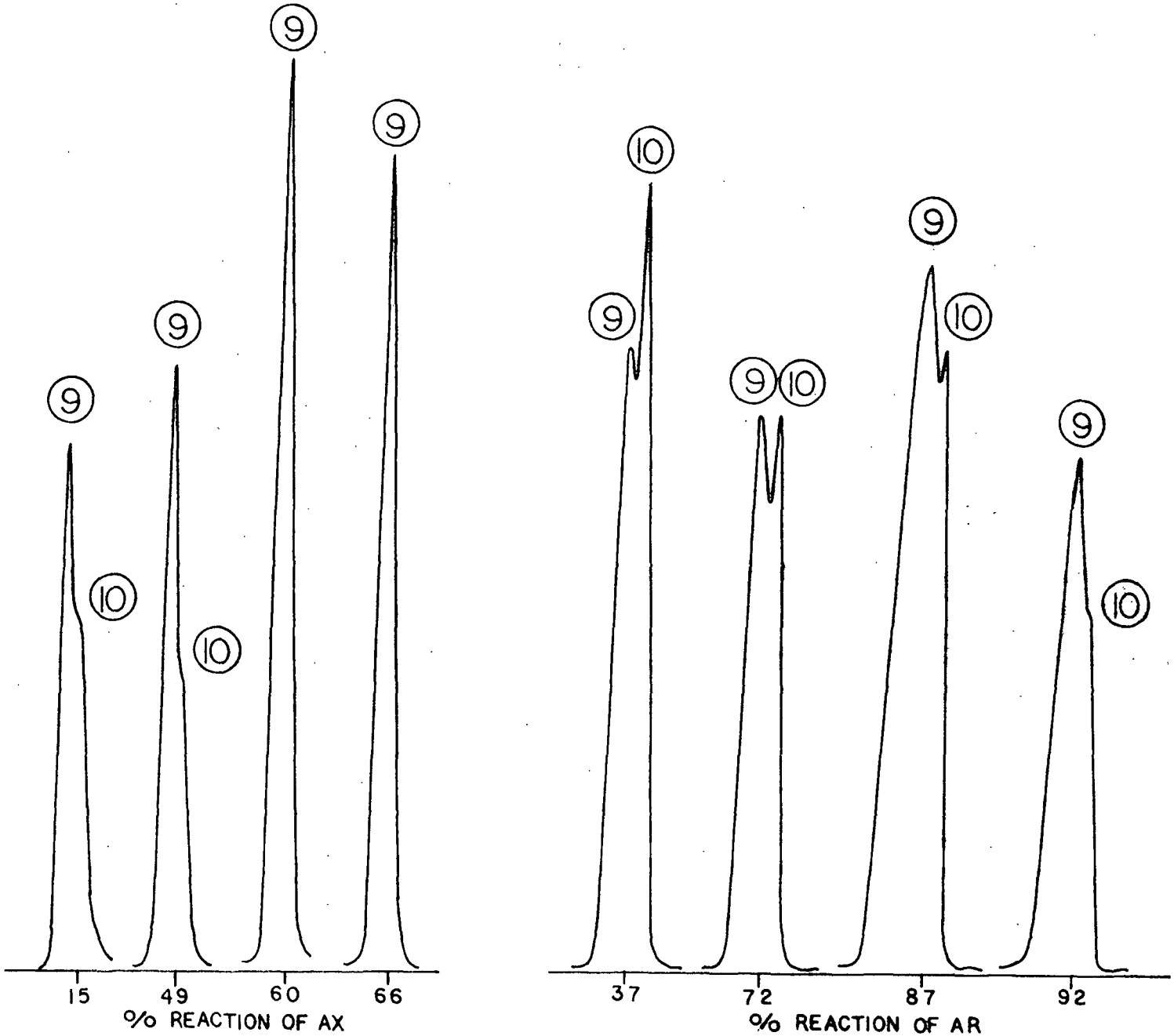

Figure 34. GLC Peaks Showing Relative Proportions of 1,4-Anhydrotetritols (AX and AR Products (9) and (10)) as a Function of Percent Reaction of AX and AR

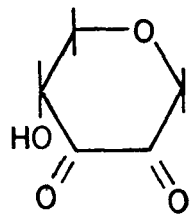

another intermediate with a stereochemical directing effect operating at C-3 must also be important. Figure 35 gives one possibility for the AR and AX systems.

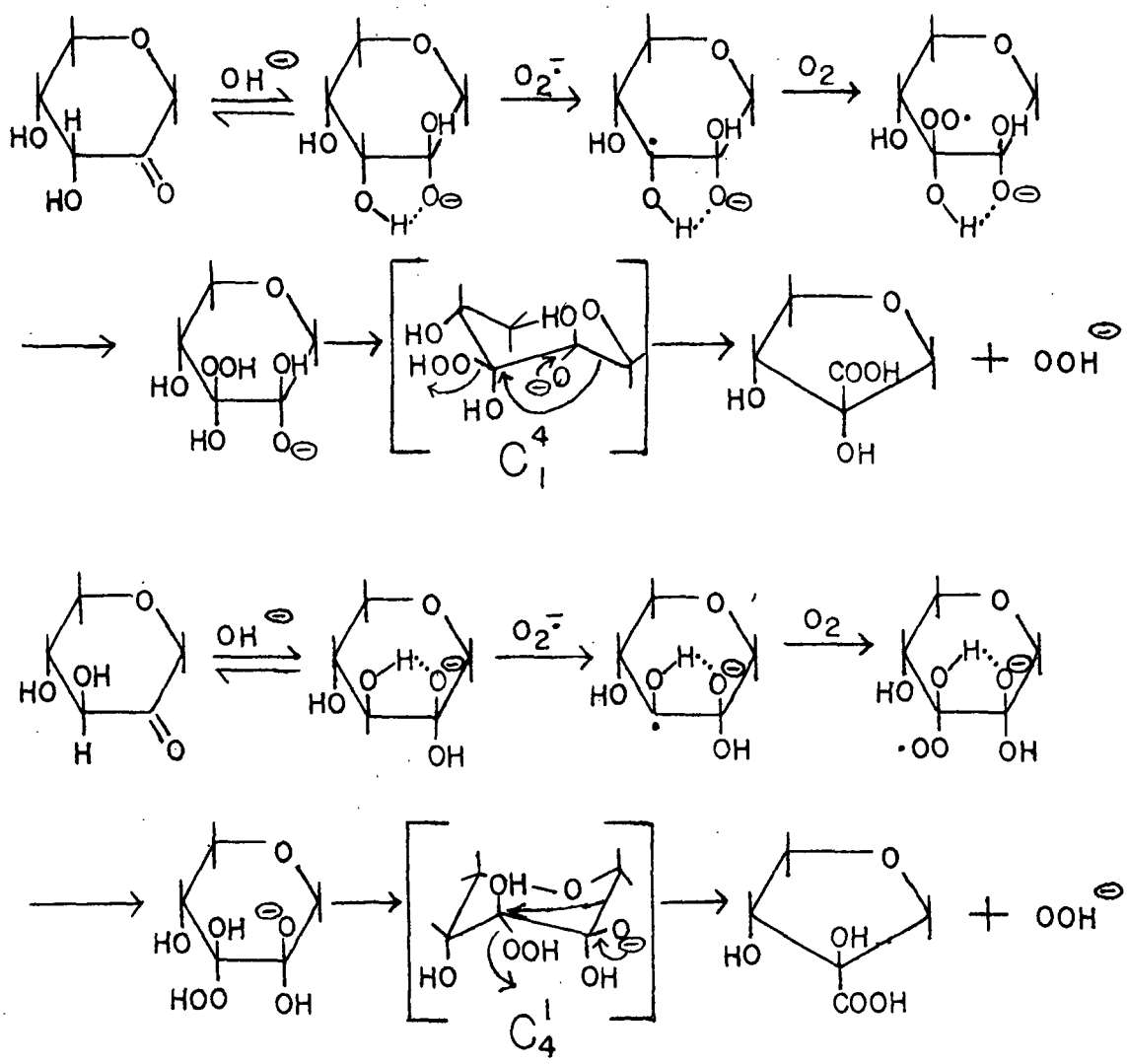

Figure 35. Formation of 1,4-Anhydro-2-C-carboxy-tetritols via Intermediates Which Possibly Account for Differences in Stereoselectivity in the AR and AX Systems

Step 1 of both reaction pathways involves reversible addition of hydroxyl ion to the carbonyl. Because of steric considerations, the point of hydroxyl ion attack on the carbonyl preferentially occurs opposite the hydroxyl group on the adjacent carbon atom. In both systems, the resulting anionic species can hydrogen bond to the hydroxyl group as illustrated. Step 2 is abstraction of the C-3 hydrogen by the superoxide radical ($O_2\overline{\cdot}$) to form an alkyl free radical. Normally, rapid inversion of the radical and its resulting equilibrium would produce equivalent intermediates in the A and AR reactions, eliminating any difference in stereoselectivity of the furanoid products between the two systems. Therefore, if a substantial amount of the reaction proceeds as shown in Fig. 35, Step 3 must be the rapid oxidation of the alkyl radical by molecular oxygen to give the alpha-hydroxyhydroperoxy free radical before much inversion takes place. The stereospecific addition of oxygen is facilitated by radical stabilization to inversion via hydrogen bonding. The alpha-hydroxy-hydroperoxy free radical is converted to the alpha-hydroxyhydroperoxide, followed by ring contraction via a benzylic acid-type rearrangement to yield the 1,4-anhydro-2-C-carboxy-tetritol. The rearrangement must take place from specific conformations (C_1^4 for AR, and C_4^1 for AX) so that the molecular orbitals of the (C-1)-(C-2) bond and the carbon-oxygen bond of the hydroperoxide are parallel, permitting back-side displacement of the perhydroxy anion (S_N2 type) as shown in Fig. 35 (50). This parallel relationship does not exist for the "AR hydroperoxide" in the C_4^1 conformation and the "AX hydroperoxide" in the C_1^4 conformation.

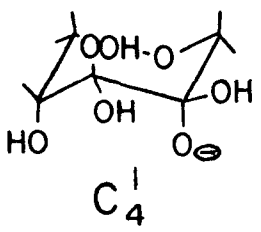

C_4^1

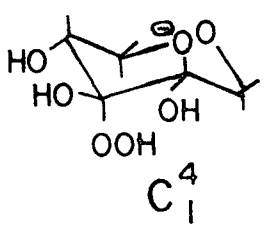

C_1^4

Like S_N2 reactions, the rearrangements should result in inversion of the hydroxyl group as shown in Fig. 35. Therefore, since Product ⑨ is the preferred isomer formed in the AX system, it is postulated that this compound is 1,4-anhydro-2-C-carboxy-D-, and -L-threitol. Throught similar logic based on the AR system, Product ⑩ is postulated to be 1,4-anhydro-2-C-carboxy-D-, and -L-erythritol. Furthermore, if these designations are correct, the erythritol isomer seems to be more reactive than the threitol isomer under the reaction conditions studied. This is consistent with the finding that carbohydrates having cis-vincinal hydroxyl groups are more reactive than those containing trans-vincinal hydroxyl groups under oxygen alkaline degradative conditions (23). Of the major degradation products, those with vicinal glycol groups were non-termination and the rest were termination products.

The formation patterns of the minor degradation products in the AX and AR systems are shown in Fig. 31 and 33, respectively. 3-Hydroxypropanoic acid [Product ③] was a nontermination product in both systems. 3-O-Carboxymethyl-glyceric acid [Product 11], 2,4-dihydroxybutyric acid [Product ⑦], and Product ⑧ (unknown) were termination products and showed similar patterns in both systems. The level of 2-hydroxybutyric acid [Product ④] continually increased in the AX reaction while it was a nontermination product in the AR system. The GLC results were subject to relatively large error, as seen by the scatter in the data points in Fig. 31 and 33. Therefore, the curves in Fig. 31 and 33 may, or may not, represent the actual formation patterns of Products ③, ④, ⑦, and ⑧. However, it should be remembered that the sum of Products ③, ④, ⑦, and ⑧ accounted for no more than 11% of either reaction at any given time.

MECHANISM

THE KETO INTERMEDIATE

Most investigators who have studied degradation of carbohydrates by molecular oxygen in alkali agree that the reaction proceeds via a keto derivative (5,7,8,10,12,14,16,18-20,40,45-47,51-57) which rapidly degrades to acidic products (7,8,10,18,20,21). However, the mechanism of formation of the keto derivative has not been clarified.

Information gained in the present research, in conjunction with the results of other workers, allows the postulation of a reaction scheme (Fig. 36) which may be important during AR degradation by molecular oxygen in alkali. The scheme illustrates the formation of a carbonyl at C-2 only. However, formation at C-3 and C-4 is also possible.

Equations (7)-(29) reflect the reactions shown in Fig. 36, but also include important radical reactions not indicated in the figure. Equations (7)-(29) were used to derive the rate expression for the mechanism depicted in Fig. 36.

$$A + OH^- \underset{}{\overset{K_6}{\rightleftharpoons}} A^- + H_2O \qquad (7)$$

$$A^- + O_2 \xrightarrow{k_7} A^{-}\cdot + HOO\cdot \qquad (8)$$

$$HOO\cdot + OH^- \underset{k_{-8}}{\overset{k_8}{\rightleftharpoons}} O_2^{-}\cdot + H_2O \qquad (9)$$

$$O_2^{-}\cdot + H_2O \xrightarrow{k_9} HO\cdot + HOO^- \qquad (10)$$

$$HOO^- + M^{+n+1} \underset{k_{-10}}{\overset{k_{10}}{\rightleftharpoons}} HOO\cdot + M^{+n} \qquad (11)$$

$$A^{-}\cdot + H_2O \underset{k_{-11}}{\overset{k_{11}}{\rightleftharpoons}} A\cdot + OH^- \qquad (12)$$

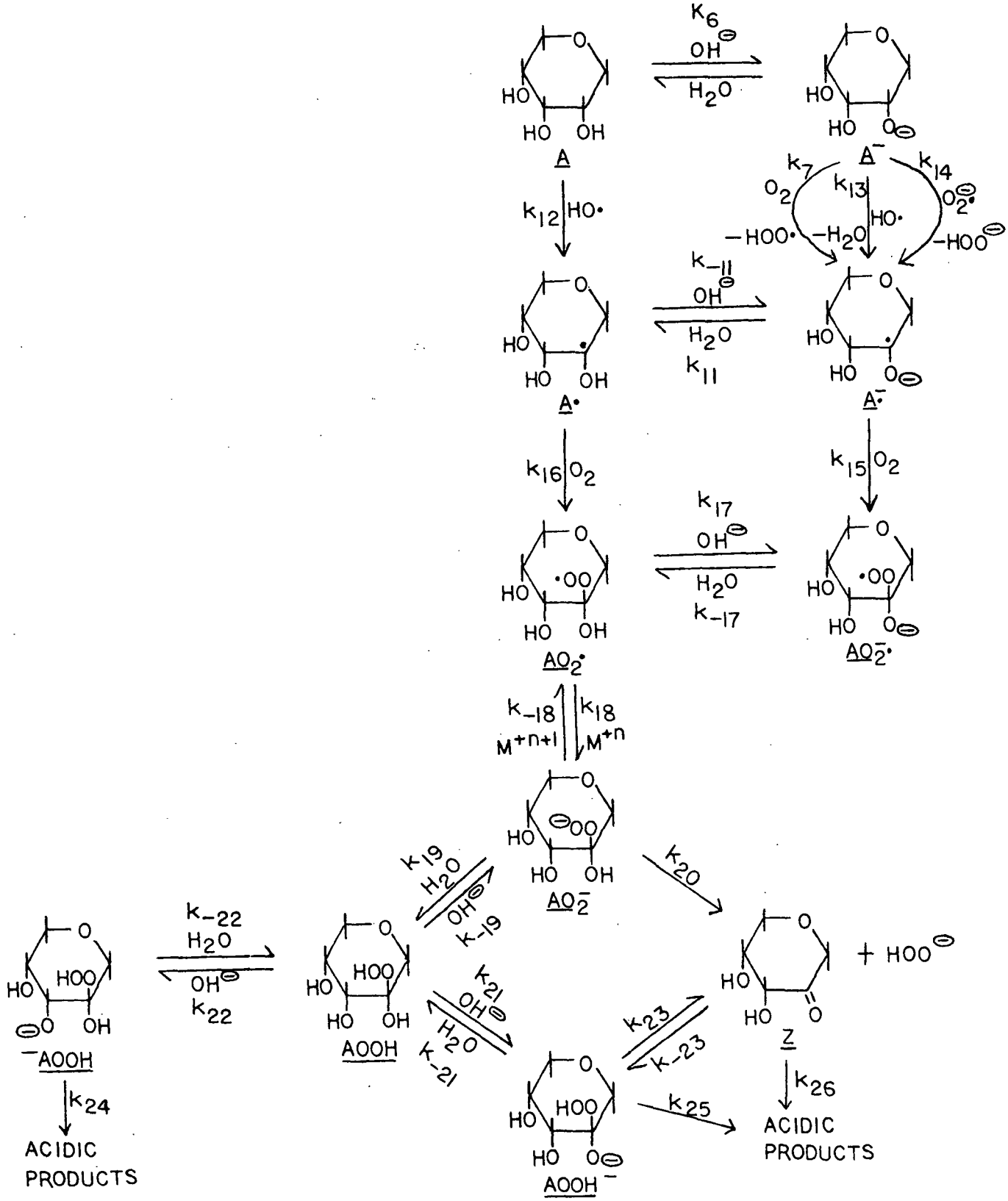

Figure 36. Proposed Mechanism of Formation of the Keto Intermediate During the Degradation of 1,5-Anhydroribitol by Molecular Oxygen in Alkali

$$A + HO\cdot \xrightarrow{k_{12}} A\cdot + H_2O \quad (13)$$

$$A^- + HO\cdot \xrightarrow{k_{13}} A^{-}\cdot + H_2O \quad (14)$$

$$A^- + O_2^{-}\cdot \xrightarrow{k_{14}} A^{-}\cdot + HOO^- \quad (15)$$

$$A^{-}\cdot + O_2 \xrightarrow{k_{15}} AO_2^{-}\cdot \quad (16)$$

$$A\cdot + O_2 \xrightarrow{k_{16}} AO_2\cdot \quad (17)$$

$$AO_2\cdot + OH^- \underset{k_{-17}}{\overset{k_{17}}{\rightleftharpoons}} AO_2^{-}\cdot + H_2O \quad (18)$$

$$AO_2\cdot + M^{+n} \underset{k_{-18}}{\overset{k_{18}}{\rightleftharpoons}} AO_2^- + M^{+n+1} \quad (19)$$

$$AO_2^- + H_2O \underset{k_{-19}}{\overset{k_{19}}{\rightleftharpoons}} AOOH + OH^- \quad (20)$$

$$AO_2^- \xrightarrow{k_{20}} Z + HOO^- \quad (21)$$

$$AOOH + OH^- \underset{k_{-21}}{\overset{k_{21}}{\rightleftharpoons}} AOOH^- + H_2O \quad (22)$$

$$AOOH + OH^- \underset{k_{-22}}{\overset{k_{22}}{\rightleftharpoons}} {}^{-}AOOH + H_2O \quad (23)$$

$$AOOH^- \underset{k_{-23}}{\overset{k_{23}}{\rightleftharpoons}} Z + HOO^- \quad (24)$$

$${}^{-}AOOH \xrightarrow{k_{24}} \text{Products} \quad (25)$$

$$AOOH^- \xrightarrow{k_{25}} \text{Products} \quad (26)$$

$$Z \xrightarrow{k_{26}} \text{Products} \quad (27)$$

$$O_2^{-}\cdot + M^{+n+1} \xrightarrow{k_{27}} O_2 + M^{+n} \quad (28)$$

$$HO\cdot + M^{+n} \xrightarrow{k_{28}} OH^- + M^{+n+1} \quad (29)$$

where M = catalytic metal ion.

The proposed reaction scheme is the first attempt at incorporating a reactive hydroperoxide intermediate into the mechanism of degradation of a carbohydrate by molecular oxygen in alkali. The scheme also includes important ionizations and subsequent reactions which are unique to a particular species. In the postulated mechanism, Equations (7)-(9) reflect the only important reactions during the induction period. The production of superoxide radical ($O_2^{\bullet -}$) [Equation (9)] predominates over the reverse reaction because of the relatively high sodium hydroxide concentration (58). For this reason, the superoxide radical, and not the perhydroxyl free radical (HOO•), is considered one of the important radical species. The superoxide radical can also be converted to the hydroxyl free radical (HO•) [Equation (10)]. When the concentration of the reacting radical species ($O_2^{\bullet -}$ and HO•) reaches steady state, the free radical mechanism is propagated [Equations (9)-(24)]. Carbonyl formation is postulated to proceed through an ionized alpha-hydroxyhydroperoxide (Equations (21) and (24)]. Acidic degradation products are formed from the carbonyl (Equation (27)] and/or the ionized alpha-hydroxyhydroperoxide directly [Equations (25) and (26)], as proposed by Isbell (54) (Fig. 37).

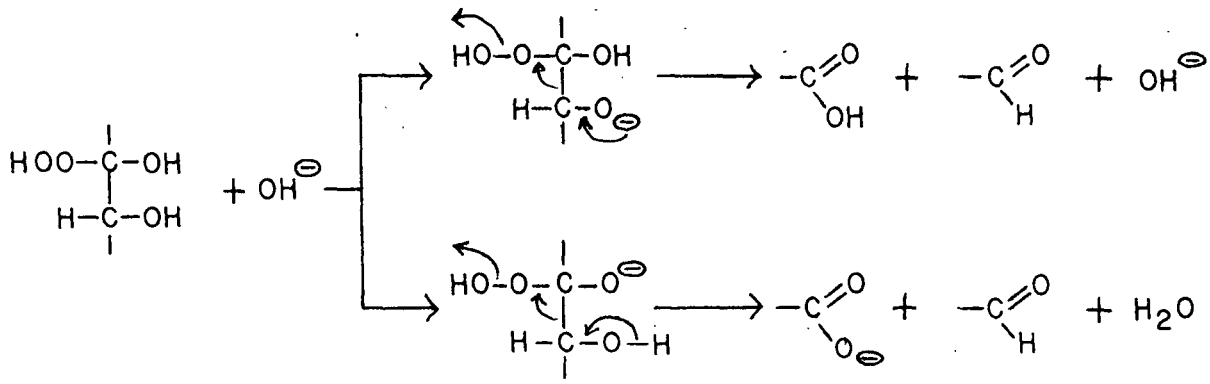

Figure 37. Acidic Degradation Products Formed Directly from Ionized Alpha-hydroxyhydroperoxide Proposed by Isbell (54)

Equations (28), (29), and the reverse reaction of Equation (11) reflect chain termination reactions. Formation of the alpha-hydroxyhydroperoxy anion by a reversible one-electron transfer reaction of the alpha-hydroxyhydroperoxy free radical with metal ion [Equation (19)] is also proposed. The alpha-hydroxyhydroperoxy anion thus formed can react with water to yield the alpha-hydroxyhydroperoxide [Equation (20)]. This is in contrast to the frequently postulated formation of the alpha-hydroxyhydroperoxide via hydrogen abstraction by the hydroperoxy radical as shown (39,59):

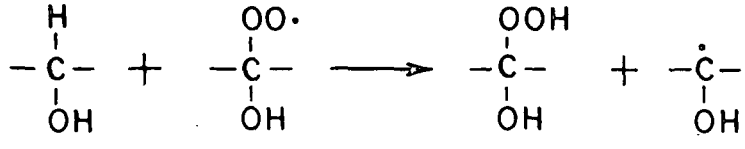

(30)

Making the steady-state approximation that all radical species are very reactive and therefore present in very small concentration and that the concentration of each metal ion remains constant during the reaction, a kinetic expression for the proposed mechanism was derived (see Appendix VI):

$$-d[A]/dt = K_6k_7[A][OH^-][O_2] + K_6^2k_7k_{14}[A]^2[OH^-]^2[O_2]/k_{27}[M^{+n+1}] + K_6k_7k_9[H_2O][A][OH^-][O_2]/k_{27}[M^{+n+1}] \quad (31)$$

The first term kinetically describes the induction period. During this time, the reaction would be first order in alditol, alkali, and oxygen. The second term is indicative of the importance of the superoxide radical in the chain reaction [Equation (15)]. The metal ion concentration term in the denominator, being very small, makes this term large relative to the first term after initiation of the free radical reaction. The third term includes the rate constant for formation of the hydroxyl radical from the superoxide radical

[Equation (10)] and also a metal ion concentration term in the denominator. A derivation of the kinetic expression considering the superoxide radical to be the only important radical species [i.e., excluding Equations (10), (13), (14), and (29)] afforded Equation (32):

$$-d[A]/dt = K_6k_7[A][OH^-][O_2] + K_6^2k_7k_{14}[A]^2[OH^-]^2[O_2]/k_{27}[M^{+n+1}] \qquad (32)$$

Equation (32) is identical to the first two terms of Equation (31). Thus, the third term of Equation (31) represents the role of the hydroxyl radical in the free radical mechanism.

From the kinetic expression [Equation (31)], the reaction could display an order with respect to carbohydrate between 1 and 2, depending on the relative importance of one term to another. The reaction of AR was found to be second order in carbohydrate after the inducation period. Therefore, if the proposed mechanism is correct, the second term of Equation (31) would have to be predominant under the conditions investigated. This leads to several interesting conclusions. The second term can predominate over the first term because of the metal ion dependence discussed earlier. There is also a term for the metal ion concentration in the denominator of the third term. Therefore, in order for the second term to be very large relative to the third term, $K_6k_{14} >> k_9$. This means that the reaction of the superoxide radical with the conjugate base of the alditol [Equation (15)] is much more important than formation of the hydroxyl radical from the superoxide radical [Equation (10)]. This would indicate that the hydroxyl radical does not play a major role in the free radical mechanism under the reaction conditions studied. This is consistent with the postulate that in minimum metal-catalyzed systems, the perhydroxyl radical (HOO•), and it conjugate base, the superoxide radical (O_2^{-}•), are more important than the hydroxyl radical (20,40).

If the second term in Equation (31) predominates, the reaction would be expected to exhibit a second order dependence on hydroxide ion concentration. This is in contrast to the first order relationship postulated by previous investigators (18,19). McCloskey's data (18) for the degradation of methyl β-D-glucopyranoside by molecular oxygen in alkali indicate that the reaction order with respect to alkali may be variable, attaining higher orders with increasing alkali concentration. In studying the degradation of pentoses by molecular oxygen (14.7 psi) and alkali (0.883M potassium hydroxide) at 25°C, Gleason and Barker (22) concluded that the reaction was greater than first order in alkali. Thus, there seems to be some evidence that during the alkaline oxygen degradation of carbohydrates, the order in alkali can be variable. The derived kinetic expression [Equation (31)] could account for a variable order in alkali as the third term becomes more important relative to the second term; that is, as the hydroxyl radical begins to play a major role in the free radical mechanism. This could be accomplished by adding transition metals to the reaction solution which facilitate the formation of the hydroxyl radical (20,21,40). Also, as the hydroxide ion concentration decreases, the relative importance of the first and third terms of Equation (31) increases due to the squared alkaline dependence in the second term. If the decrease in alkali concentration is severe enough to permit the first and third term to contribute significantly to the degradation rate, the result would be a mixed alkali order between one and two. It has been postulated that the variable alkaline dependence, if it truly exists, could result from a change in mechanism with a change in hydroxide ion concentration (18,22), salt effects (18), or variations in dissolved oxygen at different alkali concentrations (18).

AUTOINHIBITION IN THE AX SYSTEM

General

The AX reactions displayed higher reaction orders with respect to carbohydrate than did the AR reactions. This phenomenon is postulated to be the result of autoinhibition. The mechanism of degradation of AX is viewed to be the same as AR [Equations (7)-(29)], except that termination reactions involving the alpha-hydroxyhydroperoxy free radical ($AO_2\cdot$) [Equations (33) and (34)] are postulated to play a major role in the AX system. Reaction (34) is proposed to occur through the decomposition of a tetroxide intermediate via a cyclic

$$AO_2\cdot + A\cdot \longrightarrow AOOA \qquad (33)$$

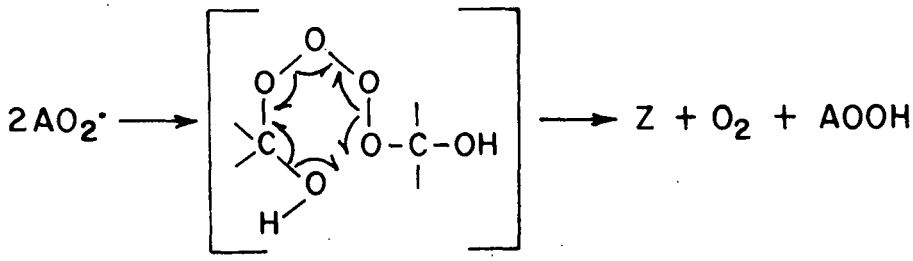

(34)

transition state (60). Evidence for the existence of tetroxides as quasi-stable species is available, at least for tertiary peroxy radicals (61). The autoinhibition is proposed to operate through these two reactions. The products are inactive (nonradical) and do not include the perhydroxyl anion (HOO^-). The concentration of the superoxide radical is related to the concentration of HOO^- [Equations (11) and (9)]. Therefore, reaction pathways which lead to nonradical products, and do not concurrently produce HOO^-, cause a slowing of the propagating reactions which retards the overall rate of carbohydrate degradation.

Stabilization of the Alpha-Hydroxyhydroperoxide Formed in the 1,5-Anhydroxylitol Reaction

In order for the termination reactions [Equations (33) and (34)] to be important in the AX reaction, the concentration of the alpha-hydroxyhydroperoxy radical ($AO_2\cdot$) must be substantially greater in the AX system than it is in the AR system. As seen in Fig. 36, $AO_2\cdot$ is involved in a reversible electron transfer reaction with the alpha-hydroxyhydroperoxy anion (AO_2^-); which is the predominant ionized hydroperoxidic species in the system (62). Unlike its counterpart in the AR reaction, the peroxy anion of the AX system can form good hydrogen bonds with the hydroxyl groups on adjacent carbon atoms (63) (Fig. 38), regardless of which carbon atom the perhydroxyl group is formed at and in what chair conformer* the molecule exists. The interatomic distances shown in Fig. 38 are minimum distances that the respective atoms can approach one another based on measurements taken from Dreiding Molecular Models. In solution, the O•••O distance is critical in determining the strength of a hydrogen bond; the strongest bond occurring at approximately 2.5 A (64). Therefore, oxygen atoms that can theoretically approach each other at distances less than 2.5 A can also swing away to attain the optimum distance for hydrogen bonding. From Fig. 38, the hydroperoxy anion produced in the AR reaction can achieve good hydrogen bonding when formed at C-3 in the C1 conformation and when formed at C-2 and C-4 in the 1C conformation. The hydroperoxy anion in the AX system can achieve good hydrogen bonding when formed at C-2, C-3, or C-4 in either conformer. Pitzner and Atalla (65) have shown that the ratios of C1 to 1C conformers in the AX and AR systems in water at 25°C are 95:5 and 74:26, respectively. The 1C conformation probably becomes more important at 120°C with both alditols.

*The C_1^4 and C_4^1 conformations will be referred to as the C1 and 1C conformations since no ambiguity can arise from these optically inactive molecules.

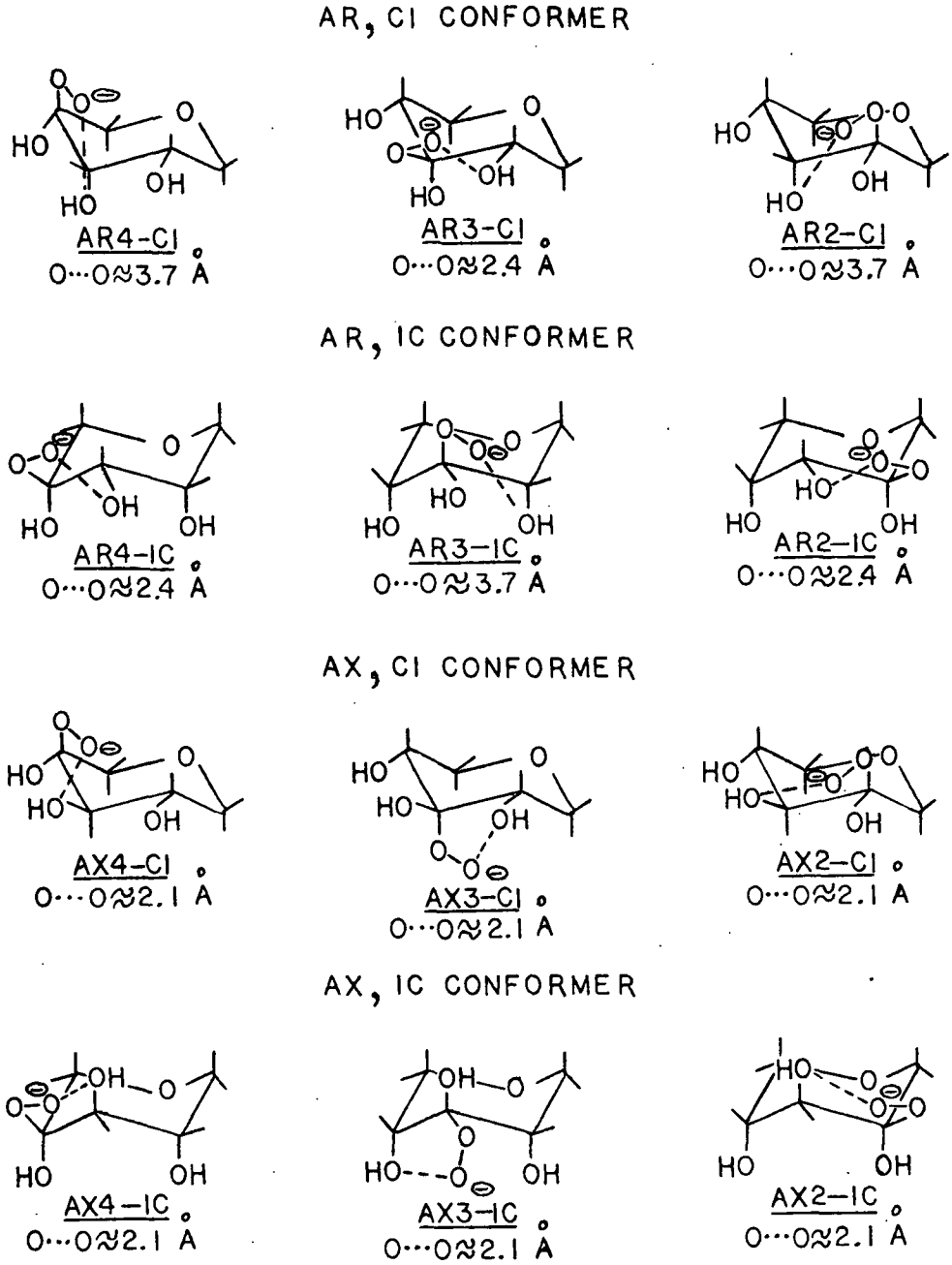

Figure 38. Minimum Hydrogen Bond Distances in Alpha-hydroxyhydroperoxides Formed at C-2, C-3, and C-4 in the 1,5-Anhydroribitol (AR) and 1,5-Anhydroxylitol (AX) Molecules (Both Chair Conformers Shown). (Distances were Measured from Dreiding Molecular Models.)

Assuming that, under the reaction conditions investigated, at least 25% of AR exists in the 1C conformation and that the alpha-hydroxyhydroperoxide can form equally well at C-2, C-3, or C-4, approximately 42% of the anionic alpha-hydroxyhydroperoxy molecules (AO_2^-) formed should be stabilied by hydrogen bonding. This would seem to be ample stabilization to produce detectable organic peroxides in the AR system. Intermediate organic peroxides were not detected in the AR reactions. Furthermore, based on the AX data in which autoinhibition was evident at very low organic peroxide levels, the AR system would also be expected to show autoinhibition. Experimentally, no autoinhibition was found. Therefore, formation of the hydroperoxy anions AR3-C1, AR4-1C, and AR2-1C, which could potentially be stabilized by hydrogen bonding, must not be important relative to the production of the other three AR species (AR4-C1, AR2-C1, and AR3-1C). The following explanation possibly accounts for a stereospecific reaction of oxygen and the alkyl free radicals [Equation (16)] and, in turn, the preferential production of AR4-C1, AR2-C1, and AR3-1C in the AR system. Normally, free radicals of carbon are thought to exist as either planar structures or rapidly inverting pyramids* (59). This would result in a racemic mixture of hydroperoxides upon reaction of the free radical with oxygen.

There is evidence that functional groups containing ionizable hydrogens in equatorial positions are more acidic than those in axial positions since the resulting equatorial anion, being less hindered than its axial epimer, is more easily solvated (66). The resulting anionic species can be pictured as follows:

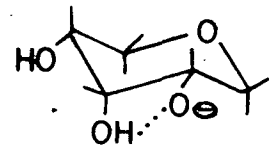

*Alkyl radicals have been proposed to be planar in which the carbon atom is sp^2-hybridized and the unpaired electron is in a p orbital perpendicular to the plane of the sp^2 orbitals. Also, alkyl radicals have been postulated to be pyramidal with the carbon atom sp^3-hybridized. Thus, there could be rapid inversion of the two enantiomeric configurations of the pyramidal radical.

The anion is not only stabilized by solvation but also by hydrogen bonding to the hydroxyl group on the adjacent carbon atom. This would also be true for ionization at C-4. In the event that ionization takes place at C-3, an equivalent hydrogen bonded species can be imagined in which the hydrogen of the C-2 hydroxyl group is transferred to the C-3 oxy group because of the solvation effect just discussed. The next step in the mechanism is abstraction of the C-2 hydrogen by the superoxide radical [Equation (15)] to form the free radical $A^{\bullet}$. This radical is now stabilized against inversion (via hydrogen bonding) so that the subsequent reaction with oxygen [Equation (16)] retains the stereochemistry at C-2. This preferential production of ionized hydroperoxy

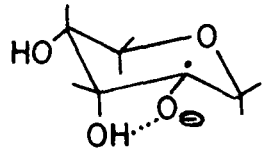

radicals at carbon atoms containing equatorial hydroxyl groups would make the formation of AR3-C1, AR4-1C, and AR2-1C unimportant relative to the other three AR species. This concept is also consistent with the postulate that the hydroxyl radical (HO•) is not an important radical species in the reactions under investigation. If it were, abstraction of hydrogen from the unionized carbohydrate [Equation (13)], followed by reaction with oxygen [Equation (17)] to form $AO_2^{\bullet}$, would be important. This reaction would not have the stereospecificity previously discussed. The result in the AR reaction would be hydroperoxy radicals stabilized by hydrogen bonding and autoinhibition similar to that found in the AX system.

Another factor which could contribute to the stereospecificity of the reaction of $A^{\bullet}$ and oxygen [Equation (16)] is that the reaction is very rapid, having essentially a zero activation energy (38,39,67). Once formed, $A^{\bullet}$ would

react rapidly with oxygen in its vicinity, perhaps before the radical has a chance to invert.

The reaction of the hydroperoxy anion to form the carbonyl [Equation (35)] is postulated to proceed through a cyclic mechanism. Hydrogen bonding of the

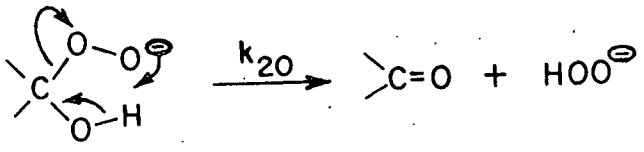

(35)

hydroperoxy anion with the hydroxyl group on the adjacent carbon atom would greatly hinder carbonyl formation via the cyclic mechanism shown, resulting in stabilization of the anion. The reaction of the anion with water to form the alpha-hydroxyhydroperoxide [Equation (20)] would also be hindered because of hydrogen bonding. Thus, the concentrations of $^{-}$AOOH and AOOH^{-}, other conjugate bases of the alpha-hydroxyhydroperoxide [Equations (22) and (23)] which react to form products [Equations (24)-(27)], decrease. In conclusion, intramolecular hydrogen bonding can potentially account for the stabilization of the alpha-hydroxyhydroperoxy anion by decreasing the rates of subsequent reactions which lead to acidic degradation products.

Autoinhibition Mechanism

Autoinhibition in the AX system is postulated to be the result of termination reactions [Equations (33) and (34)] which do not produce radical species or the perhydroxyl anion (HOO^{-}). As previously discussed, this adversely affects the free radical reactions. Consequently, the carbohydrate degradation rate is decreased, resulting in autoinhibition. Evidence for the formation of dialkyl peroxides (AOOA) [Equation (33)] is presented in Fig. 14. The organic peroxide curve is explained as a rapid build-up and subsequent degradation of alpha-hydroxyhydroperoxides in conjunction with slow formation of dialkyl peroxides.

The relatively slow rate of AOOA formation is accounted for by the low concentration of A• in solution. Since the hydroxyl free radical (HO•) does not seem to be an important intermediate, formation of A• probably occurs mainly through the reaction of $A^{\overline{\bullet}}$ and water [Equation (12)], as opposed to the reaction of the unionized carbohydrate with HO• [Equation (13)]. Because of the very rapid reaction of $A^{\overline{\bullet}}$ with oxygen, the concentration of A• should be relatively low compared to AO_2•. Thus, the termination reaction [Equation (33)] to produce dialkyl peroxides should be slow relative to the self-termination of AO_2• that produces a carbonyl moiety, oxygen, and AOOH [Equation (34)].

Because the reaction of $A^{\overline{\bullet}}$ and oxygen is extremely rapid, only hydroperoxy radicals are of importance in chain termination reactions at high partial pressures of oxygen (39). At relatively low concentrations of hydroperoxides, the rate of decomposition is generally first order in hydroperoxide (39); owing to unimolecular decomposition reactions, e.g., Equations (21) and (24)-(27). At higher concentrations, there are substantial deviations (39) caused by the increasing importance of bimolecular decompositions [Equation (34)]. The bimolecular decomposition has a lower activation energy than the unimolecular decomposition (60). Therefore, as the concentration of hydroperoxide increases, the bimolecular decomposition attains greater importance because of probability and thermodynamic considerations. Actually, the viability of the bimolecular reaction depends on the concentration of hydroperoxy radicals (AO_2•) and not on the concentration of hydroperoxide (or its conjugate bases) itself. The concentration of AO_2• is related to the concentration of AO_2^- through the reaction with metal ion [Equation (19)]. Therefore, increasing the concentration of AO_2^- via stabilization (hydrogen bonding) subsequently increases the concentration of AO_2•.

Another factor that could increase the concentration of $AO_2\cdot$ is hydrogen bonding. Rust and Youngman (68) have noted a substantial modification of peroxy radical properties by the proximity of a hydroxyl group. In studying the autoxidation of various pentane diols (68), it was concluded that when sterically feasible, intramolecular hydrogen bonded radicals were the important product determinants. It was also reasoned that subsequent peroxy radical-peroxy radical interactions assumed increased importance because of the augmented radical stability brought about by hydrogen bonding. The final products were nonradical in nature, without the formation of hydrogen peroxide.

In the AX system, hydroperoxy radicals ($AO_2\cdot$) can be imagined to hydrogen bond with hydroxyl groups on adjacent carbon atoms in a manner similar to AO_2^- as previously discussed. Such hydrogen bonding is not sterically favored in the AR system. As in the systems investigated by Rust and Youngman (68), it is proposed that hydrogen bond-enhanced radical stability in the AX reaction also aids radical-radical termination reactions [Equation (33)] to produce nonradical products. This would cause a decrease in the rate of carbohydrate degradation which manifests itself as autoinhibition.

Based on the previous discussion, the inhibiting effect of the stabilized hydroperoxy radical should become greater as the concentration of hydroperoxide increases. From Fig. 14, the hydroperoxide concentration is greatest at very early reaction time. Figures 12 and 13 show that, as predicted, the order with respect to carbohydrate in the AX system is greatest at early reaction times corresponding to the highest concentration of hydroperoxides.

The autoinhibition mechanism should apply to other carbohydrates in which the hydroxyl groups are in the "xylo" configuration (vicinal hydroxyl groups at C-2, C-3, and C-4 trans to one another). The differential method

of kinetic analysis used in this investigation was applied to methyl β-D-glucopyranoside degradation data obtained by McCloskey [0.01N carbohydrate, 1.25N alkali, 74.5 psi oxygen pressure (25°C), and 120°C] (18) and Sinkey [0.031M carbohydrate, 1.25N alkali, 75 psi oxygen pressure (25°C), and 120°C] (19) (Fig. 39). As seen from Fig. 39, the order with respect to methyl β-D-glucopyranoside is 2.9 in both cases. This is consistent with the AX orders (3.0→3.5) found in the present investigation. Also in agreement with the AX system, Sinkey's data rise to higher orders at early reaction times. McCloskey's data do not rise because kinetic samples were not taken at early reaction times (less than 6 hours).

As stated previously, no definite conclusions regarding the MAX reaction order could be reached. However, the reaction does produce detectable organic peroxides at early reaction times (probably hydroperoxides) (Fig. 16). The hydroperoxide can be stabilized by hydrogen bonding to the C-3 methoxyl group.

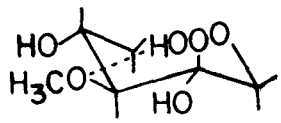

It has been shown that methoxyl groups are better hydrogen bond formers than hydroxyl groups (63), although weaker than carbinolate ions. However, unlike the AX system, the corresponding hydroperoxy radical in the MAX reaction cannot be stabilized. Therefore, the concentration of the hydroperoxy radical (which is related to the hydroperoxide concentration) is increased because of stabilized hydroperoxides; but hydrogen bonding does not stabilize the radical itself. It is postulated that the MAX reaction order with respect to the alditol is between two and three; but closer to two since the hydroperoxy radical concentration is probably less in the MAX system than it is in the AX system.

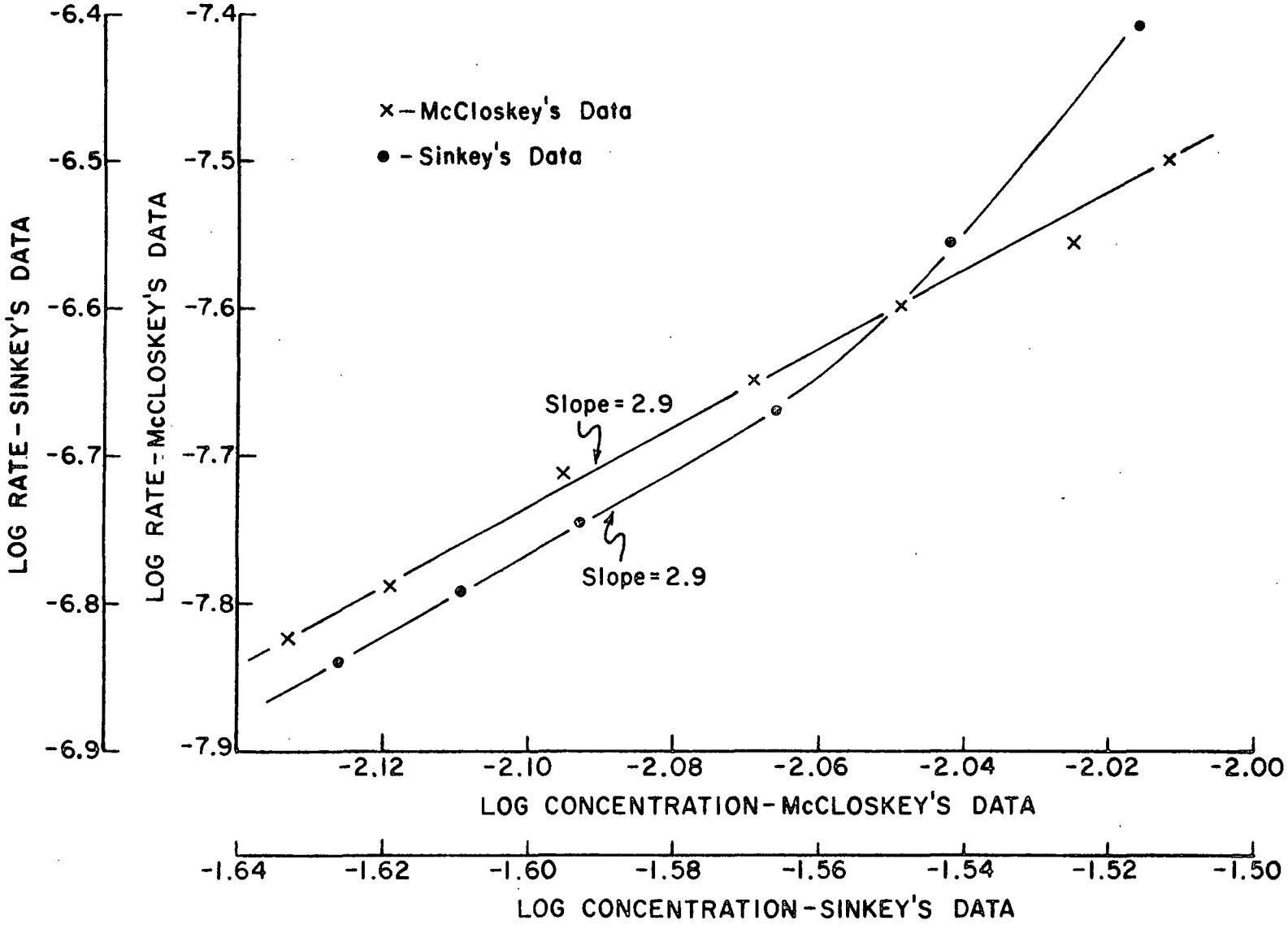

Figure 39. Representative Degradations of Methyl-D-glucopyranoside (x - McCloskey's Data at 0.01N Carbohydrate; ⊙ - Sinkey's Data at 0.031N Carbohydrate) in 1.25N NaOH at 120°C and 75 PSI Oxygen Pressure (25°C). Data Plotted According to the Differential Method

FORMATION OF ACIDIC REACTION PRODUCTS

All reaction products are postulated to form via $^{-}$AOOH, AOOH^{-}, and/or carbonyl intermediates (Fig. 36). Once a carbonyl is introduced into an alditol ring, rapid alkaline rearrangement can shift the carbonyl moiety to any carbon atom containing a hydroxyl group. The carbohydrate ring can then cleave to form acidic products. However, before cleavage, a second carbonyl can be introduced adjacent to the first, followed by carbon-carbon cleavage to form dibasic acids. The alpha-dicarbonyl intermediate can also undergo a benzylic acid-type rearrangement to produce 1,4-anhydro-2-C-carboxy-tetritols. The tetritols are also postulated to form via stereoselective reactions as proposed earlier (Fig. 35). Formation of the tetritols is a major reaction pathway in the AX and AR systems. Figures 40 and 41 illustrate possible reeaction pathways for the formation of the acidic products identified in the AX and AR reactions. No plausible route could be found for the formation of 2,4-dihydroxybutyric acid (a minor degradation product).

Ring cleavage by the following process seems to be a viable reaction pathway:

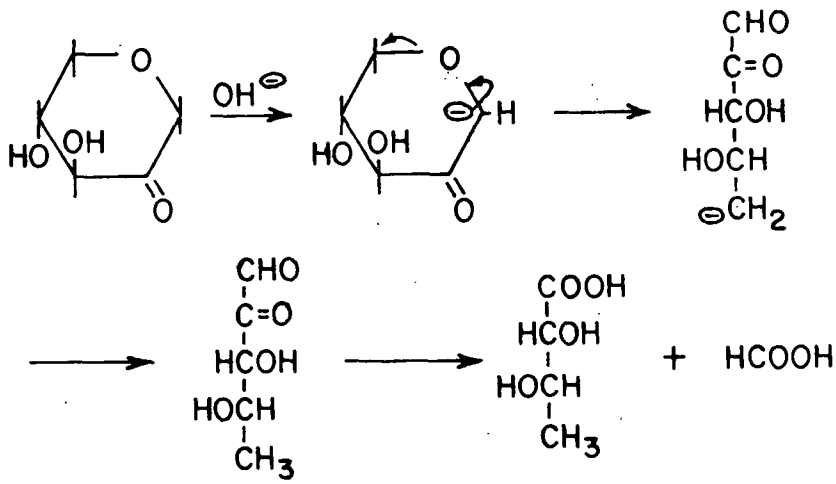

The scheme accounts for the formation of 2,3-dihydroxybutyric acid in the AR and AX systems. The pathway also accounts for the production of 3-hydroxy-2-methoxy-butyric acid in the MAX reaction. This compound is the analog of

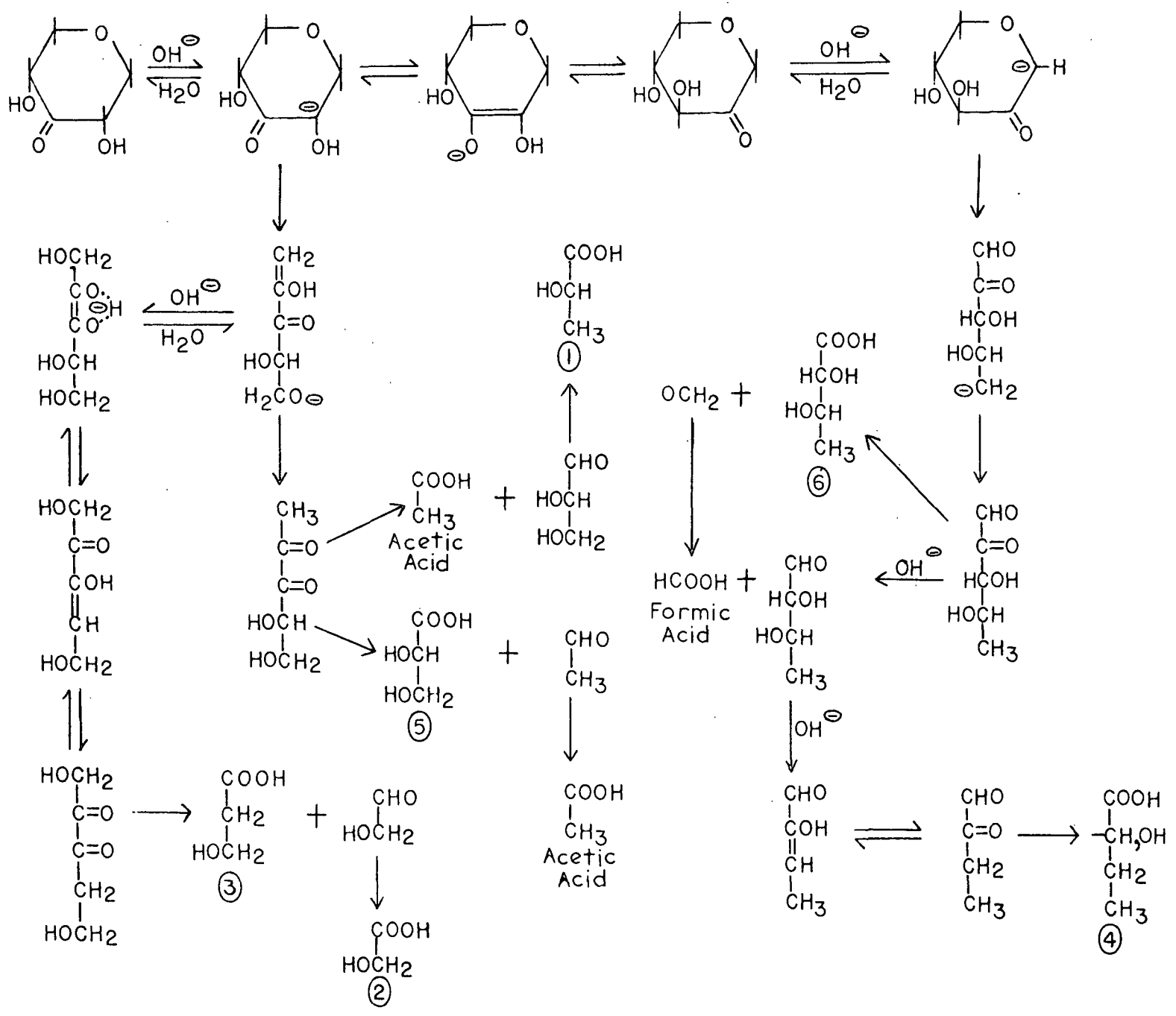

Figure 40. Possible Degradative Pathways for Product Formation Involving the C-2 and C-3 Carbonyl Functions (AX and AR Systems)

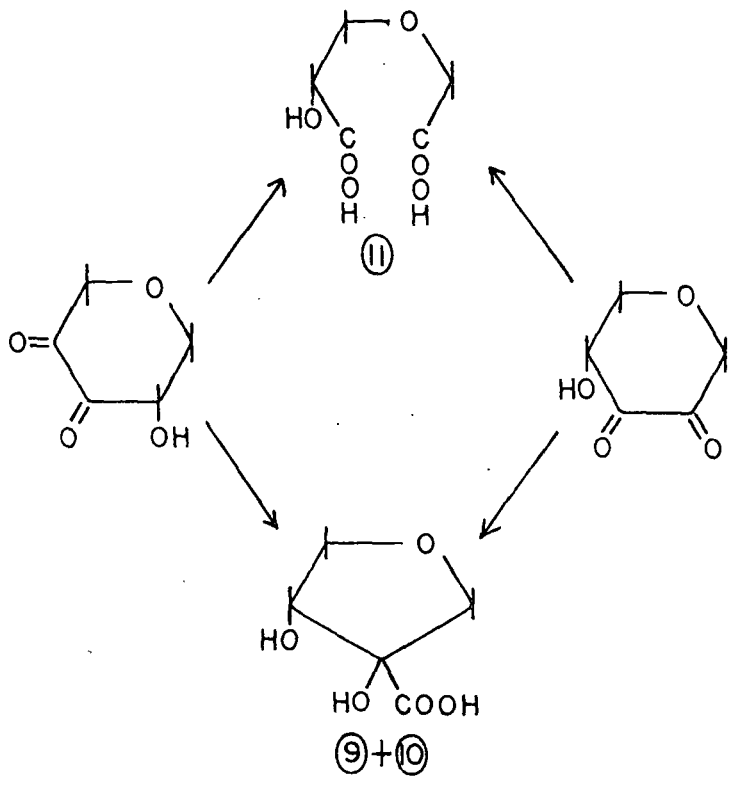

Figure 41. Possible Degradative Pathways for Product Formation Involving the Alpha-Dicarbonyl Intermediate (AX and AR Systems)

2,3-dihydroxybutyric acid in the AX and AR system and is the only major product produced during the MAX degradation. It should also be noted that formic acid was detected in the MAX reaction. This is consistent with the above reaction scheme. The scheme could also be pictured as a free radical reaction in which a reactive radical species abstracts a C-1 hydrogen. One electron shifts produce a primary free radical as the leaving group. A primary free radical, although

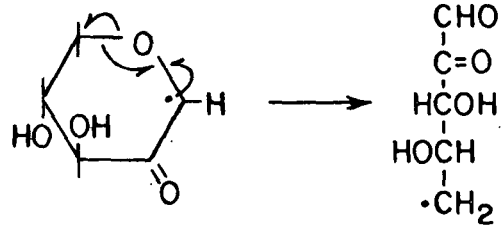

least stable of all free radicals, is much less energetic than a primary carbanion. The primary free radical is considered as a viable leaving group in free radical reactions (59,69).

CONCLUSIONS

The results obtained from the model compounds (AR, AX, and MAX) by molecular oxygen in alkaline medium indicate that the configuration, as well as the number, of hydroxyl groups present on the pyranoid ring influence the rate and mode of degradation. The order of reactivity of the alditols was AR>AX>MAX. The AR system was second order in carbohydrate with respect to time, while AX displayed a complex relationship indicative of autoinhibition by a reactive intermediate. The intermediate is postulated to be an alpha-hydroxyhydroperoxy free radical ($AO_2\cdot$) which is stabilized via hydrogen bonding in the AX system. The radical is also involved in a reversible reaction with the alpha-hydroxyhydroperoxy anion (AO_2^-), which is stabilized via hydrogen bonding. Thus, hydrogen bonding of $AO_2\cdot$ and AO_2^- causes an increase in the concentration of $AO_2\cdot$ and subsequently, increases the importance of $AO_2\cdot$ self-termination reactions. The complex kinetics of the AX reaction are proposed to result from these self-termination reactions between alpha-hydroxyhydroperoxy radicals which produce only nonradical species, causing an abnormal decrease in the rate of the free radical propagation reactions which kinetically manifests itself as autoinhibition. No definite conclusions were reached regarding the order of the MAX reaction with respect to the alditol.

The acidic degradation products of the AX and AR reactions were identical. Of the seven major acids formed in the two systems, those having vicinal glycol groups (glyceric, 2,3-dihydroxybutyric, 1,4-anhydro-2-C-carboxy-tetritols, and 3-O-carboxymethyl-glyceric acids) were nontermination products. Lactic and glycolic acids, not having vicinal glycol groups, were termination products (rate of formation $\geq$ rate of degradation at all times). However, there was no apparent inhibition related to any of the acidic degradation products. The

only major product formed in the MAX reaction was 3-hydroxy-2-methoxybutyric acid. This demonstrates that ring cleavage between C-5 and the ring oxygen is a viable reaction pathway during the degradation of carbohydrates by molecular oxygen in alkali. Major differences in the relative ratio of 1,4-anhydro-2-C-carboxy-D-, and -L-, erythritol and threitol between the AX and AR reactions indicate that, besides the alpha-dicarbonyl, another intermediate with a stereochemical directing effect acts as a precursor to these furanoid acids.

A mechanism proposed for the alkaline oxygen degradation of the model compounds accounts for an induction period, the formation of hydrogen peroxide and organic peroxides, the kinetics of the AX and AR systems, and the formation of final acidic degradation products. Assuming that the proposed mechanism is operative, several interesting conclusions can be reached. The AR reaction was second order in carbohydrate. Therefore, the second term of the derived kinetic expression [Equation (36)] must predominate over the other two terms.

$$-d[A]/dt = K_6k_7[A][OH^-][O_2] + K_6^2k_7k_{14}[A]^2[OH^-]^2[O_2]/k_{27}[M^{+n+1}] + K_6k_7k_9[H_2O][A][OH^-][O_2]/k_{27}[M^{+n+1}] \quad (36)$$

Hence, under the reaction conditions studied, the AR degradation would be predicted to have a second order dependence on hydroxide ion concentration. No experimental evidence is available to verify this supposition. Also, the hydroxyl radical does not seem to play a major role in the mechanism. If it did, a mixed carbohydrate order between one and two would be expected.

EXPERIMENTAL

GENERAL ANALYTICAL PROCEDURES

Melting points were determined on a Thomas Hoover capillary melting point apparatus which had been calibrated against known compounds.

A Perkin-Elmer 141 MC recording polarimeter was used to measure optical rotations.

Thin-layer chromatography (TLC) was done on microscope slides coated with Silica gel G (Brinkman Instruments, Inc.). Detection was accomplished with methanolic sulfuric acid spray (20%, v/v) and subsequent charring. Developing solvents were as follows: Solvent 1 — chloroform:ethyl acetate, 2:1, v/v; Solvent 2 — chloroform:ethyl acetate, 19:1, v/v; Solvent 3 — benzene:methanol, 3:1, v/v.

Gas-liquid chromatography (GLC) studies were done on a Varian Aerograph 1200 gas chromatograph equipped with a hydrogen flame ionization detector and a Honeywell Electronic 16 recorder with a Disc integrator. Prepurified nitrogen (Matheson Gas Products) was used as the carrier gas. Column descriptions and operating conditions are given in Appendices II and IV.

Mass spectral analyses were done on a Dupont 21-491 mass spectrometer interfaced via a jet separator with a Varian Aerograph 1400 gas chromatograph equipped with a hydrogen flame ionization detector and a Hewlett-Packard 7128A recorder. Helium (UHP Helium, minimum purity 99.999%; Matheson Gas Products) was used as the carrier gas. Mass spectra were recorded with a Century GPO 460 oscillographic recorder. Chromatographic conditions and mass spectrometer control settings are reported in Appendix IV.

Colorimetric analyses were performed on a Beckman DU spectrophotometer.

SOLUTIONS, REAGENTS, AND CATALYSTS

Ethanol (70), ethyl acetate (71), pyridine (71), and triethylamine (71) were purified according to standard procedures. Triply-distilled water (72) was prepared according to standard procedure.

SODIUM HYDROXIDE STOCK SOLUTION

A 50% (w/w) solution of sodium hydroxide in triply-distilled water was prepared from reagent grade pellets. Most transition metal ions were eliminated from the solution by complexation with phenyl-2-pyridyl ketoxime as described by Trusell and Diehl (73). The final solution was boiled for 15 minutes and stored in a paraffin-lined glass bottle.

SODIUM THIOSULFATE SOLUTION (19)

Anhydrous sodium thiosulfate (5.0 g) and sodium carbonate (0.2 g) were dissolved in triply-distilled water (2 liters). The solution was shaken, allowed to stand for one day, and then standardized against a standard solution of potassium iodate using starch indicator.

TITANIUM SULFATE REAGENT (21)

Titanium sulfate (10.0 g, $TiOSO_4 \cdot H_2SO_4 \cdot 8H_2O$, Fisher Scientific Co.) was dissolved in concentrated sulfuric acid (10 ml) and diluted to 100 ml with triply-distilled water. After standing for 1 day, the solution was filtered and stored in a glass bottle.

PALLADIUM ON CHARCOAL CATALYST (10%)

The catalyst was prepared as described by Mozingo (74). The powdered catalyst was stored in a desiccator over calcium chloride.

RANEY NICKEL CATALYST (W-2 TYPE)

Raney nickel catalyst was prepared as an aqueous slurry according to the method of Mozingo (75). The water was exchanged for absolute ethanol, and the ethanolic slurry was stored in a bottle for later use.

SILVER OXIDE CATALYST

The catalyst was prepared as described by Bayer (76) with a modification to the washing procedure. Once the catalyst was prepared, it was washed with hot water (to a negative sliver test), acetone, and petroleum ether (b.p. 30-60°C), dried *in vacuo* (50°C), and stored in a foil-covered bottle.

SYNTHESIS OF COMPOUNDS

1,5-ANHYDROXYLITOL (AX)

1,2,3,4-Tetra-*O*-acetyl-D-xylopyranose (I) (180.7 g as a sirup) [prepared from D-xylose by acetylation with pyridine-acetic anhydride (77)] was reacted with 32% (w/w) hydrogen bromide-acetic acid solution (140 ml) for 1 hour (78). The reaction was followed by TLC using Solvent 1. The reaction mixture was diluted with 1,2-dichloroethane (300 ml), washed with ice water (3 x 200 ml), dried ($CaCl_2$), and filtered. The 2,3,4-tri-*O*-acetyl-α-D-xylopyranosyl bromide (II) was not crystallized.

The 1,2-dichloroethane solution of (II) was added to ethanolic potassium hydroxide (1000 ml, 0.61N) containing thiophenol (65 ml) and heated on a steam bath for 45 minutes (77) (TLC-Solvent 1). The clear liquid, with its deposit of potassium bromide, was washed with water (200 ml), aqueous sodium hydroxide (3 x 200 ml, 0.3N), and water (200 ml), dried ($CaCl_2$), and concentrated *in vacuo* to a thick sirup. Crystallization from absolute ethanol yielded phenyl 2,3,4-tri-O-acetyl-1-thio-β-D-xylopyranoside (III) (168.0 g, 80.0%); m.p. 77-78°C, $[\alpha]_D^{20}$ -60.0° ($CHCl_3$). Literature: m.p. 78-79°C, $[\alpha]_D^{20}$ -60.8° ($CHCl_3$) (78).

Compound III (82.4 g) was dissolved in absolute ethanol (450 ml). Raney nickel catalyst (200.0 g) was added to the solution and the mixture was warmed (60-65°C) for 2.5 hours (79) (TLC-Solvent 1). The catalyst was removed by filtration (Celite), and washed with hot absolute ethanol (2 x 100 ml) and acetone (100 ml). The clear filtrate and washings were concentrated *in vacuo* to a sirup. Crystallization from absolute ethanol afforded 2,3,4-tri-O-acetyl-1,5-anhydroxylitol (IV) (49.4 g, 84.7%); m.p. 121-123°C, $[\alpha]_D^{20}$ 0° ($CHCl_3$). Literature: m.p. 122-123°C, $[\alpha]_D^{20}$ 0° ($CHCl_3$) (79).

Compound IV (46.8 g), dissolved in methanol (500 ml), was deacetylated with methanolic sodium methoxide (50 ml, 1%, w/w) (TLC-Solvent 1). The reaction solution was treated with Amberlite IR-120 (H^+) resin until neutral, decolorized, filtered through Celite, and concentrated *in vacuo* to a sirup. The sirup was dissolved in aqueous sodium hydroxide (5 ml, 0.1N). After 0.5 hours at room temperature, the solution was treated with Amberlite MB-3 resin until neutral, decolorized, filtered through Celite, and concentrated *in vacuo* to a sirup. Crystallization from absolute ethanol yielded 1,5-anhydroxylitol (AX) (21.9 g, 90.8%); m.p. 115-116°C, $[\alpha]_D^{20}$ 0° (H_2O). Literature: m.p. 116-117°C, $[\alpha]_D^{20}$ (H_2O).

1,5-ANHYDRORIBITOL (AR)

D-Ribopyranose (V) (76.0 g) was reacted for 45 minutes at 0°C with a mixture of pyridine (304 ml), benzoyl chloride (293 ml), and 1,2-dichloroethane (630 ml) which had been previously chilled to -20°C using acetone-dry ice (80). After refrigeration overnight, the reaction mixture was left at room temperature for 5 hours (TLC-Solvent 2). The reaction mixture was poured into ice and water, agitated, diluted with chloroform (1000 ml), washed with ice cold sulfuric acid (3 x 500 ml, 3N), saturated sodium bicarbonate (2 x 500 ml), and distilled water (3 x 500 ml), and dried (Na_2SO_4). The solution was filtered through a bed of decolorizing carbon and concentrated in vacuo to a clear sirup. The 1,2,3,4-tetra-O-benzoyl-β-D-ribopyranose (VI) could not be crystallized.

Compound VI (363.8 g as a sirup) was dissolved in 1,2-dichloroethane (910 ml) and reacted with 32% hydrogen bromide-acetic acid solution (200 ml) for 2.5 hours (81) (TLC-Solvent 2). The reaction mixture was diluted with chloroform (500 ml), washed with ice water (3 x 500 ml), dried ($CaCl_2$), and concentrated in vacuo (40-45°C bath). The sirupy 2,3,4-tri-O-benzoyl-β-D-ribopyranosyl bromide (VII) was dissolved in diethyl ether (700 ml) and crystallization was initiated with petroleum ether (b.p. 30-60°C) (213.8 g, 80.3%); m.p. 150-141°C, $[\alpha]_D$ -198° ($CHCl_3$). Literature: m.p. 151-153°C, $[\alpha]_D$ -199° ($CHCl_3$) (80).

Compound VII (13.4 g), in absolute ethyl acetate (160 ml), was reacted with palladium on charcoal catalyst (1.0 g) and triethylamine (9 ml) in a Paar bomb under 50 psi hydrogen pressure for 24 hours (81) (TLC-Solvent 2). The reaction mixture was filtered through Celite and the residue was washed with chloroform. The filtrate was washed with hydrochloric acid (2 x 200 ml, 0.5N), saturated sodium bicarbonate (2 x 200 ml), and distilled water (2 x 200 ml).

The solution was shaken with silver nitrate (10 ml, 3% in aqueous acetone), dried ($CaCl_2$), filtered through Celite, and concentrated *in vacuo* to a thick sirup (11.3 g). In all, 66.4 g of 2,3,4-tri-*O*-benzoyl-1,5-anhydroribitol (VIII) were prepared this way.

Compound VIII (66.0 g as sirup), dissolved in methanol (600 ml) and chloroform (30 ml), was debenzoylated with methanolic sodium methoxide (10 ml, 1%, w/w) (TLC-Solvent 2). After 19 hours the reaction solution was treated with Amberlite IR-120 (H^+) resin until neutral, decolorized, filtered through Celite, and concentrated *in vacuo* to a clear sirup (18.2 g). The sirup was dissolved in aqueous sodium hydroxide (200 ml, 0.125*N*) and refluxed for 2 hours. The solution was neutralized with Amberlite MB-3 resin, decolorized, filtered through Celite, and evaporated *in vacuo* to a clear sirup. Crystallization from absolute ethanol-ethyl acetate (50:50, v/v) afforded pure 1,5-anhydroribitol (AR) (13.6 g, 80.1%); m.p. 128-129°C, $[\alpha]_D$ 0° (H_2). Literature: m.p. 128-129°C, $[\alpha]_D$ 0° (H_2O) (80).

3-*O*-METHYL-1,5-ANHYDROXYLITOL (MAX)

Compound AX (20.0 g), dissolved in dimethylformamide (500 ml), was treated with methyl iodide (14.3 ml) and silver oxide catalyst (66.0 g, in increments over a 48-hr period). At approximately 90% reaction of AX (estimated by TLC-Solvent 3), the major product was the monomethylated derivative with a substantial amount of the di-*O*-methyl-1,5-anhydroxylitol present. The reaction mixture was decolorized, filtered through Celite, and concentrated *in vacuo* to a clear sirup (24.2 g), the mixture was then separated by column chromatography on Silica gel (Sargent Welch, 60-200 mesh) using Solvent 3 as the elution solvent. The second component eluted was a mixture of monomethyl (2, 3, and 4-*O*-methyl)-1,5-anhydroxylitols (clear sirup upon concentration, 16.2 g).

The sirup (16.2 g) was dissolved in aqueous sodium metaperiodate (250 ml, 0.33N) contained in a light-protected beaker, allowed to stand at room temperature for 24 hours, and treated with Amberlite MB-3 resin to remove all ions from solution. The volume of the solution was increased to 800 ml (distilled water) and bromine was added (10 ml) (to oxidize the aldehydes to acids); the solution was shaken intermittently for 2 hours and allowed to stand at room temperature for 15 hours. Excess bromine was removed by aeration. The solution was treated with aqueous silver nitrate, filtered through Celite, treated with Amberlite MB-3 resin, and evaporated *in vacuo* to a clear, colorless sirup (3.7 g). The sirup of 3-O-methyl-1,5-anhydroxylitol (MAX) was dissolved in ethyl acetate and crystallization was initiated with petroleum ether (b.p. 30-60°C) (2.6 g, 11.8%); m.p. 104-105°C, $[\alpha]_D$ 0° (H_2O). Literature: m.p. 105-106°C, $[\alpha]_D$ 0° (H_2O) (82).

(±)-ERYTHRO-2,3-DIHYDROXYBUTYRIC ACID (83)

Hydrogen peroxide solution (30%, 106 ml) containing tungstic acid (0.54 g) was added in portions over 10 minutes to a hot (50°C), vigorously stirred aqueous solution (500 ml) of *trans*-crotonic acid (86.0 g). The reaction temperature was raised to 70°C for 4 hours. The mixture was cooled to room temperature and extracted with chloroform (2 x 250 ml). The chloroform extracts were back-extracted with distilled water (2 x 200 ml). The reaction solution and the aqueous extracts were combined, filtered, and concentrated *in vacuo* (50°C) to a clear, colorless sirup. The sirup was dissolved in an equivalent volume of boiling ethyl acetate (anhydrous) and refrigerated. Crystallization produced (±)-erythro-2,3-dihydroxybutyric acid (52.6 g, 43.8%); m.p. 79-81°C. Literature: m.p. 80-83°C (83).

KINETIC ANALYSIS

CONDITIONING OF REACTOR AND GLASSWARE

Prior to each kinetic experiment, all teflon surfaces of the reactor that would come into contact with the reaction solution (inside of reactor, reactor cover, and sampling lines) and all glassware used to prepare the reaction solution were washed successively with aqueous sodium hydroxide (5%, w/w, 80°C), distilled water, hydrochloric acid (5%, w/w, 80°C), nitric acid (5%, w/w, 80°C), several times with triply-distilled water, and dried.

PREPARATION OF REACTION SOLUTIONS

Triply-distilled water was boiled for 10 minutes and allowed to cool to room temperature while being purged with nitrogen. Sodium hydroxide stock solution (ca. 35.5 g) was mixed with a portion of this water (ca. 300 ml) under a nitrogen atmosphere. The inert atmosphere was provided by a glove bag in which the air had been replaced by prepurified nitrogen (Matheson Gas Products, Inc.) maintained at a slightly positive pressure. The alkaline solution was titrated against potassium acid phthalate and, if necessary, the proper adjustment was made to attain 1.25N sodium hydroxide. The solution was then retitrated to confirm the results. A portion of the solution (ca. 200 ml) was weighed and, from the density (1.0529 g/ml), the volume calculated. The proper amount of carbohydrate (depending on the desired concentration) was dissolved in the solution, which was then ready for loading into the reactor.

LOADING THE REACTOR

The solution was placed in the reactor (under a nitrogen atmosphere); the reactor was sealed, bolted into place on the oil bath, lowered into the oil, and heated to reaction temperature.

SAMPLING

After attaining the desired reaction temperature, the sampling lines were purged by drawing a sample which was discarded. A time-zero sample was taken and then the reactor was pressurized with oxygen to initiate the reaction*. At the desired sampling times the sampling system was purged, and duplicate samples were drawn into tared, 4-ml vials. The precise amount of sample and internal standard (added as an aqueous solution) was determined gravimetrically.

The samples (ca. 1.5 ml) (containing internal standard) were deionized over an Amberlite MB-3 column (6-8 ml) and eluted with triply-distilled water (20 ml). The eluate was concentrated in vacuo to a small volume (ca. 2 ml) in a pear shaped flask (100 ml), transferred to an Erlenmeyer flask (10 ml, GGS), and concentrated to dryness.

ACETYLATION

The dried samples were acetylated with a mixture of dry pyridine (0.75 ml) and acetic anhydride (0.25 ml) with mechanical shaking. After 18 hours, distilled water (8 ml) was added to the acetylation mixture, and the mixture was shaken for 0.5 hours. The aqueous mixture was extracted with chloroform (2 x 5 ml). The combined chloroform extracts were washed with hydrochloric acid (15 ml, 1N) and distilled water (10 ml), dried (Na_2SO_4), decanted, and concentrated in vacuo to dryness. The acetylated sample was dissolved in chloroform (0.2-1.0 ml) and analyzed (in triplicate) by GLC (Appendix II). In the case of 3-O-methyl-1,5-anhydroxylitol (MAX), the water solubility of the partially methylated-partially acetylated material was such that a modified work-up procedure was used (84). The aqueous mixture of acetates was extracted with chloroform (4 x 5 ml)

*Calculation of the actual gage pressure can be found in Institute Research Notebook No. 2984.

and the combined chloroform extracts were washed with hydrochloric acid (15 ml, 2N) saturated with sodium chloride, and water (10 ml) saturated with sodium chloride. The aqueous phase at each step was back-extracted with chloroform (5 ml) and the chloroform phases combined for the succeeding stage. Sample chromatograms are shown in Fig. 40.

PEROXIDE ANALYSIS

Peroxide analyses were performed using a chlorimetric method involving a titanium complex (30,85-88). A straight-line calibration curve [peroxide concentration versus absorbance (Appendix III, Fig. 46)] was obtained by analyzing various hydrogen peroxide concentrations by the iodine-thiosulfate titration technique (89), and by the titanium sulfate colorimetric method (Appendix III).

SAMPLING AND ANALYSIS

At the desired sampling times, the sampling lines were purged and a sample (3.2 ml) drawn into a beaker. An aliquot (1 ml) of the peroxide test solution was placed in each of 3 volumetric flasks (10 ml). The solutions were neutralized (ca. pH 7) with sulfuric acid (0.5N), followed by addition of the titanium sulfate reagent (4 drops, bringing the solution to ca. pH 1.0). For the hydrogen peroxide analysis the sample was diluted to volume with distilled water, and the absorbance at 420 nm was determined within 0.5 hours of sampling. For the organic peroxides the remaining 2 samples were diluted to volume with distilled water, and the absorbancies taken over a period of 1.5 days, with the maximum occurring between 20-28 hours.

PRODUCT ANALYSIS

The major tool employed for product analysis was GLC-MS of the trimethylsilyl (TMS) derivatives of the acidic reaction products. The TMS derivatives were

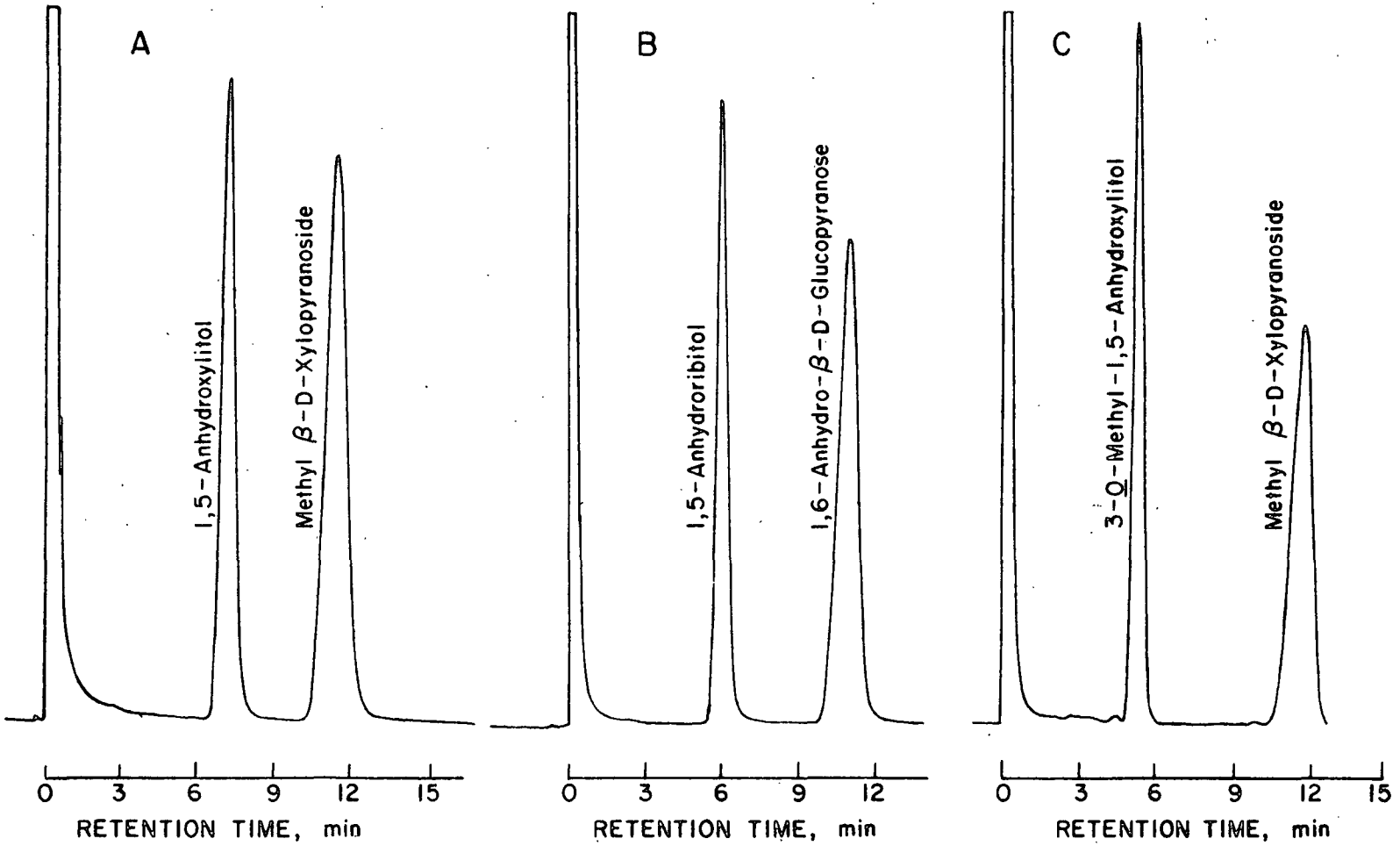

Figure 42. Sample Chromatograms for Kinetic Analyses of: A - 1,5-Anhydroxylitol; B - 1,5-Anhydroribitol; C - 3-O-Methyl-1,5-anhydroxylitol

prepared via a two-phase system involving dimethylsulfoxide and Tri-Sil Concentrate (Pierce Chemical Co.).

TRIMETHYLSILYLATION

At the completion of selected kinetic trials, the remaining reaction solution was eluted through an appropriate size column of IR-120 (H^+) resin. The resin was washed with distilled water and the combined eluates were concentrated *in vacuo* to a sirup (as much water as possible was removed as an azeotrope of 1,2-dichloroethane). The sirup was dissolved in dimethylsulfoxide (0.3 ml, silylation grade, Pierce Chemical Co.), transferred to a Reacti-Vial (Pierce Chemical Co.), treated with Tri-Sil Concentrate (0.5 ml), and shaken for 1 hour. Samples of the Tri-Sil Concentrate (top layer of the two-phase system containing the TMS derivatives) were drawn off with a microsyringe and analyzed directly by GLC (Appendix II). Sample chromatograms are shown in Fig. 17-19.

MASS SPECTRAL ANALYSIS

All major reaction products were analyzed by GLC-MS (see Appendix IV for GLC and MS control settings) as their TMS derivatives, employing a standard (heptacosafluorotributylamine, alone and in conjunction with each compound) to facilitate mass marking. The fragmentation patterns of the neutral carbohydrates (AX, AR, and MAX) were determined employing the nomenclature devised by Kochetkov and Chizhov (49). For the mass spectra and relative abundance data of all compounds analyzed, see the Results and Discussion section and Appendix IV, Tables VII-XVIII, respectively. When the presence of the parent ion was in doubt, a lower ionizing voltage (*ca.* 7.5 ev) was used to enhance the molecular ion (since this ion has the lowest appearance potential) relative to the other peaks in the spectrum. Where possible, mass spectra and GLC retention times of authentic samples were used to verify the reaction products' identities.

SEMIQUANTITATIVE PRODUCT ANALYSIS

The sampling procedure was as described previously (see Sampling) except that the alkaline solution of products and internal standard (ca. 3.0 ml) was deionized over Amberlite IR-120 (H^+) resin (5 ml) and concentrated to a sirup in a 4-ml vial. Trimethylsilylation of the products and internal standard was as described previously (see Trimethylsilylation) except that the samples were shaken for 24 hours to ensure complete derivatization. Sample chromatograms of the AX and AR reaction products (including internal standard) are shown in Fig. 17 and 18, respectively.

PREPARATION OF BENZYL ESTERS OF FORMIC AND ACETIC ACIDS (90)

The alkaline solution (ca. 3.0 ml) containing formic and acetic acids was deionized by passing it through a column of Amberlite IR-120 (H^+) resin (5 ml). The column was eluted with distilled water (3 x 5 ml) and the combined eluate was titrated to ca. pH 8 with tetra-n-butyl ammonium hydroxide (0.03M). The solution was concentrated in vacuo to a sirup, dissolved in anhydrous acetone, treated with benzyl bromide, allowed to stand for 2 hours, and injected directly into the gas chromatograph for analysis (Appendix II).

METAL ION DETERMINATIONS

Samples taken after the trials on AX, AR, and MAX (at 0.1N carbohydrate) were analyzed by the Analytical Department using atomic absorption techniques for the following metals: cadmium, cobalt, copper, chromium, iron, magnesium, manganese, nickel, and zinc. Results are reported in Appendix V, Table XXVII.

NOMENCLATURE

AX	1,5-anhydroxylitol
AR	1,5-anhydroribitol
MAX	3-O-methyl-1,5-anhydroxylitol
GLC	gas-liquid chromatography
TLC	thin-layer chromatography
MS	mass spectrometry
GLC-MS	gas chromatography-mass spectrometry
M	molar, moles/liter
N	normality, equivalents/liter
TMS	trimethylsilyl derivative
m.p.	melting point
b.p.	boiling point
w/w	weight to weight ratio
v/v	volume to volume ratio
m/e	mass to charge ratio (mass spectrometry)
psi	pounds/square inch
$[\alpha]_D$	specific optical rotation at 589 nm

ACKNOWLEDGMENTS

The author gratefully acknowledges the assistance and encourgement of his Thesis Advisory Committee: Drs. L. R. Schroeder, Chairman, D. C. Johnson, and N. S. Thompson. In particular, the author extends his deepest appreciation to Dr. Schroeder, not only for his professional guidance but also for his personal friendship. The invaluable aid of Messrs. M. C. Filz and P. E. Van Rossum in constructing the reaction system is appreciated. To other faculty and staff members who contributed in many ways, the author expresses his thanks.

The generous support provided by The Institute of Paper Chemistry is gratefully acknowledged.

The author also wishes to thank his fellow students and, where appropriate, their wives for making life at the Institute enjoyable.

On a very personal note, I thank my family for their unending encouragement and support. The huge phone bills amassed by my parents are testimony to their continuing interest in my welfare. Finally, I wish to thank my wife, Sherry, for her love and patience, and for being the better half of my life.

LITERATURE CITED

1. Robert, A., Rerolle, P., Viallet, A., and Martin-Borret, O., ATIP Bull. 18 (4):151(1964).

2. Robert, A., Viallet, A., Rerolle, P., and Andreolety, J. P., ATIP Revl. 20 (5):207(1966); Paper Trade J. 152(2):49(1968).

3. Golova, O. P., Nosova, N. I., Andrievskaya, E. A., and Mayat, N. S., Tsellyul. Proizvodyne, Sb. Statei 1963:100; ABIPC 35:A58.

4. Golova, O. P., Nosova, N. I., Andrievskaya, E. A., and Volkova, L. A., Vysokomol. Soedin. 7(9):1619(1965).

5. Akim, G. L., Papper och Tra 55(5):389(1973).

6. Mayat, N. S., Golova, O. P., and Nikolaeva, I. I., Vysokomol. Soedin. 5(6): 873(1963).

7. Samuelson, O., and Stolpe, L., Tappi 52(9):1709(1969).

8. Kolmodin, H., and Samuelson, O., Svensk Papperstid. 73(4):93(1970).

9. Malinen, R., and Sjostrom, E., Papper och Tra 55(8):547(1973).

10. Samuelson, O., and Thede, L., Tappi 52(1):99(1969).

11. Lindberg, B., and Theander, O., Acta Chem. Scand. 72:1782(1968).

12. Haskins, J. F., and Hogsed, M. J., J. Org. Chem. 15:1264(1950).

13. Kolmodin, H., and Samuelson, O., Svensk Papperstid. 76(2):71(1973).

14. Samuelson, O., and Stolpe, L., Svensk Papperstid. 72:662(1969).

15. Samuelson, O., and Thede, L., Acta Chem. Scand. 22:1913(1968).

16. Brooks, R. D. A kinetic study of the rate of cleavage of the glycosidic bond of methyl β-D-glucopyranoside in an alkaline medium. Doctoral Dissertation. Appleton, WI, The Institute of Paper Chemistry, 1965.

17. Minor, J. L., and Sanyer, N., J. Polymer Sci., Part C, 36:73(1971).

18. McCloskey, J. T. The degradation of methyl β-D-glucopyranoside by oxygen in alkaline solution. Doctoral Dissertation. Appleton, WI, The Institute of Paper Chemistry, 1971.

19. Sinkey, J. D. The function of magnesium compounds in an oxygen-alkali-carbohydrate system. Doctoral Dissertation. Appleton, WI, The Institute of Paper Chemistry, 1973.

20. Ericsson, B., Lindgren, B. O., Theander, O., and Petersson, G., Carbohyd. Res. 23(2):323(1972).

21. Weaver, J. W. The alkaline hydrogen peroxide reaction of methyl β-D-glucopyranoside by oxygen in alkaline solution. Doctoral Dissertation. Appleton, WI, The Institute of Paper Chemistry, 1971.

22. Gleason, W. B., and Barker, R., Can. J. Chem. 49:1425(1971).

23. Malinen, R., and Sjostrom, E., Cell. Chem. Tech. 9:231(1975).

24. Ericsson, B. Oxygen oxidation of cellulose in aqueous alkaline medium. Doctoral Dissertation. Stockholm, Sweden, The Royal University of Technology, 1974.

25. McCloskey, J. T., Schroeder, L. R., Sinkey, J. D., and Thompson, N. S., Papper och Tra 57(3):131(1975).

26. Dewilt, H. G. J., and Kuster, B. F. M., Carbohyd. Res. 19:5(1971).

27. Thompson, N. S., and Green, J. W. Personal communication, 1976.

28. Laidler, K. J. Reaction kinetics. Vol. 1. p. 18. New York, MacMillan, 1963.

29. Bruhn, G., Gerlach, J., and Pawlek, F., Z. Anorg. Allgem. Chem. 337(1-2): 68(1965).

30. Satterfield, C. N., and Bonnell, A. H., Anal. Chem. 27:1174(1955).

31. Probiner, H., Anal. Chem. 33(10):1423(1961).

32. Marklund, S., Acta Chem. Scand. 25:21(1971).

33. Schumb, W. C., Satterfield, C. N., and Wentworth, R. L. Hydrogen peroxide. New York, Reinhold Publishing Corp., 1955. 759 p.

34. Barb, W. G., Baxendale, J. H., George, P., and Hargrave, K. R., Trans. Faraday Soc. 47:591(1951).

35. Baxendale, J. H., Adv. Catalysis 4:31(1952).

36. Uri, N., Chem. Rev. 50:375(1952).

37. Mair, R. D., and Hall, R. T. Determination of organic peroxides by physical, chemical, and colorimetric methods. In Swern's Organic peroxides. Vol. II. p. 535. New York, Wiley-Interscience, 1971.

38. Russell, G. A., Bemis, A. G., Geels, E. J., Janzen, E. G., and Moye, A. J., Adv. Chem. Ser. 75:174(1968).

39. Ingold, K. U., Chem. Rev. 61:563(1961).

40. Michie, R. I. C., and Neale, S. M., J. Polymer Sci., Part 2A:2063(1964).

41. McCloskey, J. T., Sinkey, J. D., and Thompson, N. S., Tappi 58(2):56(1975).

42. Schultze, H., and Schulte-Frohlude, D., J. Chem. Soc. (Faraday Trans. I) 71 (5):1099(1975).

43. Sosnovski, G., and Rawlinson, D. J. The chemistry of hydroperoxides in the presence of metal ions. In Swern's Organic peroxides. Vol. II. p. 153. New York, Wiley-Interscience, 1971.

44. Mageli, O. L., and Sheppard, C. S. Organic peroxides and peroxy compounds-general description. In Swern's Organic peroxides. Vol. I. p. 153. New York, Wiley-Interscience, 1970.

45. Lewin, M., and Ettinger, A., Cell. Chem. Tech. 3:9(1969).

46. Isbell, H. S., and Frush, H. L., Carbohyd. Res. 28:295(1973).

47. Isbell, H. S., Frush, H. L., and Martin, E. T., Carbohyd. Res. 26:287(1973).

48. Petersson, G., Tetrahedron 26:3413(1970).

49. Kochetkov, N. K., and Chizhov, O. S., Adv. Carbohyd. Chem. 21:29(1966).

50. McKelvey, R. D. Personal communication, 1975.

51. Kolmodin, H., and Samuelson, O., Svensk Papperstid. 74:301(1971).

52. Entwistle, D., Cole, E. H., and Wooding, N. S., Textile Res. J. 19:609 (1949).

53. MacDonald, D. M., Tappi 48:708(1965).

54. Isbell, H. S., Adv. Chem. Ser. 117:71(1975).

55. Theander, O., Acta Chem. Scand. 12:1887(1958).

56. Malinen, R., Paperi ja Puu 57(4a):193(1975).

57. Mellor, A., Holzforschung 14:79(1960).

58. Behar, D., Czapski, G., Rabini, J., Dorfman, L. M., and Schwarz, H. A., J. Phys. Chem. 74:3209(1970).

59. Nonhebel, D. C., and Walton, J. C., Free-radical chemistry. p. 78. London, Cambridge University Press, 1974.

60. Russel, G. A., J. Am. Chem. Soc. 79:3871(1957).

61. Hiatt, R. Hydroperoxides. In Swern's Organic peroxides. Vol. II. p. 88. New York, Wiley-Interscience, 1971.

62. Curci, R., and Edwards, J. O. Peroxide reaction mechanisms-polar. In Swern's Organic peroxides. Vol. I. p. 205. New York, Wiley-Interscience, 1970.

63. Rendleman, J. A., Adv. Chem. Ser. 117:55(1975).

64. Atalla, R. H. Personal communication, 1975.

65. Pitzner, L. J., and Atalla, R. H., Spect. Acta, Vol. 31A:911(1975).

66. Eliel, E. L., Allinger, N. L., Angyal, S. J., and Morrison, G. A. Conformational analysis. p. 274. New York, Interscience, 1966.

67. Fish, A. Rearrangement and cyclization reactions of organic peroxy radicals. In Swern's Organic peroxides. Vol. I. p. 143. New York, Wiley-Interscience, 1970.

68. Rust, F. F., and Youngman, E. A., J. Org. Chem. 27:3778(1962).

69. Swern, D. Organic peroxides. Vols. I and II. New York, Wiley-Interscience, 1971.

70. Lund, H., and Bjerrum, J., Ber. 64:210(1931).

71. Perrin, D. D., Armarego, W. L. F., and Perrin, D. R. Purification of laboratory chemicals. New York, Pergamon Press, 1966. 362 p.

72. Bauer, N., and Lewin, S. Z. In Weissberger's Techniques in organic chemistry. Vol. I. Part 1. p. 136. New York, Interscience, 1959.

73. Trusell, F., and Diehl, H., Anal. Chem. 31(12):1978(1959).

74. Mozingo, R., Org. Syn. 26:77(1946).

75. Mozingo, R., Org. Syn. Col. Vol. III:181(1955).

76. Bayer, G. F. A study of the iron-tartrate-alkali system and its complexing reaction with cellulose-related polyhydroxy compounds. Doctoral Dissertation. Appleton, WI, The Institute of Paper Chemistry, 1964.

77. Wolfrom, M. L., and Thompson, A. T. In Methods in carbohydrate chemistry. Vol. II. p. 212. New York, Academic Press, Inc., 1963.

78. Purves, C. B., J. Am. Chem. Soc. 51:3619(1929).

79. Fletcher, H. G., and Hudson, C. S., J. Am. Chem. Soc. 69:921(1947).

80. Jeanloz, R., Fletcher, H. G., and Hudson, C. S., J. Am. Chem. Soc. 70: 4052(1948).

81. Pitzner, L. J. An investigation of the vibrational spectra of the 1,5-anhydro-pentitols. Doctoral Dissertation. Appleton, WI, The Institute of Paper Chemistry, 1973.

82. Lonngren, J., and Pilotti, A., Acta Chem. Scand. 25(3):1144(1971).

83. Bachelor, F. W., and Miana, G. A., Can. J. Chem. 47:4089(1969).

84. Brandon, R. E. Alkaline degradation of 1,5-anhydro-cellobiitol. Doctoral Dissertation. Appleton, WI, The Institute of Paper Chemistry, 1973.

85. Ledaal, T., and Bernatek, E., Anal. Chim. Acta 28:322(1963).

86. MacNevin, W. M., and Urone, P. F., Anal. Chem. 25:1760(1953).

87. Furmanek, C., and Monikowski, K., Rocen. Panstiv. Zakl. Hig. 4:447(1953); Anal. Abstr. 2:1678(1955).

88. Meloan, C. E., and Brandt, W. W., Anal. Chem. 33:102(1961).

89. Kolthoff, I. M., and Sandell, E. B. Textbook of quantitative inorganic chemistry. p. 574. New York, MacMillan, 1956.

90. Bethge, P. O., and Lindstrom, K., Analyst 99:137(1974).

APPENDIX I

THE REACTOR SYSTEM

REACTION VESSEL AND COVER

The basic design, which provides a reactor capable of being sampled while hot and under pressure, was conceived by McCloskey (18). The reactor was a completely teflon-lined brass system with considerable versatility and with commercially available components wherever possible. Details of reactor construction are illustrated in Fig. 41.

The reaction vessel consisted of a brass pot lined with a machined teflon insert. The brass cover, bolted to the pot by means of flange fittings, was protected from the reaction solution by a teflon shield, which was fashioned from teflon sheeting (1/32" thickness, Eagle Supply and Plastics, Inc.). The contact between this shield and the reactor insert provided an effective main seal.

Figure 42 illustrates the design of the sampling and pressurizing ports in the reactor cover. The stainless steel connectors were Gyrolok 2COS-316 fittings (Hoke Mfg. Co.). The holes in the teflon plugs were bored with diameters smaller than the tubing which, when drawn through the holes, formed excellent seals. The plugs were also fashioned with "O" rings which, when screwed into place, formed good seals with the teflon shield.

HEAT EXCHANGER

The heat exchanger was constructed from copper tubing and Gyrolok heat exchange tees and reducer (numbers XT and 2RUI-316, respectively, Hoke Mfg. Co.).

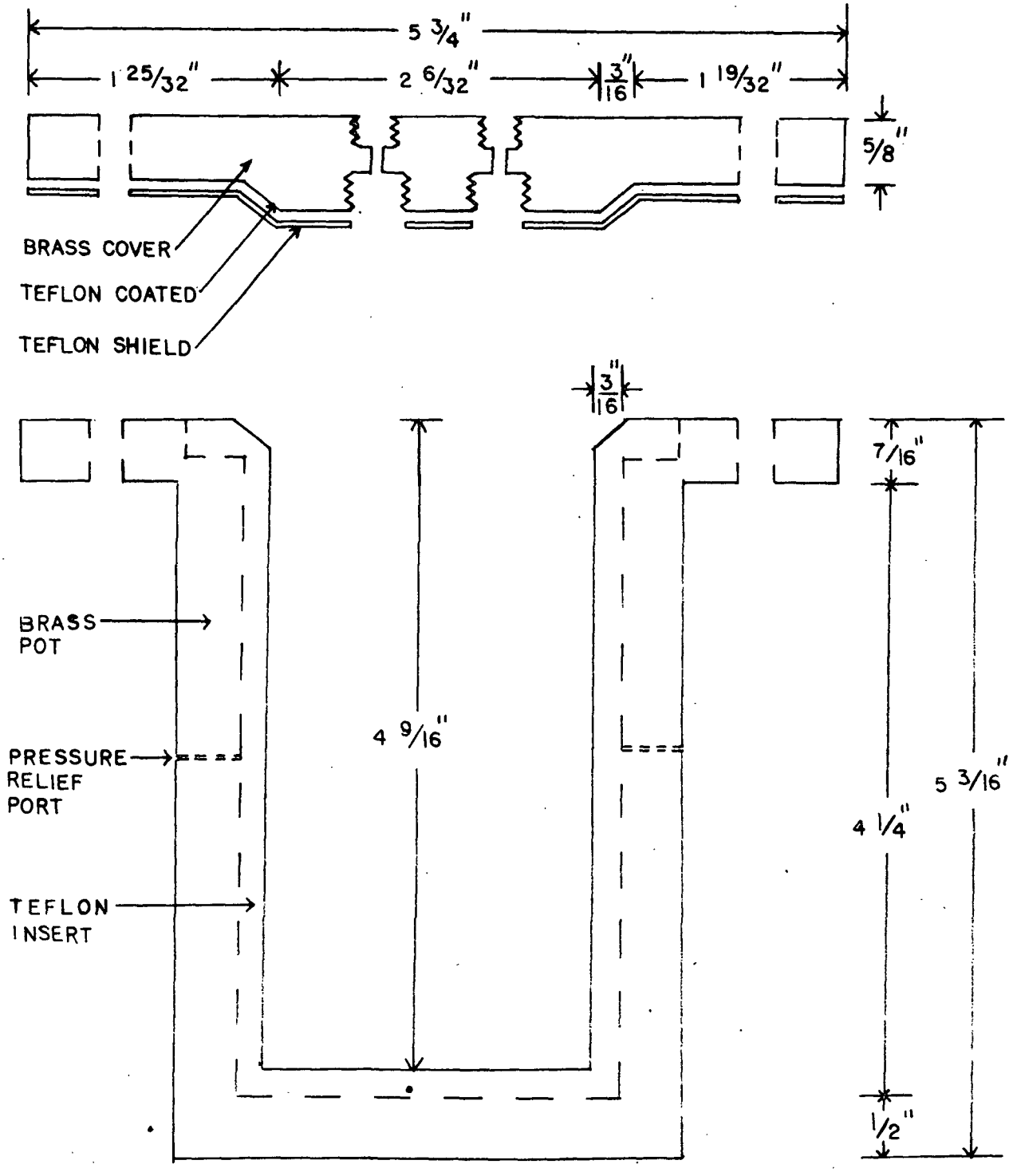

Figure 43. Details of Reactor and Cover

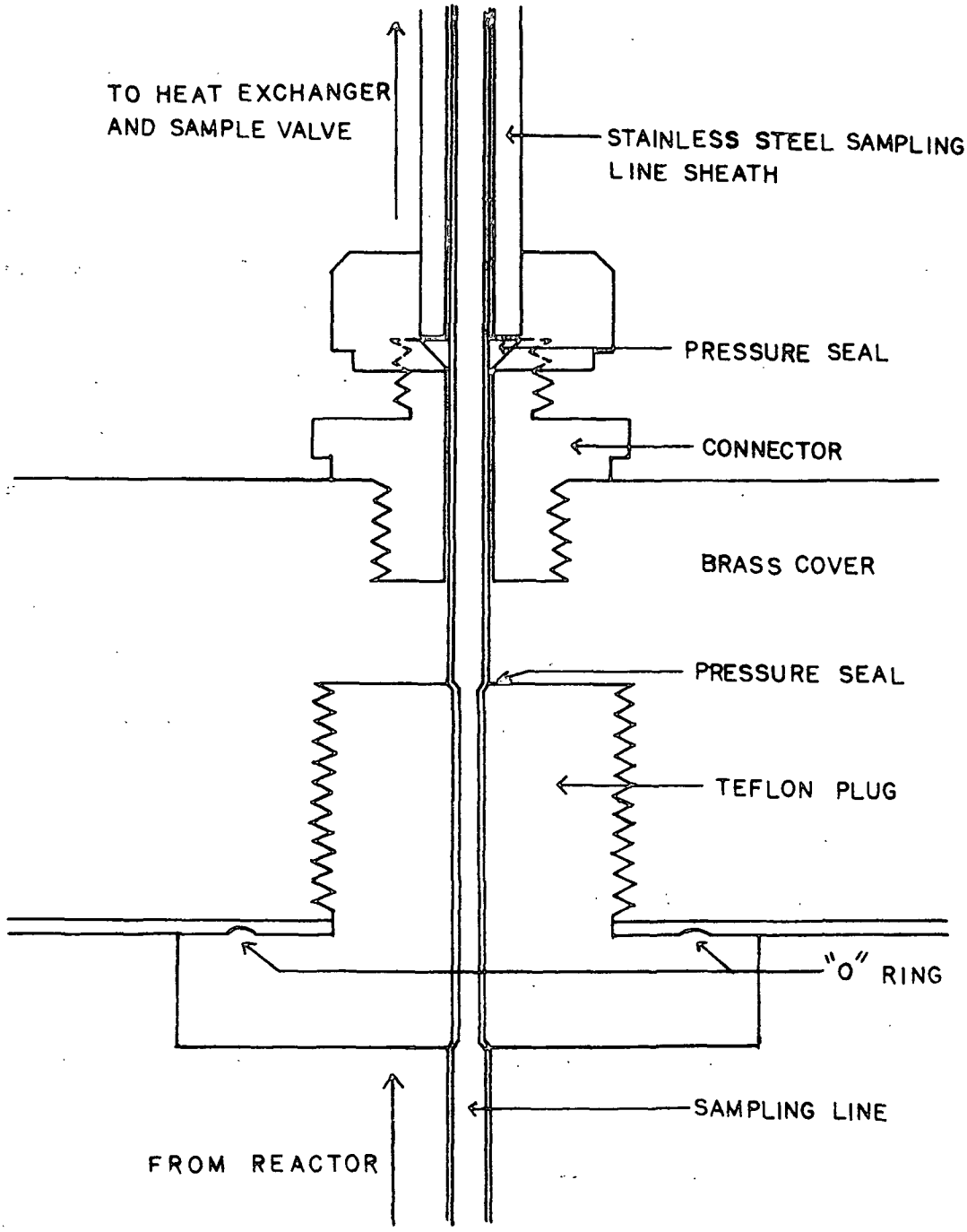

Figure 44. Details of the Sampling and Pressurizing Ports in the Reactor Cover

The reducer provided a final seal against gas leakage between the stainless steel jacket and teflon tubing.

OIL BATH AND TEMPERATURE CONTROL APPARATUS

Upon assembly, the reactor was attached to an oil bath apparatus equipped with a movable carriage for raising and lowering the reactor and sampling system (sampling lines, heat exchanger, and face plate containing the valving system) and a constant temperature controller. The controller consisted of the following components: Bronwell Constant Temperature Circulator (100-200 watt heater, mercury contact thermoregulator rated at ±0.02°C; Matheson Scientific); Inconel clad iron-constantan grounded thermocouple (Omega Engineering, Inc.) for monitoring reaction mixture temperature (Fig. 43 and 44); precision potentiometer (Leeds and Northrup No. 8691-2 mv potentiometer); recorder (Leeds and Northrup Speedomax W Model 101112) for providing continuous record of temperature; and an adjustable, bucking-current circuit (3.0-10.5 mv, Fig. 44) for bringing the thermocouple output into the recorder's range. For a detailed illustration of the oil bath assembly and temperature controlling system, see Brandon (84).

MAGNETIC STIRRER

The magnetic stirrer was an air-driven "Mag-Jet" (Matheson Scientific, Inc.). Its two small magnets were replaced by a 1.5 inch cylindrical magnet to give better tracking of the stirring bar inside the reactor. The stirrer was clamped to the bottom of the reactor before the reactor was positioned on the oil bath assembly.

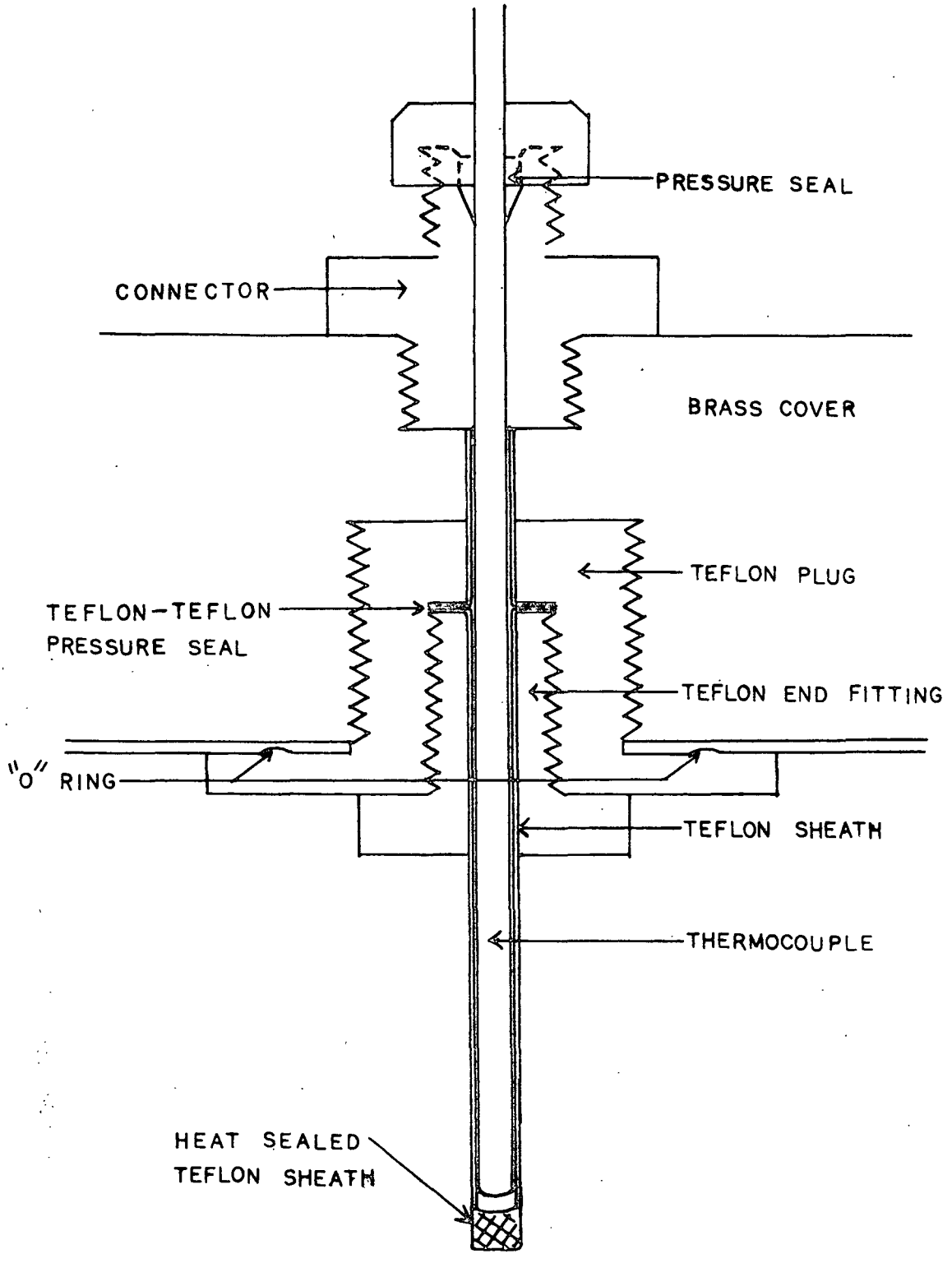

Figure 45. Details of the Installation of the Thermocouple in the Reactor Cover

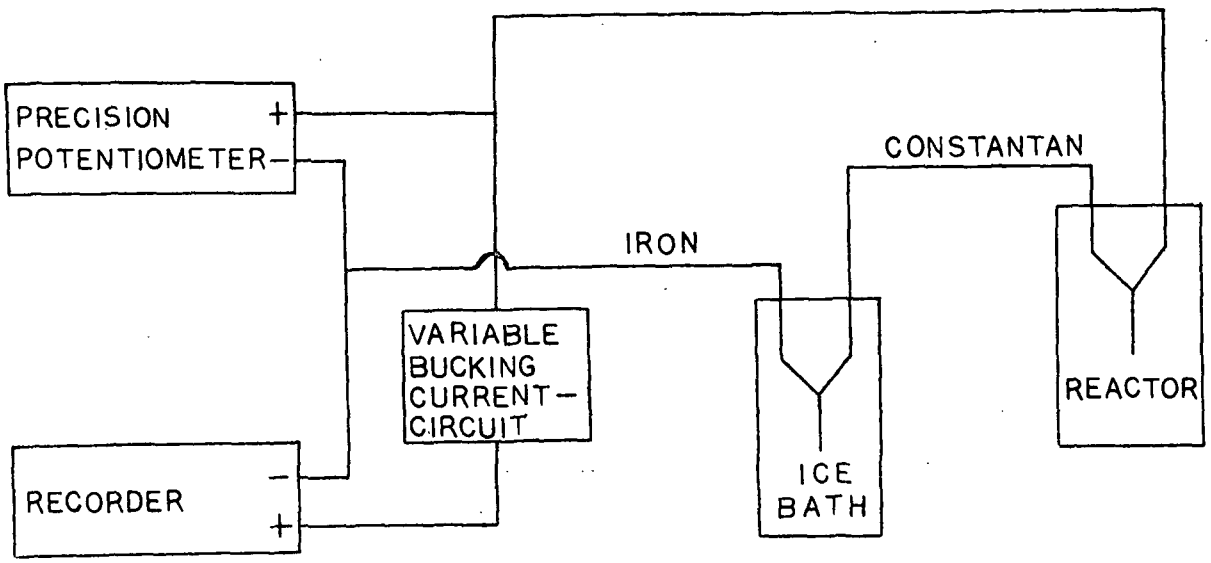

Figure 46. Schematic of Temperature Monitoring System

THE SAMPLING SYSTEM

The sampling and pressurizing lines consisted of teflon tubing (0.063 inch OD x 0.031 inch ID, Chromatoronix, Inc.). In order to ensure against bursting at high temperature and pressure, the sample line was reinforced with a close-fitting, stainless steel jacket from the connector through the heat exchanger (Fig. 42). At room temperature, the teflon tubing can withstand pressures of at least 500 psi. Figure 45 is a schematic representation of the valving system used in connection with the reactor. All valves were Chromatronix, two-position, sampling valves (Chromatronix, Inc.). The system allows for sampling of the reaction mixture under pressure, back-flushing and drying of the sample lines, and injecting liquids into the reactor while under pressure. To illustrate these points, consider the following procedures in connection with Fig. 45.

SAMPLING OF REACTOR UNDER PRESSURE

Connect Ports A3, A4, A1', and A2' of the sample injection valve with the on-off valve, B, closed. Fill sample Loop 2. Connect Ports A3', A2', A4, and A1

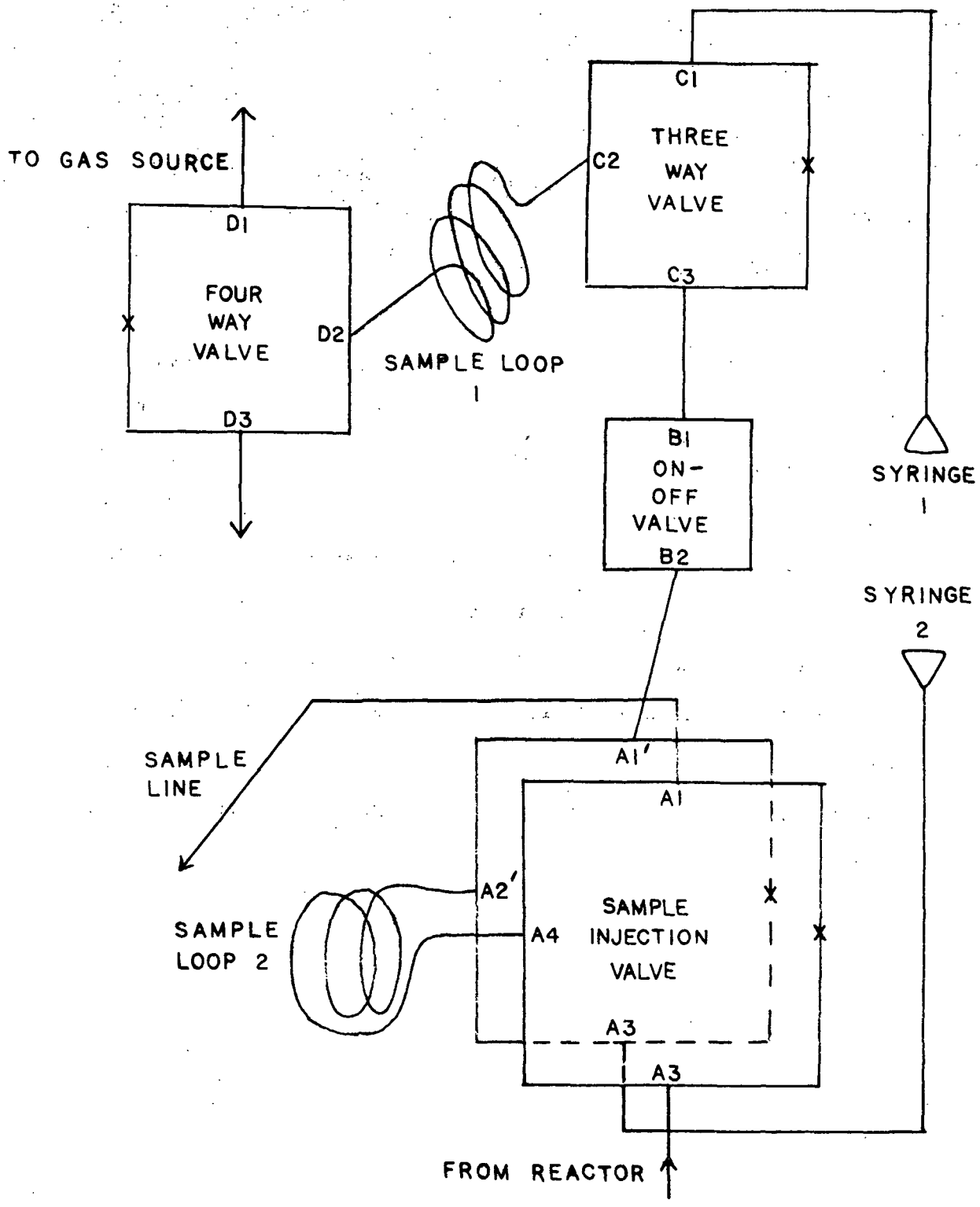

Figure 47. Schematic Representation of the Valving System

and force the sample out of sample Loop 2 through Port A1 by use of syringe 2. After taking the sample, the line can be back-flushed with distilled water and ethanol and vacuum dried.

INJECTING LIQUIDS INTO REACTOR WHILE UNDER PRESSURE

1. Fill sample Loop 1 with liquid by withdrawing the plunger of syringe 1 while Ports D3 and D2 of the four-way valve and Ports C2 and C1 of the three-way valve are connected.
2. With the on-off valve, B, open, connect Ports D1 and D2 of the four-way valve; connect C2 and C3 of the three-way valve; pressurize the line with nitrogen (at a slightly greater pressure than exists inside the heated reactor); and connect A1', A2', A4, and A3 of the sample injection valve. This will force the sample into the reactor.
3. Close the sample injection valve and nitrogen source. Relieve the pressure in sample loops by connecting Ports D2 and D3 of the four-way valve. Close on-off valve. The reactor is now ready to be sampled.
4. With valves adjusted as in Step 1, sample Loop 1 can be back-flushed with water and ethanol and vacuum dried.

APPENDIX II

GAS-LIQUID CHROMATOGRAPHY

Molar response factors were calculated according to Equation (37):

$$F_X = A_R \times M_R \tag{37}$$

where F_X = response factor for Compound X relative to the selected internal standard

A_R = ratio of peak area of Compound X to the peak area of the internal standard

M_R = mole ratio of the internal standard to Compound X

For each response factor, four solutions were prepared with varying mole ratios and treated in the manner of samples taken from the reactor (see Experimental). Four GLC analyses were performed on each sample and the response factor determined from the average of the values for each set of analyses.

Table V lists the GLC conditions used in this work, and Table VI gives GLC retention times and response factors (where possible) for the compounds involved in the kinetic and semiquantitative product analyses of the alkaline oxygen degradation of 1,5-anhydroxylitol, 1,5-anhydroribitol, and 3-O-methyl-1,5-anhydroxylitol.

The response factors were used to calculate the concentration of Compound "X" in the reaction mixtures from Equation (38):

$$X' = 10^3(A_R)(IS)\rho/(S)(F_X) \tag{38}$$

where IS = internal standard, moles

ρ = density of reaction mixture, g/liter

S = reaction sample, g

X' = Compound X in reaction mixture, moles/liter

TABLE V

GAS-LIQUID CHROMATOGRAPHIC CONDITIONS

Conditions	A	B	C	D	E
Column type	SE-30[a]	SE-30[a]	SE-30[a]	OV-17[b]	OV-17[b]
Derivative	acetylated	acetylated	acetylated	benzylated	trimethyl-silylated
Column temp. programming, °C	165	185	160	120	iso. at 70°C for 21.6 min; then 4°C/min for 17.1 min; then 1°C/min to completion
Injector temp., °C	260	260	265	160	265
Detector temp., °C	260	260	265	190	265
N_2 flow rate, ml/min	15	8.3	15	30	15

[a]Stainless steel column (5 ft x 0.125 inch) rigged for on-column injection and packed with 10% SE-30 on 60/80 mesh DMCS-AW Chromosorb W.

[b]Stainless steel column (10 ft x 0.125 inch) rigged for on-column injection and packed with 3% OV-17 on 80/100 mesh Supelcoport.

TABLE VI

RETENTION TIMES (T_R) AND RESPONSE FACTORS (F_X)

Conditions	Compound	T_R, min	F_X
A	Methyl β-D-xylopyranoside	11.6	1.000[a]
	1,5-Anhydroxylitol	7.4	0.905 ± 0.013[a]
B	1,6-Anhydro-β-D-gluco-pyranose	11.7	1.000[b]
	1,5-Anhydroribitol	6.8	0.955 ± 0.008[b]
C	Methyl β-D-xylopyranoside	11.9	1.000[a]
	3-O-Methyl-1,5-anhydro-xylitol	5.3	0.393 ± 0.006[a]
D	Formic acid	9.7	N.D.[d]
	Acetic acid	11.6	N.D.[d]
E[c]	Methyl β-D-xylopyranoside	58.2	1.000[a]
	Lactic acid	21.5	0.473 ± 0.046[a]
	Glycolic acid	25.6	0.480 ± 0.021[a]
	3-Hydroxypropanoic acid	35.9	0.473[e]
	2-Hydroxybutyric acid	37.6	0.500[e]
	Glyceric acid	38.6	0.566 ± 0.028[a]
	2,3-Dihydroxybutyric acid	38.6	0.566[e]
	2,4-Dihydroxybutyric acid	40.5	0.566[e]
	Unknown	44.0	0.566[e]
	1,5-Anhydroribitol	48.0	1.166 ± 0.027[a]
	1,4-Anhydro-2-C-carboxy-D-, and -L-, erythritol and threitol	51.6 52.3	1.000[e]
	1,5-Anhydroxylitol	54.1	1.330 ± 0.021[a]
	3-O-Carboxymethyl-glyceric acid	60.5	1.100[e]

[a] Calculated relative to the internal standard, methyl β-D-xylopyranoside, under the specified conditions.

[b] Calculated relative to the internal standard, 1,6-anhydro-β-D-glucopyranose, under the specified conditions.

[c] Retention times varied with column age and loading.

[d] N.D. = not determined.

[e] Interpolated response factor.

APPENDIX III

PEROXIDE ANALYSIS

Peroxides were determined using the acidic titanium sulfate colorimetric method of Marklund (32). At pH 1 the complexing of hydrogen peroxide is immediate. Organic peroxides are slow to hydrolyze to hydrogen peroxide at this acid level. Thus, organic peroxides may be distinguished from hydrogen peroxide by an increase in absorbance with time. A straight-line calibration curve (Fig. 46) was obtained by analyzing various hydrogen peroxide solutions by the standard iodometric titration technique (19) and by the titanium sulfate colorimetric determination.

STANDARD IODOMETRIC TITRATION TECHNIQUE

The peroxide solution (1 ml) was delivered to a volumetric flask (10 ml) containing sulfuric acid (2 ml, 6N). Ammonium molybdate (3 drops, 3% solution, w/w) and aqueous potassium iodide (2 ml, 10% solution, w/w) were added and the sample diluted to the mark with triply-distilled water. Three duplicate titrations (1 ml aliquots) were performed against standardized aqueous sodium thiosulfate (0.0016N) to a starch end point. The peroxide concentration was calculated from Equation (39):

$$[\text{Peroxide}] = V_T C_T / 2V_S \qquad (39)$$

where V_T = volume of sodium thiosulfate solution, liters

C_T = concentration of sodium thiosulfate solution, moles/liter

V_S = volume of peroxide sample, liters

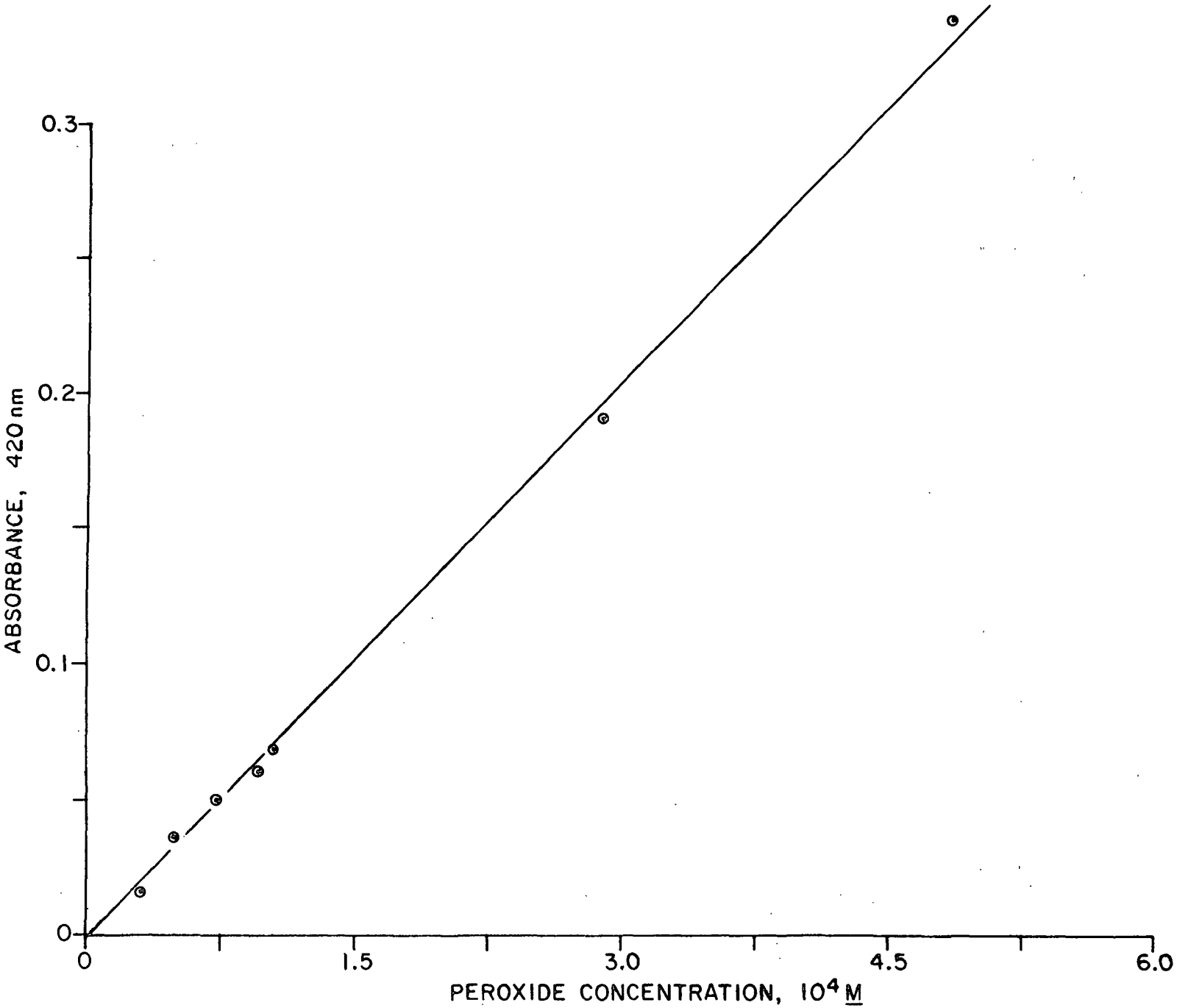

Figure 48. Absorbance at 420 nm vs. Peroxide Concentration, as Determined by the Standard Iodometric Titration Technique

TITANIUM SULFATE COLORIMETRIC DETERMINATION

The alkaline peroxide test solution (1 ml, 3 samples) was delivered to a volumetric flask (10 ml). The sample was neutralized with sulfuric acid (0.5N) to ca. pH 7, treated with titanium sulfate reagent (4 drops), diluted to the mark with triply-distilled water, and, if necessary, adjusted to pH 1 with sulfuric acid (0.5N). Absorbancies were determined on Sample 1 within 0.5 hour of sampling for hydrogen peroxide and over a 36 hour period (Samples 2 and 3) for organic peroxides (maximum absorbance usually occurring between 20-28 hours). Absorbance determinations were performed at 420 nm using triply-distilled water in the reference cell (19).

APPENDIX IV

GAS CHROMATOGRAPHIC-MASS SPECTROMETRIC ANALYSES

As described previously, a Varian Aerograph 1400 GC interfaced with a Dupont 21-491 mass spectrometer was used in this work. Chromatographic separations were performed on a 3% OV-17 on 80/100 mesh Supelcoport column (10 ft x 0.125 inch, stainless steel) under the following conditions: helium, 15 ml/min; column temperature, isothermal at 70°C for 21.6 min, then 4°C/min for 17.1 min, and then 1°C/min to completion; injector, 265°C, and detector, 265°C.

Separated compounds were routed from the GC to the mass spectrometer via a splitter valve located before the GC detector. The components of the interfacing system were all maintained at 300°C.

Control settings for the mass spectrometer were: oven, 105-115°C; source, 215-225°C; sensitivity, 7.5; ionizing voltage, 75 ev; filament, GC mode; scan, 10 sec/decade; chart speed, 4 inches/sec; initial pressure, 5×10^{-8}-2×10^{-7} Torr; and pressure during sample introduction, ca. 1×10^{-6} Torr. Heptacosafluorotributylamine was used as a standard to facilitate marking mass units of the spectra. Experiments using 7.5 ev ionizing voltage instead of 75 ev were also performed to help determine molecular weights. All of the mass spectral data, along with fragmentation patterns for several compounds, are found in the following tables and figures (Tables VII-XX and Fig. 47-51).

Product designations in parentheses refer to GLC results as follows: 1,5-anhydroxylitol (AX) — Fig. 17, p. 39; 1,5-anhydroribitol (AR) — Fig. 18, p. 40; and 3-O-methyl-1,5-anhydroxylitol (MAX) — Fig. 19, p. 41.

TABLE VII

MASS SPECTRAL DATA FOR 1,5-ANHYDROXYLITOL (TMS DERIVATIVE)[a]

m/e	Relative Abundance, %	m/e	Relative Abundance, %	m/e	Relative Abundance, %
352	22	193	5	101	77
351	26	192	6	90	11
350	53	191	53	89	6
337	4	189	15	88	9
336	12	171	23	82	12
335	20	149	13	77	7
306	5	148	22	76	13
305	22	147	64	75	81
304	7	143	19	74	55
303	9	135	7	73	98
247	4	134	18	72	22
246	17	133	73	71	12
245	38	131	56	69	13
234	13	130	64	61	13
233	27	129	91	60	7
232	55	119	11	59	49
230	8	118	24	58	9
220	7	117	79	55	11
219	40	116	100	54	8
218	37	115	7	47	7
217	67	113	7	46	12
216	29	105	7	45	65
206	8	104	15	44	17
205	37	103	79	43	15
204	58	102	25	41	25
203	58				

[a]Figure 47 gives fragmentation pattern for some major ions in AX spectrum.

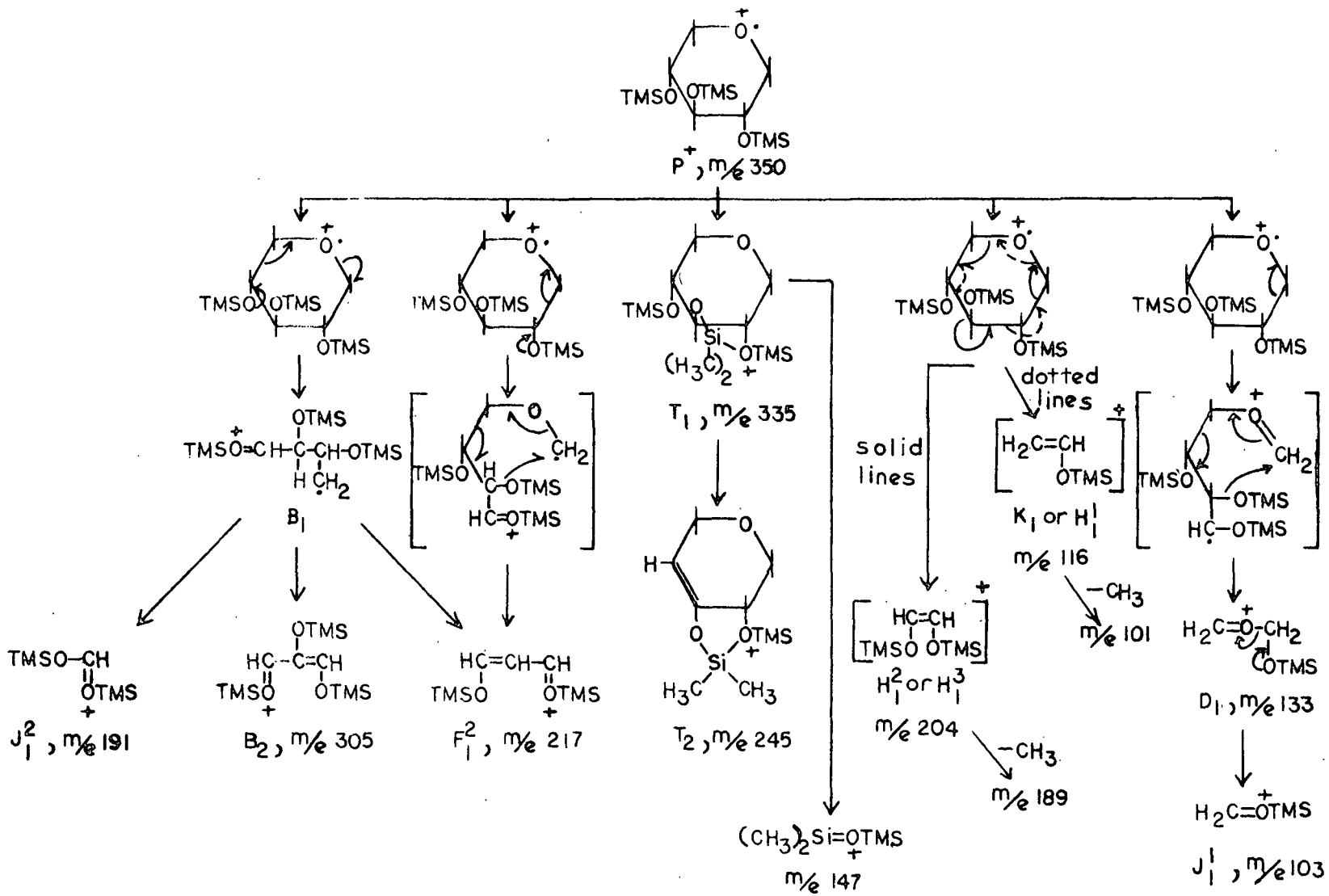

Figure 49. Fragmentation Pattern for Some Major Ions in the AX Mass Spectrum. Fragments are Labeled According to the Nomenclature of Kochetkov and Chizhov (49)

TABLE VIII

MASS SPECTRAL DATA FOR 1,5-ANHYDRORIBITOL (TMS DERIVATIVE)[a]

m/e	Relative Abundance, %	m/e	Relative Abundance, %	m/e	Relative Abundance, %
352	4	192	14	102	14
351	8	191	46	101	48
350	17	190	9	90	3
337	3	189	30	86	4
336	11	173	4	82	11
335	16	172	7	77	7
306	4	171	17	76	5
305	4	149	21	75	51
304	4	148	35	74	34
303	8	147	77	73	100
247	5	145	6	72	7
246	2	143	17	70	3
245	12	135	9	69	4
234	6	133	33	67	5
233	6	132	18	61	6
232	36	131	18	60	3
230	2	130	4	59	20
220	6	129	76	58	7
219	19	119	7	57	4
218	21	118	6	55	6
217	65	117	57	54	5
216	12	116	93	47	2
207	6	115	9	46	3
206	14	113	2	45	38
205	34	105	6	44	8
204	74	104	6	43	10
203	80	103	54	41	4
193	5				

[a]Fragmentation pattern (Fig. 47) identical to AX.

TABLE IX

MASS SPECTRAL DATA FOR 3-O-METHYL-1,5-ANHYDROXYLITOL (TMS DERIVATIVE)[a]

m/e	Relative Abundance, %	m/e	Relative Abundance, %	m/e	Relative Abundance, %
294	1	156	1	89	1
293	2	155	2	88	1
292	4	148	2	87	1
277	2	147	14	86	2
249	7	146	18	84	3
247	1	145	7	82	5
245	4	143	1	78	1
219	4	142	2	77	4
217	4	134	2	76	3
206	2	133	9	75	28
205	3	131	11	74	12
204	8	130	7	73	100
203	1	129	64	72	5
202	1	127	2	71	2
193	3	118	4	70	1
192	5	117	18	61	2
191	36	116	91	60	2
190	1	115	3	59	13
189	5	114	2	58	2
188	1	113	7	57	1
187	5	112	1	55	1
175	8	104	3	54	1
173	2	103	7	52	1
172	3	102	7	48	1
171	22	101	4	47	1
161	9	100	2	46	1
160	12	99	2	45	35
159	48	92	2	44	1
158	3	91	3	43	3
157	4	90	29	41	2

[a]Figure 48 gives fragmentation pattern for some major ions in MAX spectrum.

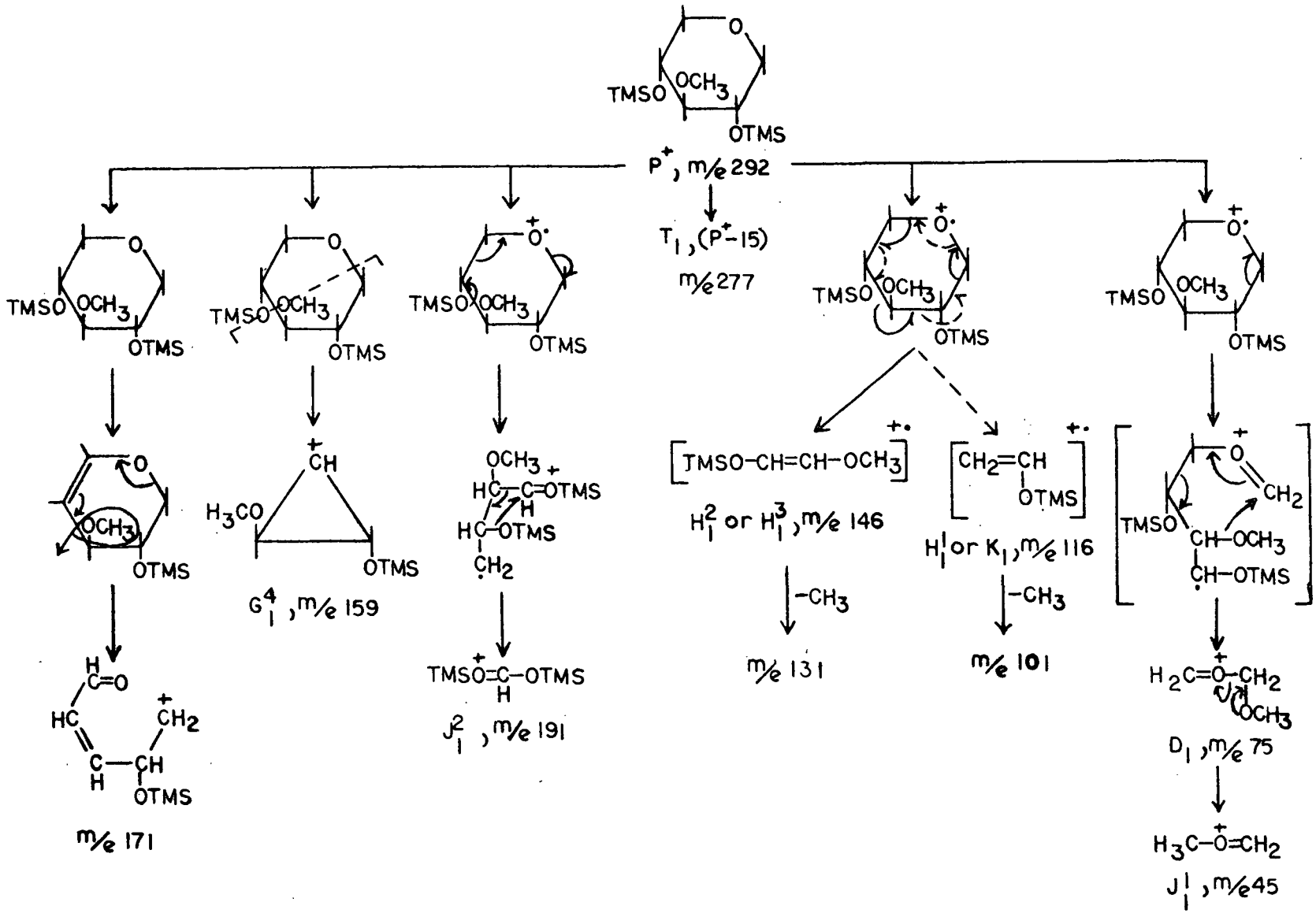

Figure 50. Fragmentation Pattern for Some Major Ions in the MAX Mass Spectrum. Fragments are Labeled According to the Nomenclature of Kochetkov and Chizhov (49)

TABLE X

MASS SPECTRAL DATA FOR LACTIC ACID (TMS DERIVATIVE)
(AX AND AR PRODUCT (1))[a]

m/e	Relative Abundance, %	m/e	Relative Abundance, %	m/e	Relative Abundance, %
234	2[b]	133	13	75	30
219	18	131	7	74	18
203	6	129	5	73	85
192	6	119	14	72	10
191	28	118	27	66	18
190	41	117	100	61	6
149	14	102	6	59	12
148	25	89	7	45	22
147	80				

[a]Mass spectra from the AX and AR reaction systems are identical within operating variation of the mass spectrometer.

[b]Determined at ionizing voltage 7.5 ev (VIV mode).

TABLE XI

MASS SPECTRAL DATA FOR GLYCOLIC ACID (TMS DERIVATIVE)
(AX AND AR PRODUCT (2))[a]

m/e	Relative Abundance, %	m/e	Relative Abundance, %	m/e	Relative Abundance, %
220	--[b]	148	28	74	14
207	4	147	97	73	100
206	12	135	12	72	12
205	33	133	23	66	25
197	9	131	8	59	5
177	7	117	9	58	6
176	32	103	12	57	8
162	7	89	6	47	7
161	24	75	20	45	18
149	12				

[a]Mass spectra from the AX and AR reaction systems are identical within operating variation of the mass spectrometer.

[b]No parent ion evident, even at ionizing voltage 7.5 ev (VIV mode).

TABLE XII

MASS SPECTRAL DATA FOR 3-HYDROXYPROPANOIC ACID (TMS DERIVATIVE) (AX AND AR PRODUCT (3))[a]

m/e	Relative Abundance, %	m/e	Relative Abundance, %	m/e	Relative Abundance, %
234	--[b]	133	3	81	7
221	1	131	1	76	6
220	4	129	3	75	68
219	22	118	1	74	12
179	2	117	3	73	100
178	4	116	5	72	6
177	12	110	3	65	3
151	4	103	2	61	5
149	7	102	3	59	13
148	12	89	2	58	7
147	83	88	3	55	18
145	2	87	7	44	37

[a] Mass spectra from the AX and AR reaction systems are identical within operating variation of the mass spectrometer.

[b] No parent ion in evidence.

TABLE XIII

MASS SPECTRAL DATA FOR 2-HYDROXYBUTYRIC ACID (TMS DERIVATIVE)
(AX AND AR PRODUCT (4))[a]

m/e	Relative Abundance, %	m/e	Relative Abundance, %	m/e	Relative Abundance, %
248	1	135	1	102	4
235	1	134	1	101	3
234	1	133	3	96	9
233	4	132	1	94	16
219	2	131	1	91	2
204	2	130	3	90	5
191	1	128	1	78	1
190	2	125	1	77	2
189	2	119	1	76	3
175	1	118	1	75	40
163	2	117	11	74	1
159	1	116	1	73	100
149	1	115	1	72	2
148	5	114	1	71	1
147	12	105	1	70	2
146	1	104	1	65	6
145	1	103	14		

[a]Mass spectra from the AX and AR reaction systems are identical within operating variation of the mass spectrometer.

TABLE XIV

MASS SPECTRAL DATA FOR GLYCERIC ACID AND 2,3-DIHYDROXYBUTYRIC ACID (TMS DERIVATIVES) (AX AND AR PRODUCTS ⑤ AND ⑥)[a]

m/e	Relative Abundance, %	m/e	Relative Abundance, %	m/e	Relative Abundance, %
322	4	204	56	130	11
309	10	203	5	129	5
308	14	191	14	119	5
307	30	190	26	117	29
294	24	189	75	116	7
293	35	175	6	104	8
292	76	149	17	103	44
278	4	148	17	102	41
222	5	147	88	101	12
220	7	135	5	75	18
217	9	133	20	74	34
206	12	131	7	73	100
205	21				

[a] Mass spectra from the AX and AR reaction systems are identical within operating variations of the mass spectrometer.

TABLE XV

MASS SPECTRAL DATA FOR 2,4-DIHYDROXYBUTYRIC ACID
(TMS DERIVATIVE)
(AX AND AR PRODUCT (7))[a]

m/e	Relative Abundance, %	m/e	Relative Abundance, %	m/e	Relative Abundance, %
336	--[b]	149	7	77	4
323	1	148	14	76	3
322	2	147	74	75	28
321	6	135	2	74	15
306	1	134	1	73	100
294	4	133	12	72	4
293	13	132	1	71	2
292	17	131	6	69	2
263	1	130	12	66	4
246	3	129	2	65	1
221	1	119	1	61	2
220	2	118	2	59	10
219	6	117	6	58	3
218	1	116	2	57	2
217	2	105	3	56	2
216	1	104	10	55	3
206	1	103	49	47	5
205	2	102	5	46	2
191	1	97	2	45	31
190	2	95	1	44	7
189	2	89	2	43	6
161	2	87	2	41	1

[a]Mass spectra from the AX and AR reaction systems are identical within operating variations of the mass spectrometer.

[b]Parent ion not in evidence.

TABLE XVI

MASS SPECTRAL DATA FOR ISOMERIC MIXTURE OF 1,4-ANHYDRO-2-C-CARBOXY-D-ERYTHRITOL AND THREITOL (TMS DERIVATIVES) (AX AND AR PRODUCTS (9) AND (10)) [a,b]

m/e	Relative Abundance, %	m/e	Relative Abundance, %	m/e	Relative Abundance, %
364	2	217	47	132	73
350	9	205	11	131	18
349	27	204	36	129	36
305	25	203	72	118	5
291	7	190	7	117	32
259	9	189	7	116	60
249	5	159	5	115	48
247	18	158	8	103	18
235	14	157	50	101	33
234	28	149	36	76	7
233	65	148	64	75	54
232	7	147	93	74	30
231	26	145	5	73	100
219	10	143	10	72	11
218	14	133	48		

[a] Mass spectra from the AX and AR reaction systems are identical within operating variations of the mass spectrometer.

[b] Figure 49 gives fragmentation pattern for some major ions in mass spectrum of AX and AR Products (9) and (10).

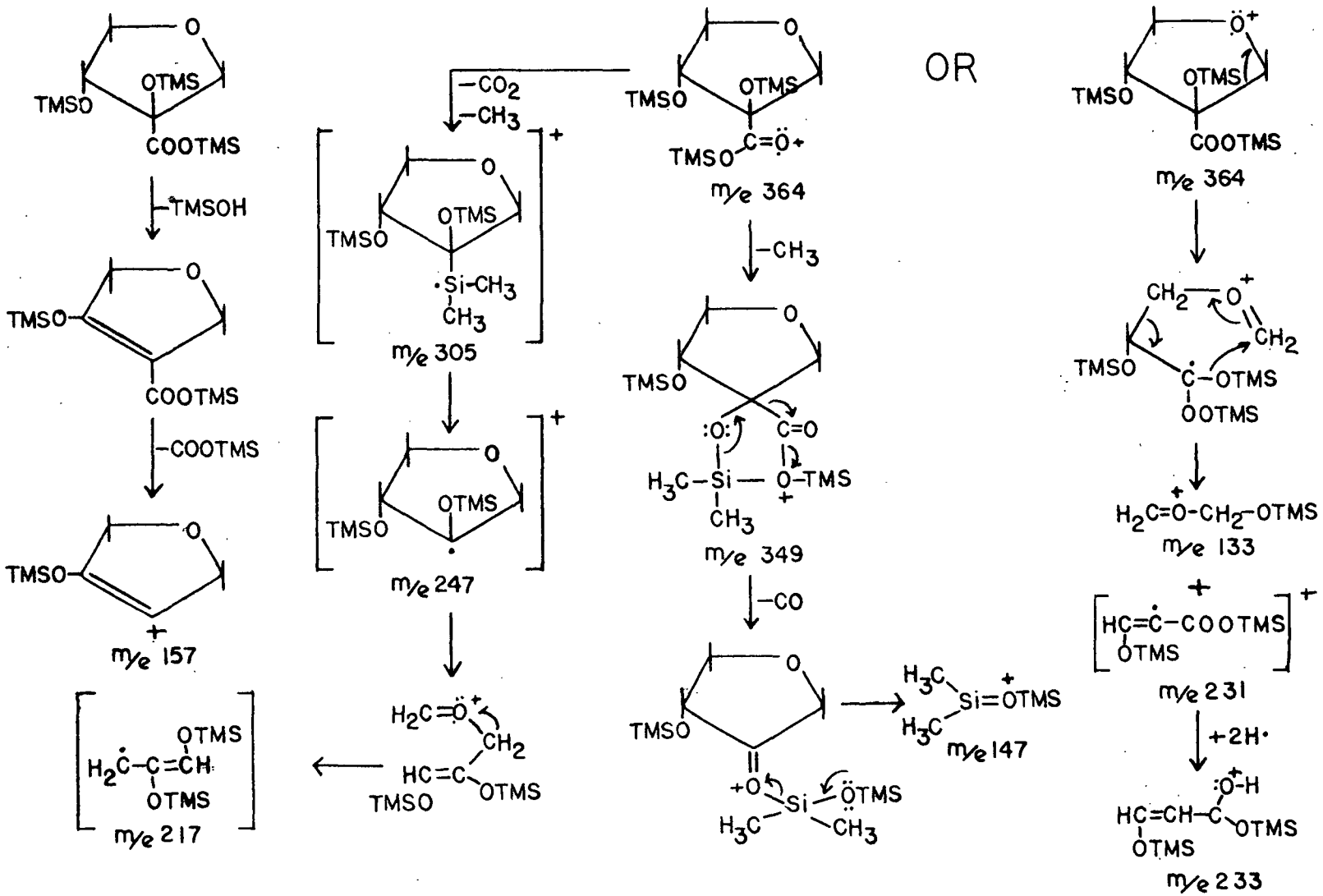

Figure 51. Fragmentation Pattern for Some Major Ions in the Mass Spectrum of AX and AR Products (9) and (10)

TABLE XVII

MASS SPECTRAL DATA FOR 3-O-CARBOXYMETHYL-GLYCERIC ACID
(TMS DERIVATIVE)
(AX AND AR PRODUCT (11))[a,b]

m/e	Relative Abundance, %	m/e	Relative Abundance, %	m/e	Relative Abundance, %
380	--[c]	220	22	134	3
336	2	219	81	133	9
322	1	206	9	132	1
321	1	205	26	131	7
307	3	204	66	130	2
306	2	203	3	129	12
305	4	193	3	119	1
290	1	192	7	118	2
264	1	191	30	117	4
263	3	190	6	116	4
249	2	189	13	113	1
248	1	161	1	105	2
247	4	157	2	104	4
235	1	149	5	103	31
234	1	148	8	101	7
233	2	147	40	77	2
223	3	145	3	75	21
222	3	143	3	74	14
221	9	135	1	73	100

[a] Mass spectra from the AX and AR reaction systems are identical within operating variation of the mass spectrometer.

[b] Figure 50 gives fragmentation pattern for some major ions in 3-O-carboxymethyl-glyceric acid spectrum.

[c] No parent ion in evidence.

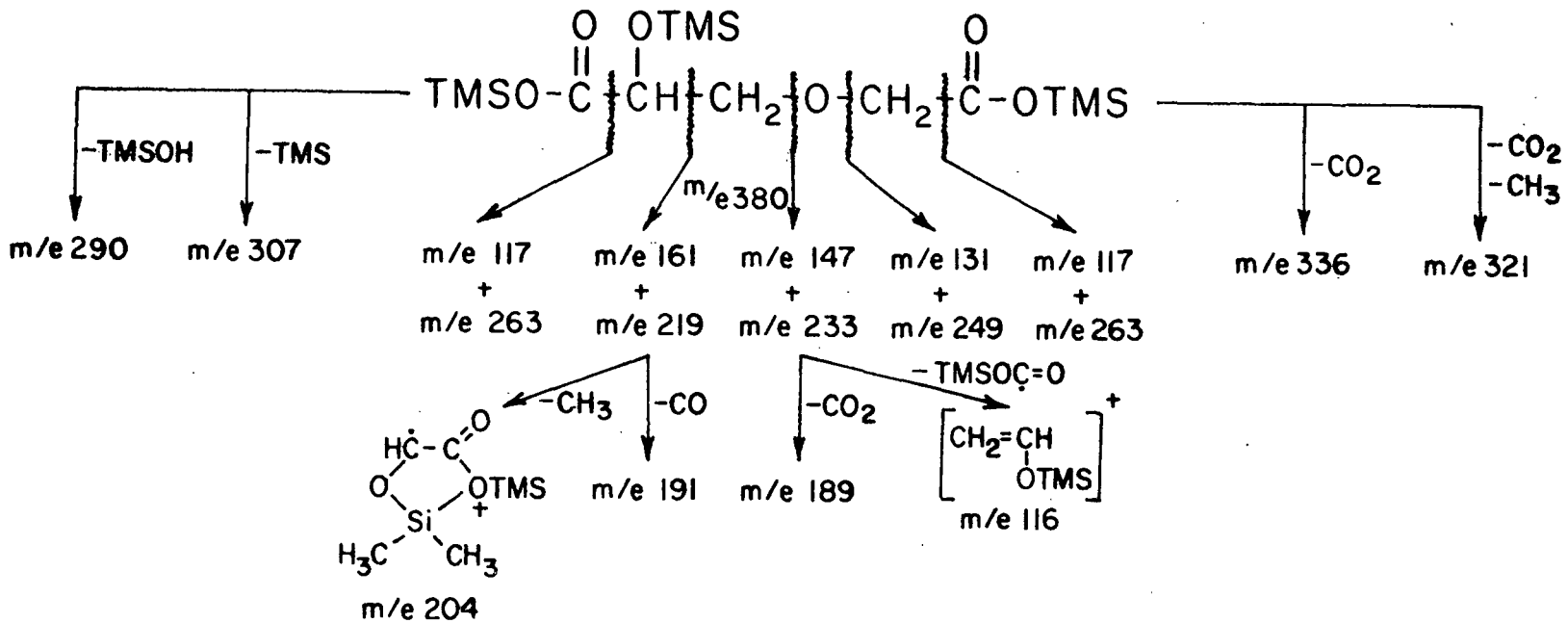

Figure 52. Fragmentation Pattern for Some Major Ions in the 3-O-Carboxymethyl-glyceric Acid Mass Spectrum

TABLE XVIII

MASS SPECTRAL DATA FOR 3-HYDROXY-2-METHOXYBUTYRIC ACID
(TMS DERIVATIVE)
(MAX PRODUCT ③)[a]

m/e	Relative Abundance, %	m/e	Relative Abundance, %	m/e	Relative Abundance, %
280	2	189	2	131	19
279	6	188	10	130	33
278	17	164	12	129	43
263	5	163	41	119	29
248	5	162	74	118	50
247	4	161	29	117	98
246	12	158	5	115	6
236	20	149	18	104	6
235	48	148	32	103	19
234	77	147	78	102	60
232	6	146	1	101	14
217	7	145	3	75	69
204	10	144	9	74	65
203	19	135	4	73	100
202	56	134	10	72	11
192	3	133	48	71	32
191	13	132	7		

[a]Figure 51 gives fragmentation pattern for some major ions in 3-hydroxy-2-methoxybutyric acid spectrum.

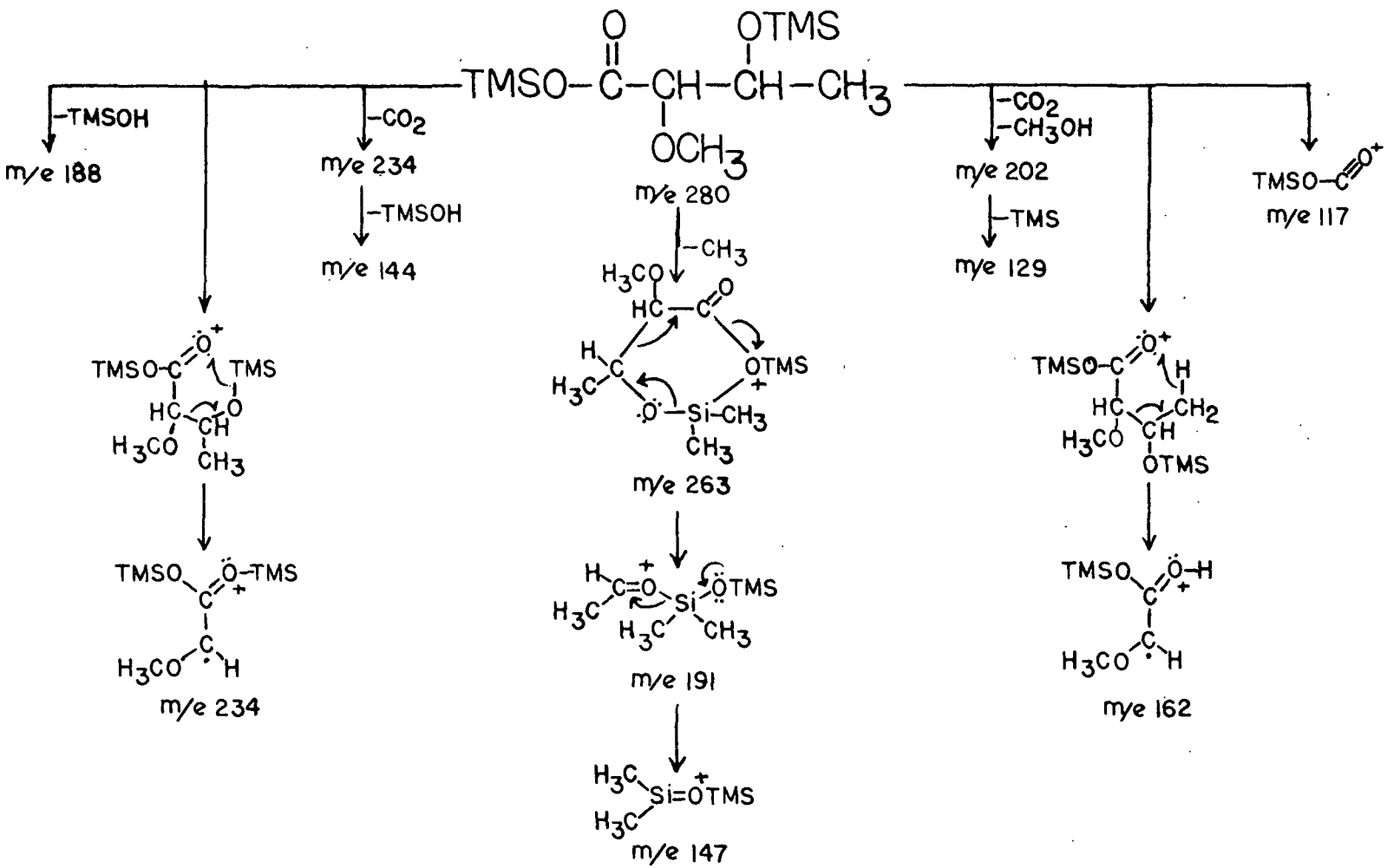

Figure 53. Fragmentation Pattern for Some Major Ions in the 3-Hydroxy-2-methoxybutyric Acid Mass Spectrum

TABLE XIX

MASS SPECTRAL DATA FOR GLYCERIC ACID (GA), 2,3-DIHYDROXYBUTYRIC ACID (2,3-DHB), AND AX PRODUCTS ⑤ AND ⑥ (AT VARIOUS % REACTION OF AX) (TMS DERIVATIVES)

m/e	GA, relative abundance, %	2,3-DHB, relative abundance, %	Products ⑤ and ⑥, % reaction of AX — Relative Abundance, %						
			16	29	42	50	56	61	64
323	3	2	--[a]	2	--	--	--	--	--
322	4	8	2	3	1	1	1	1	1
321	--	22	--	2	4	1	1	1	--
309	5	--	--	1	1	--	2	--	2
308	7	--	2	--	2	1	2	--	2
307	21	--	8	9	3	3	5	4	3
295	4	10	1	3	--	--	2	1	1
294	13	36	2	7	4	5	7	3	4
293	25	65	12	10	10	7	12	6	4
292	67	83	34	36	27	19	36	20	21
222	--	15	1	1	2	1	1	1	1
221	4	43	3	5	4	4	3	2	1
220	2	74	8	8	8	8	8	2	1
219	2	17	1	2	2	2	2	2	3
218	3	3	2	--	1	1	1	--	1
217	7	--	1	2	1	3	2	3	2
206	4	3	3	2	1	1	2	2	3
205	12	2	1	1	1	2	3	3	3
204	42	11	4	12	6	9	17	14	8
203	6	16	--	3	1	2	2	1	1
202	--	49	4	4	6	3	1	2	--
192	2	--	--	--	--	--	--	--	--
191	11	6	3	3	3	4	5	3	2
190	22	5	5	6	2	5	9	9	7
189	76	20	16	28	14	28	30	25	27
177	3	--	--	--	--	--	--	--	--
176	3	--	--	--	--	--	--	--	--
175	9	--	--	--	--	--	--	--	--
151	--	3	1	1	1	--	2	--	--
150	4	4	1	2	1	1	1	1	9
149	15	39	3	4	5	9	9	3	5
148	29	40	4	11	5	10	11	7	10
147	83	81	43	49	33	60	66	44	40
135	3	7	1	1	1	1	1	--	--
134	5	6	--	1	1	1	2	1	2
133	35	58	5	9	7	9	11	12	11
132	2	7	1	2	1	1	1	1	--
131	7	26	5	7	7	5	7	5	4
130	10	49	9	11	8	5	6	6	5
129	--	38	1	4	8	2	2	1	1

Footnotes next page.

TABLE XIX (Continued)

MASS SPECTRAL DATA FOR GLYCERIC ACID (GA), 2,3-DIHYDROXYBUTYRIC ACID (2,3-DHB), AND AX PRODUCTS ⑤ AND ⑥ (AT VARIOUS % REACTION OF AX) (TMS DERIVATIVES)

m/e	GA, relative abundance, %	2,3-DHB, relative abundance, %	Products ⑤ and ⑥, % reaction of AX — Relative Abundance, %						
			16	29	42	50	56	61	64
119	5	30	3	3	2	3	1	2	1
118	5	54	4	8	8	4	4	2	1
117	32	96	15	55	69	44	42	31	19
116	5	6	--	3	2	2	5	4	2
115	3	12	--	2	3	4	1	1	--
105	5	2	--	--	1	--	1	3	2
104	8	4	2	4	3	3	3	4	2
103	68	16	19	22	12	17	25	21	21
102	32	64	18	21	17	12	14	12	7
101	15	10	1	4	6	3	5	2	4
75	32	76	22	15	22	15	10	13	16
74	35	61	9	9	10	8	10	11	8
73	100	100	100	100	100	100	100	100	100
72	7	15	4	1	2	3	3	2	2

[a] Ion not in evidence.

TABLE XX

MASS SPECTRAL DATA FOR AR PRODUCTS (5) AND (6) (AT VARIOUS % REACTION OF AR) (TMS DERIVATIVES)

	Products (5) and (6), % reaction of AR							
	Relative Abundance, %							
m/e	16	29	37	44	54	72	88	92
323	2	1	1	1	1	1	--[a]	1
322	5	2	2	2	1	2	1	1
321	--	--	3	5	5	2	--	--
309	1	--	1	1	2	1	2	3
308	2	2	1	1	1	2	3	3
307	8	4	3	5	3	6	11	10
295	3	1	2	2	3	2	2	1
294	7	8	8	8	6	7	7	5
293	16	13	13	19	17	7	22	12
292	40	29	40	41	51	28	37	35
223	--	--	--	--	--	1	--	--
222	2	--	4	4	1	1	2	--
221	3	3	5	4	7	3	3	1
220	12	12	11	17	21	11	8	2
219	1	1	2	3	4	2	2	3
218	1	2	1	1	1	--	2	2
217	3	1	1	2	2	3	3	2
206	2	--	2	3	1	1	4	3
205	3	3	1	1	3	1	9	5
204	11	7	10	8	10	7	18	13
203	2	3	1	4	7	2	2	1
202	5	3	7	9	12	3	--	2
191	4	4	4	4	3	4	3	4
190	7	2	7	5	6	5	15	5
189	28	23	7	16	22	21	49	39
151	--	--	--	--	--	--	--	--
150	1	1	1	--	--	1	1	1
149	6	3	13	6	8	5	7	4
148	9	9	5	8	8	8	7	9
147	54	49	51	49	54	54	70	53
135	--	1	2	1	1	--	2	1
134	2	2	3	1	--	1	2	1
133	11	11	10	9	13	8	15	11
132	--	3	1	1	4	1	3	3
131	9	14	13	10	13	10	3	3
130	8	11	13	10	14	8	9	7
129	3	5	8	8	8	3	3	1
119	3	4	1	3	4	5	2	2
118	8	3	11	8	11	7	5	3
117	54	53	56	68	83	54	36	22
116	2	1	1	1	4	2	2	1

[a] Ion not in evidence.

TABLE XX (Continued)

MASS SPECTRAL DATA FOR AR PRODUCTS (5) AND (6) (AT VARIOUS % REACTION OF AR) (TMS DERIVATIVES)

	Products (5) and (6), % reaction of AR							
	Relative Abundance, %							
m/e	16	29	37	44	54	72	88	92
115	1	3	3	3	6	2	1	--
105	1	--	1	1	1	2	2	2
104	2	2	1	1	1	1	4	3
103	25	21	11	12	12	23	36	35
102	15	16	16	19	15	16	29	20
101	4	3	3	2	5	6	7	4
76	2	2	--	--	1	1	2	--
75	13	17	9	22	20	18	19	9
74	12	6	7	12	14	11	8	11
73	100	100	100	100	100	100	100	100
72	2	4	4	2	2	2	2	2

APPENDIX V

EXPERIMENTAL DATA[1]

TABLE XXI

DEGRADATION OF 1,5-ANHYDROXYLITOL (AX) (ca. 0.01N) IN 1.25N NaOH AT 120°C AND 75 PSI O_2 (25°C)

Time, min	AX, 10^3M	Time, min	AX, 10^3M
	Reaction 1 AX		
0.0	9.51	90.0	9.56
1.0	9.46	474.0	8.94
3.0	9.11	1233.0	7.12
12.0	9.48	2639.0	5.59
20.0	9.46	3423.0	4.92
45.0	9.42	4429.0	4.36
	Reaction 2 AX		
0.0	9.67	840.0	7.02
5.0	9.61	1200.0	6.65
15.0	9.58	1560.0	6.13
30.0	9.46	1874.0	5.63
120.0	9.12	2305.0	5.23
180.0	8.67	2662.0	5.04
480.0	7.92	2960.0	4.68
	Reaction 3 AX		
0.0	9.53	2530.0	5.18
5.0	9.49	2925.0	5.10
15.0	9.26	3285.0	4.46
30.0	9.45	3620.0	4.61
80.0	9.31	4090.0	4.55
185.0	8.86	4455.0	4.51
495.0	7.64	4820.0	4.27
760.0	7.22	5112.0	4.25
1180.0	6.57	5580.0	4.06
1600.0	6.08	5950.0	3.98
2010.0	4.76		

[1] Carbohydrate concentrations are an average of duplicate samples.

TABLE XXII

DEGRADATION OF 1,5-ANHYDRORIBITOL (AR) (ca. 0.01N) IN 1.25N NaOH AT 120°C AND 75 PSI O_2 (25°C)

Time, min	AX, 10^3M	Time, min	AX, 10^3M
	Reaction 1 AR		
0.0	9.92	350.0	6.01
1.0	9.82	593.0	4.79
3.0	8.86	898.0	3.63
7.0	9.81	1290.0	3.27
12.0	9.74	1763.0	2.77
20.0	9.82	2214.0	2.43
45.0	9.06	2530.0	2.10
90.0	8.10	2904.0	1.86
199.0	7.31		
	Reaction 2 AR		
0.0	9.79	255.0	7.37
1.0	9.68	600.0	5.72
3.0	9.57	887.0	4.65
7.0	9.90	1244.0	3.89
12.0	9.88	1987.0	2.83
20.0	9.84	2325.0	2.50
45.0	9.66	2699.0	2.25
90.0	8.82	3017.0	2.13
	Reaction 3 AR		
0.0	10.00	862.0	3.97
15.0	9.52	1380.0	3.33
35.0	9.06	1730.0	2.93
120.0	7.87	2165.0	2.34
176.0	7.53	2750.0	2.15
490.0	5.37	3100.0	1.75

TABLE XXIII

DEGRADATION OF 3-O-METHYL-1,5-ANHYDROXYLITOL (MAX) (ca. 0.01N) IN 1.25N NaOH AT 120°C AND 75 PSI O_2 (25°C)

Time, min	MAX, 10^3M	Time, min	MAX, 10^3M
	Reaction 1 MAX		
0.0	9.86	475.0	9.75
15.0	9.85	1120.0	9.55
30.0	9.85	1959.0	9.31
60.0	9.84	2607.0	9.05
150.0	9.84	3440.0	8.94
300.0	9.82		

TABLE XXIV

FORMATION OF PEROXIDES DURING DEGRADATION OF 1,5-ANHYDRO-XYLITOL (AX) (ca. 0.1N) IN 1.25N NaOH AT 120°C AND 75 PSI O_2 (25°C)

Time, min	AX, 10^2M	H_2O_2, 10^4M	Organic Peroxides, 10^4M
	Reaction 4 AX[a]		
0.0	9.88[b]	0.00	0.00
5.0	N.D.	0.60	0.20
6.0	9.55	N.D.	N.D.
11.0	9.57	N.D.	N.D.
15.0	N.D.	0.60	0.38
16.0	9.48	N.D.	N.D.
23.0	7.90	N.D.	N.D.
25.0	N.D.	1.63	0.98
32.0	9.13	N.D.	N.D.
60.0	8.71	3.13	0.12
100.0	N.D.	1.13	1.07
120.0	7.98	N.D.	N.D.
160.0	N.D.	0.51	1.10
180.0	7.49	N.D.	N.D.
290.0	N.D.	0.20	0.60
300.0	6.79	N.D.	N.D.
555.0	5.78	N.D.	N.D.
600.0	N.D.	0.00	0.40
840.0	5.10	N.D.	N.D.
845.0	N.D.	0.00	0.00
1020.0	N.D.	0.00	0.00
1140.0	4.60	N.D.	N.D.
1170.0	N.D.	0.00	0.00
1595.0	4.22	N.D.	N.D.
2085.0	3.92	N.D.	N.D.
3805.0	3.17	N.D.	N.D.
4220.0	3.09	N.D.	N.D.
	Reaction 5 AX[c]		
0.0	9.89[b]	0.00	0.00
4.0	N.D.	0.00	0.00
6.0	9.52	N.D.	N.D.
9.0	N.D.	0.00	0.63
14.0	N.D.	0.38	2.50
19.0	N.D.	3.00	2.60
30.0	9.08	5.50	2.25
60.0	8.66	6.75	0.38
100.0	N.D.	4.75	0.13
150.0	7.80	N.D.	N.D.

Footnotes next page.

TABLE XXIV (Continued)

FORMATION OF PEROXIDES DURING DEGRADATION OF 1,5-ANHYDRO-XYLITOL (AX) (ca. 0.1N) IN 1.25N NaOH AT 120°C AND 75 PSI O_2 (25°C)

Time, min	AX, 10^2M	H_2O_2, 10^4M	Organic Peroxides, 10^4M
200.0	N.D.	4.00	0.15
290.0	N.D.	0.75	0.38
300.0	6.91	N.D.	N.D.
617.0	N.D.	0.20	0.50
714.0	5.36	N.D.	N.D.
900.0	N.D.	0.00	0.60
1314.0	4.37	N.D.	N.D.
2094.0	3.78	N.D.	N.D.
3000.0	3.40	N.D.	N.D.
3600.0	3.22	N.D.	N.D.
4200.0	3.08	N.D.	N.D.

[a]No metal ion determination taken.

[b]N.D. = not determined.

[c]Metal ion determination taken (see Table XXVII).

TABLE XXV

FORMATION OF PEROXIDES DURING DEGRADATION OF 1,5-ANHYDRO-RIBITOL (AR) (ca. 0.1N) IN 1.25N NaOH AT 120°C AND 75 PSI O_2 (25°C)

Time, min	AR, 10^2M	H_2O_2, 10^4M	Organic Peroxides, 10^4M
	Reaction 4 AR[a]		
0.0	10.32[b]	0.00	0.00
5.0	N.D.	0.00	0.00
6.0	10.08	N.D.	N.D.
11.0	9.66	N.D.	N.D.
15.0	N.D.	2.05	0.00
16.0	9.55	N.D.	N.D.
23.0	8.85	N.D.	N.D.
25.0	N.D.	6.68	0.00
32.0	8.31	N.D.	N.D.
55.0	N.D.	8.25	0.00
60.0	6.89	N.D.	N.D.
100.0	N.D.	4.00	0.00
120.0	4.83	N.D.	N.D.
160.0	N.D.	2.73	0.00
180.0	4.02	N.D.	N.D.
290.0	N.D.	1.38	0.37
300.0	2.84	N.D.	N.D.
760.0	1.62	0.00	0.00
1055.0	1.24	0.00	0.00
1400.0	1.06	0.00	0.00
1755.0	0.90	N.D.	N.D.
2275.0	0.74	N.D.	N.D.
2550.0	0.75	N.D.	N.D.
2860.0	0.65	N.D.	N.D.
3200.0	0.70	N.D.	N.D.
3638.0	0.60	N.D.	N.D.
	Reaction 5 AR[c]		
0.0	9.57[b]	0.00	0.00
4.0	N.D.	7.50	0.00
9.0	N.D.	13.70	0.00
10.0	9.07	N.D.	N.D.
15.0	N.D.	17.20	0.00
20.0	N.D.	17.50	0.00
30.0	8.10	16.25	0.00
60.0	6.93	13.75	0.00
100.0	N.D.	8.68	0.00
120.0	5.13	N.D.	N.D.

Footnotes end of table.

TABLE XXV (Continued)

FORMATION OF PEROXIDES DURING DEGRADATION OF 1,5-ANHYDRO-RIBITOL (AR) (ca. 0.1N) IN 1.25N NaOH AT 120°C AND 75 PSI O_2 (25°C)

Time, min	AR, 10^2M	H_2O_2, 10^4M	Organic Peroxides, 10^4M
180.0	3.99	4.90	0.43
410.0	2.70	3.75	0.25
800.0	N.D.	0.00	0.00
1160.0	1.22	0.00	0.00
1735.0	0.80	N.D.	N.D.
2335.0	0.31	N.D.	N.D.

[a]No metal ion determination taken.

[b]N.D. = not determined.

[c]Metal ion determination taken (see Table XXVII).

TABLE XXVI

FORMATION OF PEROXIDES DURING DEGRADATION OF 3-O-METHYL-1,5-ANHYDROXYLITOL (MAX) (ca. 0.1N) IN 1.25N NaOH AT 120°C AND 75 PSI O_2 (25°C)

Time, min	MAX, 10^2M	H_2O_2, 10^4M	Organic Peroxides, 10^4M
	Reaction 2 MAX[a]		
0.0	9.95[b]	0.00	0.00
15.0	N.D.	0.00	0.00
30.0	9.94	N.D.	N.D.
40.0	N.D.	0.32	0.13
65.0	9.93	N.D.	N.D.
70.0	N.D.	0.76	0.21
120.0	9.92	1.21	0.40
180.0	9.91	1.73	0.59
480.0	9.88	3.93	0.71
1070.0	9.57	2.97	0.37
1860.0	9.19	2.45	0.20
2400.0	N.D.	2.31	0.15
2520.0	8.89	N.D.	N.D.
3275.0	8.58	N.D.	N.D.
3600.0	N.D.	2.09	0.13
3970.0	8.41	N.D.	N.D.
4610.0	8.11	N.D.	N.D.
5620.0	7.77	N.D.	N.D.

[a] Metal ion determination taken (see Table XXVII).

[b] N.D. = not determined.

TABLE XXVII

METALS IN DEGRADATION REACTIONS OF MODEL COMPOUNDS (AX, AR, AND MAX) (*ca.* 0.1N) IN 1.25N NaOH AT 120°C AND 75 PSI O_2 (25°C)[a]

Metal	Concentration in Reaction 5 AX, µg/liter	Concentration in Reaction 5 AR, µg/liter	Concentration in Reaction 2 MAX, µg/liter
Cadmium	<34	<33	<35
Chromium	86	27	59
Cobalt	<23	<22	<21
Copper	65	46	67
Iron	980	890	920
Magnesium	83	40	16
Manganese	91	84	100
Nickel	<57	<55	<120
Zinc	160	140	120
Total	<1579	<1337	<1458

[a]Metal ion analyses were performed in the Institute's Analytical Department with atomic absorption techniques.

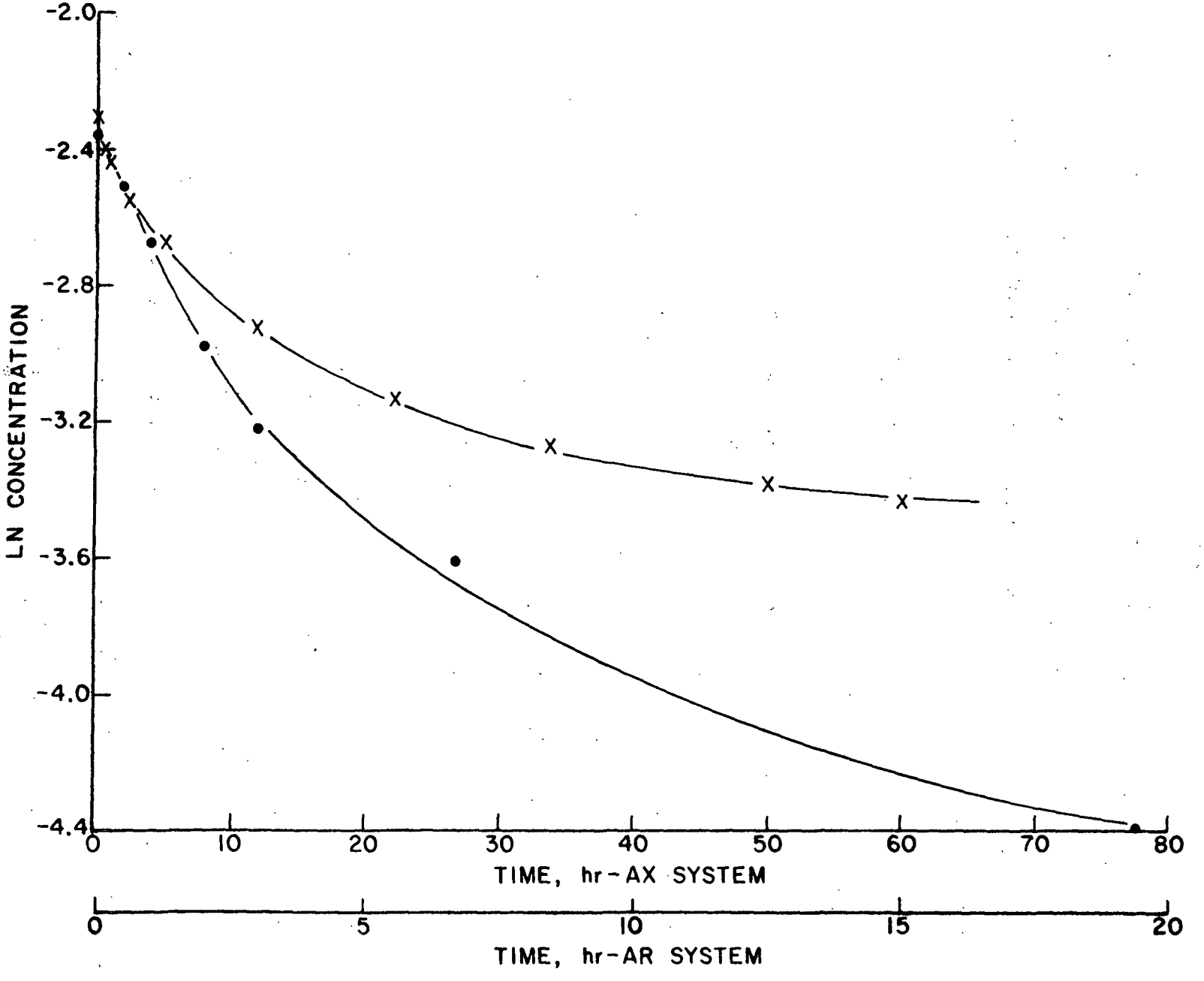

Figure 54. Degradation of 0.1N 1,5-Anhydroribitol (o - 5 AR) and 0.1N 1,5-Anhydroxylitol (x - 5 AX) in 1.25N NaOH at 120°C and 75 PSI O_2 (25°C). Data Plotted According to the Method of Integration Assuming a Carbohydrate Reaction Order of 1.0

APPENDIX VI

DERIVATION OF KINETIC EQUATION FOR 1,5-ANHYDRORIBITOL DEGRADATION

Assuming that all radical species are very reactive and therefore present in very small concentrations, the steady-state equations based on the postulated reaction mechanism can be written as follows:

$$d[HOO\cdot]/dt = 0 = k_7[A^-][O_2] - k_8[HOO\cdot][OH^-] + k_{-8}[O_2^{-\cdot}][H_2O] + k_{10}[HOO^-][M^{+n+1}] - k_{-10}[HOO\cdot][M^{+n}] \quad (40)$$

$$d[O_2^{-\cdot}]/dt = 0 = k_8[HOO\cdot][OH^-] - k_{-8}[O_2^{-\cdot}][H_2O] - k_9[O_2^{-\cdot}][H_2O] - k_{14}[A^-][O_2^{-\cdot}] - k_{27}[O_2^{-\cdot}][M^{+n+1}] \quad (41)$$

$$d[HO\cdot]/dt = 0 = k_9[O_2^{-\cdot}][H_2O] - k_{12}[A][HO\cdot] - k_{13}[A^-][HO\cdot] - k_{28}[HO\cdot][M^{+n}] \quad (42)$$

$$d[A\cdot]/dt = 0 = k_{11}[A^{-\cdot}][H_2O] - k_{-11}[A\cdot][OH^-] + k_{12}[A][HO\cdot] - k_{16}[A\cdot][O_2] \quad (43)$$

$$d[A^{-\cdot}]/dt = 0 = k_7[A^-][O_2] - k_{11}[A^{-\cdot}][H_2O] + k_{-11}[A\cdot][OH^-] + k_{13}[A^-][HO\cdot] + k_{14}[A^-][O_2^{-\cdot}] - k_{15}[A^{-\cdot}][O_2] \quad (44)$$

$$d[AO_2\cdot]/dt = 0 = k_{16}[A\cdot][O_2] - k_{17}[AO_2\cdot][OH^-] + k_{-17}[AO_2^{-\cdot}][H_2O] - k_{18}[AO_2\cdot][M^{+n}] + k_{-18}[AO_2^-][M^{+n+1}] \quad (45)$$

$$d[AO_2^{-\cdot}]/dt = 0 = k_{15}[A^{-\cdot}][O_2] + k_{17}[AO_2\cdot][OH^-] - k_{-17}[AO_2^{-\cdot}][H_2O] \quad (46)$$

If it is assumed that the concentration of each metal ion remains constant during the reaction, the following equations can also be written:

$$d[M^{+n+1}]/dt = 0 = -k_{10}[HOO^-][M^{+n+1}] + k_{10}[HOO\cdot][M^{+n}] + k_{18}[AO_2\cdot][M^{+n}] - k_{-18}[AO_2^-][M^{+n+1}] - k_{27}[O_2^{-\cdot}][M^{+n+1}] + k_{28}[HO\cdot][M^{+n}] \quad (47)$$

$$d[M^{+n}]/dt = 0 = -d[M^{+n+1}]/dt \quad (48)$$

Kinetic expressions can also be written for the concentrations of hydroperoxide, conjugate bases of the hydroperoxide, carbonyl, and products with respect to time.

$$d[AOOH]/dt = k_{19}[AO_2^-][H_2O] - k_{-19}[AOOH][OH^-] - k_{21}[AOOH][OH^-] + k_{-21}[AOOH^-][H_2O] - k_{22}[AOOH][OH^-] + k_{-22}[^-AOOH][H_2O] \quad (49)$$

$$d[AO_2^-]/dt = k_{18}[AO_2\cdot][M^{+n}] - k_{-18}[AO_2^-][M^{+n+1}] - k_{19}[AO_2^-][H_2O] + k_{-19}[AOOH][OH^-] - k_{20}[AO_2^-] \quad (50)$$

$$d[AOOH^-]/dt = k_{21}[AOOH][OH^-] - k_{-21}[AOOH^-][H_2O] - k_{23}[AOOH^-] + k_{-23}[Z][HOO^-] - k_{25}[AOOH^-] \quad (51)$$

$$d[^-AOOH]/dt = k_{22}[AOOH][OH^-] - k_{-22}[^-AOOH][H_2O] - k_{24}[^-AOOH] \quad (52)$$

$$d[Z]/dt = k_{20}[AO_2^-] + k_{23}[AOOH^-] - k_{-23}[Z][HOO^-] - k_{26}[Z] \quad (53)$$

$$d[P]/dt = k_{24}[^-AOOH] + k_{25}[AOOH^-] + k_{26}[Z] \quad (54)$$

Alditol reacts to form acidic products, carbonyl, hydroperoxide, or conjugate bases of the hydroperoxide. Therefore, the rate of alditol degradation can be written as follows:

$$-d[A]/dt = d[P]/dt + d[Z]/dt + d[AOOH]/dt + d[AO_2^-]/dt + d[AOOH^-]/dt + d[^-AOOH]/dt \quad (55)$$

Substituting Equations (50)-(54) into Equation (55) yields Equation (56).

$$-d[A]/dt = k_{18}[AO_2\cdot][M^{+n}] - k_{-18}[AO_2^-][M^{+n+1}] \quad (56)$$

Addition of Equations (40)-(42) and (47) gives

$$k_{18}[AO_2\cdot][M^{+n}] - k_{-18}[AO_2^-][M^{+n+1}] = -k_7[A^-][O_2] + k_{12}[A][HO\cdot] + k_{13}[A^-][HO\cdot] + k_{14}[A^-][O_2^{-\cdot}] + 2k_{27}[O_2^{-\cdot}][M^{+n+1}] \quad (57)$$

Substituting Equation (57) into Equation (57) yields Equation (58).

$$- d[A]/dt = - k_7[A^-][O_2] + k_{12}[A][HO\bullet] + k_{13}[A^-][HO\bullet] + k_{14}[A^-][O_2^{-\bullet}] + 2k_{27}[O_2^{-\bullet}][M^{+n+1}] \quad (58)$$

From Equation (42),

$$[HO\bullet] = k_9[O_2^{-\bullet}][H_2O]/(k_{12}[A] + k_{13}[A^-] + k_{28}[M^{+n}]) \quad (59)$$

Although the values of the rate constants $\underline{k}_{12}$, $\underline{k}_{13}$, and $\underline{k}_{28}$ are not known, they all involve the reaction of the hydroxyl free radical and, hence, they are probably similar in magnitude. Thus, since [A] is approximately 10^4 times greater than $[M^{+n}]$, it is assumed that $\underline{k}_{28}[M^{+n}] << \underline{k}_{12}[A] + \underline{k}_{13}[A^-]$. Equation (59) can now be written as

$$[HO\bullet] = k_9[O_2^{-\bullet}][H_2O]/(k_{12}[A] + k_{13}[A^-]) \quad (60)$$

Substituting Equation (60) into Equation (58) yields Equation (61).

$$- d[A]/dt = - k_7[A^-][O_2] + [O_2^{-\bullet}](k_9[H_2O] + k_{14}[A^-] + 2k_{27}[M^{+n+1}]) \quad (61)$$

Addition of Equations (40)-(47) and rearrangement expresses the concentration of superoxide radical.

$$[O_2\bullet] = k_7[A^-][O_2]/k_{27}[M^{+n+1}] \quad (62)$$

Substituting Equation (62) into Equation (61) yields Equation (63), which is devoid of all radical species.

$$- d[A]/dt = k_7[A^-][O_2] + k_7k_{14}[A^-]^2[O_2]/k_{27}[M^{+n+1}] + k_7k_9[H_2O][A^-][O_2]/k_{27}[M^{+n+1}] \quad (63)$$

Finally, from Equation (7),

$$[A^-] = K_6[A][OH^-] \tag{64}$$

Substituting Equation (64) into (63) gives

$$- d[A]/dt = K_6k_7[A][OH^-][O_2] + K_6^2k_7k_{14}[A]^2[OH^-]^2[O_2]/k_{27}[M^{+n+1}] + K_6k_7k_9[H_2O][A][OH^-][O_2]/k_{27}[M^{+n+1}] \tag{36}$$

An independent derivation of the rate of alditol degradation assuming superoxide is the only important radical [elimination of Equations (10), (13), (14), and (29) results in the following:

$$- d[A]/dt = K_6k_7[A][OH^-][O_2] + K_6^2k_7k_{14}[A]^2[OH^-]^2[O_2]/k_{27}[M^{+n+1}] \tag{32}$$

This equation is analogous to Equation (31) except for the third term which, therefore, reflects the role of the hydroxyl free radical in the reaction mechanism.